LIMIT CYCLE APPROACH FOR IDENTIFICATION AND CONTROL OF PROCESSES

A Thesis Submitted
in Partial Fulfillment of the Requirements
for the Degree of

DOCTOR OF PHILOSOPHY

by

Prabin Kumar Padhy

Department of Electronics and Communication Engineering
Indian Institute of Technology Guwahati
Guwahati-781 039, INDIA

July, 2007

CERTIFICATE

This is to certify that the thesis entitled **"Limit Cycle Approach for Identification and Control of Processes"**, submitted by Prabin Kumar Padhy, a research student in the *Department of Electronics and Communication Engineering, Indian Institute of Technology Guwahati, Guwahati,* for the award of the degree of **Doctor of Philosophy** has been carried out under my supervision. The thesis has fulfilled all the requirements as per the regulations of the institute and in my opinion it has reached the standard needed for submission. The results embodied in the thesis have not been submitted elsewhere for the award of any degree.

23rd July, 2007

(Dr. Somanath Majhi)
Associate Professor
Department of Electronics and
Communication Engineering,
Indian Institute of Technology Guwahati,
Guwahati – 781 039,
India.

Dedicated to

My Parents Premananda and Santilata

and

Wife Kunmun and Daughter Guddli

ACKNOWLEDGEMENTS

I am grateful to my Ph.D. supervisor Dr. Somanath Majhi for his patient guidance, enthusiastic encouragement and friendly behavior throughout my research works which helps in overcoming the problems encountered during the work and also for reading the thesis at the draft stage; providing useful comments and locating the errors.

I would like to thank to my Doctoral Committee members, Prof. P. K. Bora, Prof A. K. Gogoi, Dr. C. Mahanta and Dr. S. K. Dwivedy for their valuable comments from time to time that have enriched this thesis work. The cooperation I received from other faculty members of the Department is gratefully acknowledged.

I thank to all the research scholars and staffs of the Department for their help and support in carrying out my research and other thesis related works. I specifically thank Ahmad and Senthil, who have been particularly cooperative and supportive during my thesis writing.

I am grateful to my wife Kunmun and my daughter Guddli for their patience and love. Their inspiration and moral support helped me to bring this work into existence. Again, I am grateful to my parents, in-laws, sisters and brothers, whose love and encouragement made this research possible.

At last, I am grateful to Indian Institute of Technology Guwahati for financial support to carry out the present thesis work and providing scholarship during my Ph.D. period.

ABSTRACT

The thesis is concerned with identification and control of single-input-single-output (SISO) and two-input-two-output (TITO) processes based on relay induced limit cycles.

A relay based on-line identification method for stable and unstable SISO processes is proposed where the process model parameters are estimated from a single relay test. An ideal relay in parallel with a proportional-integral-derivative (PID) controller induces a limit cycle oscillation whose frequency and amplitude are used for the process identification. Firstly, the describing function (DF) analysis is used for the proposed identification method. The analysis is also accomplished by state space approach to overcome the limitations of the DF method. Load disturbance and measurement noise are the two commonly encountered problems during the process identification. These two problems are taken care of in the proposed identification method. The load disturbance is rejected successfully by the continuous action of the integral controller in the loop and the Fourier series based curve fitting technique is used to get the denoised limit cycle from the noisy one. The curve fitting method has its own limitations. Firstly, it gives an off-line noise free limit cycle signal. Secondly, the noisy signal fed to the relay results in multiple switching. To overcome these limitations, an adaptive low pass filter is placed in the feedback path during the auto-tuning test.

The proposed on-line identification method for the SISO process is extended for TITO processes. A diagonal transfer function model of the process dynamics is identified for decentralized controller design. The interaction between the loops affects the accuracy of the process model. Therefore, two proportional controllers are inserted in the inner feedback loops to reduce the loop interaction. A preload relay (P_relay) based identification scheme is also proposed to identify the diagonal transfer function models. The proposed scheme estimates the process model parameters accurately in the presence of loop interaction and measurement noise.

A PID controller design method for stable and unstable first order plus time delay (FOPDT) process models using the gain and phase margin criteria is proposed. The conventional PID controller often results in excessive overshoot in servo problem, particularly for unstable and integrating processes. Hence, a two degree of freedom PI-PD controller is designed for the FOPDT process model. The PD controller is designed so as to ensure stability of the

inner feedback loop whereas the PI controller by loop phase and gain margin criteria. The design method is extended for the decentralized PID controller design of TITO processes.

In the above controller tuning approaches, the process dynamics is first fitted to a transfer function model using the parameter estimation methods based on the relay induced oscillation signals. A model-free controller tuning approach for SISO processes is proposed where the controller is tuned based on the frequency response information obtained from the relay experiment. No structural assumption is made of the process. The distance of the Nyquist curve of the loop transfer function from the imaginary axis of complex plane and the loop phase margin are used in designing the controller parameters in this model free approach.

Contents

List of Figure

List of Tables

Nomenclatures

$G(s)$	Transfer function of a process
$G_m(s)$	Transfer function model of a process
$G_c(s)$	Transfer function of a controller
$G_{c1}(s)$	Transfer function of a feedforward controller
$G_{c2}(s)$	Transfer function of an inner feedback controller
$G_f(s)$	Transfer function of an adaptive noise filter
$G_{If}(s)$	Transfer function of an adaptive integral filter
$P(s)$	Transfer function of a fictitious process
$\overline{G}_m(s)$	Transfer function of a fictitious process model
ω_{cr}	Critical frequency of a process
T_{cr}	Critical half period of a process
K_{cr}	Critical gain of a process
K	Steady state gain of a process model
T	Time constant of a process model
D	Time delay of a process model
K_c	Proportional gain of a PID controller in parallel form
T_d	Derivative time constant of a PID controller in parallel form
T_I	Integral time constant of a PID controller in parallel form
K_c'	Proportional gain of a PID controller in series form
T_d'	Derivative time constant of a PID controller in series form
T_I'	Integral time constant of a PID controller in series form
β	Derivative filter constant of a PID controller
K_I	Proportional gain of an inner feedback PD controller
K_{b1}, K_{b2}	Gains of inner feedback proportional controllers of a TITO process
K_p	Proportional gain of a P_relay

K_I	Integral gain of a PID controller
k_I	Gain of an adaptive integral filter
T_f	Filter time constant of an adaptive noise filter
t	Time
t_s	Settling time
t_p	Peak time
t_r	Rise time
os	Overshoot
N	Gain of an ideal relay
h	Height of an ideal relay
L	Static load disturbance at the input of a process
M	Measurement noise introduced by a sensor
r(t)	Set-point / reference input
y(t)	Output signal
u(t)	Control input

Chapter 1

Introduction

1.1 Relay Based Identification

1.1.1 Identification of SISO Processes

Mathematical models of both existing and envisaged systems when made using well known techniques can result in higher order models leading to difficulties in designing control systems, in performing simulations and analysis besides creating hardware complexities. As a result, during the last couple of decades, a large number of methods for order reduction were developed to handle linear time invariant continuous and discrete systems [1]. However, a lower order transfer function model of the process dynamics can be obtained from a relay feedback experiment. Auto-tuning using relay feedback is widely used in industry because it is a closed loop method and therefore an on-off regulation of the process may be maintained even when the relay test is being conducted. It is used to find the dynamic information of the process and thereby to tune the feedback controller. The reliability of the method is used by Åström and Hägglund [2]. Process identification using auto-tuning variation (ATV) is one useful tool today in process industry. Luyben [3] is one of the pioneers to explain ATV technique for process identification of low order processes. The normal use of relay feedback is to induce a limit cycle in the process output. Process models are then obtained from the measurements made on the limit cycle output. For analysis, the nonlinear element relay is approximated by a gain using the describing function technique. The describing function technique is used by several authors to identify the transfer function models of stable and unstable processes. The accuracy and efficiency of the relay based identification have been improved in [4–14] by reducing high-order harmonic terms or using the Fourier analysis instead of the describing function method. Two relay tests are used by Li et al. [4] to identify an equivalent model of stable and unstable process. However, the use of an additional relay test is tedious and time consuming. Shen et al. [8] have used a biased relay for getting the model parameters using a single relay test. Tyagrajan and Yu [11] suggested a method that includes the effect of shape factor in identifying the stable and unstable FOPDT process models. Srinivasan and Chidambaram [12] have proposed a modified asymmetrical relay feedback method to get improved estimates of the parameters of the FOPDT model. The asymmetrical test requires an extra parameter and the value of that parameter is to be selected appropriately for accurate estimation of the model parameters. Vivek and Chidambaram [13] suggested an

improved method for calculating the FOPDT model from symmetrical relay tuning by the simultaneous solution of three nonlinear equations to estimate the three model parameters. Again, Vivek and Chidambaram [14] identified an unstable FOPDT model considering the higher harmonics. Chang et al. [15] used the z-transform method, which is one of the exact methods for relay identification. But, their method uses the amplitude ratio equation from the approximate describing function analysis. Wang et al. [16] used a time-domain approach to obtain the exact expressions for the limit cycle waveform for a FOPDT transfer function model. Atherton [17] also used a calculated exact waveform for both stable and unstable FOPDT transfer functions to produce simple corrections which can be used with the describing function method to give better accuracy. Majhi and Atherton [18] have derived a set of general expressions from a single asymmetrical relay test to identify the exact model parameters of open loop stable and unstable first order plus time delay and second order plus time delay processes using the state space approach.

Although, the relay auto-tuning is improved by some authors using modified relay based identification or by using the Fourier analysis or by exact analysis, the improvements do not overcome the practical constraints of the conventional relay based identification. First, it has a sensitivity problem in the presence of disturbance signals, which may be real process perturbation signal or equivalent one arising from varying process dynamics, nonlinearities and uncertainties present in the process. For small and constant disturbances, iterative solution [21] has been proposed by adjusting the relay bias until symmetrical limit cycle is obtained. However, for general disturbance signals, there has been no effective solution to-date. Secondly, the relay switching levels are determined with respect to the steady state operating conditions of the input and output signals and static gain of the process. Therefore, it is difficult to determine when the relay experiment is to be initiated as it is not possible to know when the above conditions are satisfied. Thirdly, the relay auto-tuning method is not applicable to certain class of processes which are not relay stabilizable, such as unstable processes and processes with more than one integrator [72]. For these processes, relay feedback does not induce stable limit cycle. Again, the conventional relay feedback test for unstable FOPDT process produces limit cycle when the ratio of time delay to unstable time constant is less than 0.693 [18]. The above ratio can be extended up to one by providing an inner feedback proportional controller during the auto-tuning test [23, 24, 40].

But, it is difficult to design the controller during the identification. Finally, the conventional relay method is an off-line identification method. Off-line tuning affects the operational process regulation which may not be acceptable for certain critical applications. Indeed, in certain key process control areas such as vacuum control, environment control, it may be too expensive or dangerous for the control loop to be broken for tuning purposes. Therefore, the tuning under tight continuous closed loop control (on-line) is necessary.

1.1.2 Identification of TITO Processes

Multivariable systems are more difficult to tune and control than the single-input-single-output systems. Such systems often called as multi-input-multi-output (MIMO) systems are commonly found in automated plants, aircrafts, chemical industries and other fields. A multivariable control system where the control loops are independently tuned according to recommendations given for the SISO systems often results in a closed loop unstable system. The main difficulty in controlling a multivariable system is the interaction between the loops and among various plant variables. This raises several issues for multivariable control system design. These include: interaction analysis, loop pairing, decoupling, robustness, implementation considerations and economy. The most basic and well-known form of a MIMO system is a TITO system. Many methods have been presented in the literature for the identification of TITO processes [45-58].

Many modern controllers are equipped with various adaptive techniques such as self-tuning, on-line tuning and auto-tuning. These features provide easy-to-use controller tuning and have proven to be well accepted among process engineers. A large majority of existing tuning methods for multivariable controllers require good process model in order to achieve satisfactory tuning. Accurate modeling of process dynamics is time consuming and requires extensive experimentation. One of the most common approaches to tune a controller automatically is to connect a relay as a feedback controller to the process during tuning [2]. The relay test for identification of TITO processes can be accomplished by the following three possible ways: a) using a single relay, b) by sequential operations of relays and c) using a decentralized relay.

In the independent single relay feedback method, one relay is used in one of the loops. This method does not excite multivariable interaction directly and therefore, it is difficult to

achieve fine-tuning of decentralized controllers when all loops are considered [45, 46]. In the case of sequential relay feedback, the multivariable system is tuned loop-by-loop, closing each loop once until all loops are tuned. Each time a relay configuration is set up to find out critical point (critical gain and frequency) of the corresponding loop [47-48]. In decentralized relay feedback, both the relays are closed at a time to tune the multivariable system. Among them the decentralized relay feedback technique is the most widely used technique in industry now a days for identification and control of TITO systems [49-58]. Using the results of relay experiment a multi-loop controller can be adopted for the TITO systems.

1.2 Controller Design

1.2.1 Model Based Controller Design

In process industry, more than 95% of the controllers are of PI/PID type. This is mainly attributed to its effectiveness and simple structure, which can be easily understood and implemented in practice. Consequently, the research on PID control algorithm development and their applications is still a very active area and many formulae have been derived to tune the PID controllers over the years [73]. The importance of PID control comes from its convenient applicability and clear effects of each proportional, integral and derivative control. Several methods are available in the literature to design the PID controller for SISO processes [24-39]. However, PID controller results in an excessive overshoot for unstable and integrating processes. Hence, two degree of freedom controllers (PI-PD, PID-P, set-point weighted PID) are designed to overcome the structural limitation of the PID controller [40-44].

Multiloop diagonal SISO controllers are often used to control multi-input-multi-output processes. The simpler structure and the easiness to handle the loop failure are most attractive advantages of such controllers. However, the controllers encounter interactions existing among the loops which have resulted in several open research topics for years. Many design methods have been reported in the literature for the control of two-input-two-output processes [59-69].

Gain and phase margins have always served as important measures of robustness for the SISO system. Phase margin is related to the damping of the system and can therefore serve

as a measure of performance. Ho et al. [31] presented simple expressions for the controller parameters of a SISO process using loop gain and phase margin criteria. In [59], the loop phase and gain margin technique is extended for controlling the TITO processes. The phase and gain margin criteria are used for the controller design for both the SISO and TITO processes in our proposed methods.

1.2.2 Model-Free Controller Design

Tuning techniques for controllers which do not require a mathematical model of the process are regularly used in industry, especially in auto-tuned PID controllers. The pioneering method was first suggested by Ziegler and Nichols [36] in 1942 for the tuning of PID controllers. The tuning method is basically based on the concepts of the critical point (critical gain and critical frequency) of the process Nyquist curve which is obtained by inserting a proportional controller of suitable gain in the feedback control loop to make the process output oscillatory. Thereafter, many further contributions have been made to improve the above tuning technique. One of the most popular methods was suggested by Aström and Hägglund [2] in 1984 for the automatic tuning of PID controller where a relay is used in the feedback control loop to obtain the critical point of the process Nyquist curve. But, the critical point obtained by the conventional relay method does not give the best possible information about the process with respect to PI / PID controller tuning. Additional information can be obtained by identifying a point in the third quadrant of the complex plane introducing an extra phase lag to the relay. Scali et al. [22] identified a point in the third quadrant using a modified relay (time delay along with the ideal relay) for the identification of completely unknown processes. However, their method requires several relay tests to determine the time delay of the modified relay. Also, the delay used during the identification is independent of the controller parameters. In [20], it is shown that the accuracy of the describing function can be improved by using an integrator along with the ideal relay during identification as per the attenuation characteristic of an integrator. The process is approximated by a low order transfer function model and the PID controller is designed by the pole-zero cancellation principle for a specified phase and gain margin. The approximations used by their method fail to give good results for many typical process models.

Tan et al. [39] proposed a robust on-line automatic tuning method for the PID controller where the controller parameters are tuned non-iteratively. In their method, the relay induces limit cycle output of the controller-stabilized process. The method is not straightforward since an initial PID controller is required to stabilize the process before initiating the relay test. Ho et al. [33] incorporated the ideas of iterative feedback tuning (IFT) into relay auto-tuning of PID controller to give specified phase margin and bandwidth. Some limitations of the conventional relay auto-tuning technique using a version of the Ziegler–Nichols formula [36] are overcome by their method. But, the time required for their on-line experiment may not be acceptable in practice. A modified relay based auto-tuning method is proposed in this thesis for stable processes to overcome problems associated with the above methods.

1.3 Outline of the Thesis

The thesis is concerned with identification of an equivalent transfer function model of a process dynamics from the relay feedback test using the describing function and state space analysis. To make the identification more realistic, static load disturbance and measurement noise are introduced during the identification. Some controller tuning methods based on the identified model are then proposed. Obtaining a good process model may require a large amount of time and the expense may not be justifiable. Therefore, a relay based auto-tuning approach is proposed where the controller can be tuned automatically on demand without identifying the process model. The thesis is divided into six chapters. Brief descriptions of the research contributions made in the four chapters (Chapter 2 to Chapter 5) of the thesis are as follows.

1.3.1 Chapter 2

In this chapter, limit cycle data based on-line identification methods for stable and unstable SISO processes are proposed. To overcome some limitations of the conventional relay auto-tuning methods, limit cycle is induced connecting an ideal relay in parallel with a PID controller. The relay sees a fictitious process whose order increases because of the PID controller. The DF analysis is used to estimate the SISO process model parameters. There are two reasons for using the DF analysis. Firstly, the generally accepted point about the DF method is that its accuracy increases with the relative order of the process transfer function. Secondly, it requires much less computational effort compared to some exact methods for

system identification. To improve the performance of the auto-tuning method, the PID controller is divided into PI and PD parts where the PD part in the inner loop and the PI part in parallel to the relay in the error path induce limit cycle output. The proposed method tries to couple the advantages of relay based identification of an inner feedback controller-stabilized process. In the DF method, only the fundamental frequency component of the nonlinear relay output is considered, thereby, affecting the accuracy of the identified model. Hence, the state space analysis is introduced to overcome the limitations of the DF method. However, one need to solve simultaneously a set of nonlinear equations to estimate the process model parameters and therefore, the describing function analysis is used extensively in subsequent studies. Estimation errors of the process model parameters increase with the asymmetrical and noisy limit cycle output data due to the presence of static load disturbance and sensor. However, the static disturbances during the on-line identification are successfully rejected due to the continuous action of the integral controller in the loop and smooth limit cycles are obtained from the noisy one using the Fourier series based curve fitting method. The Fourier series based curve fitting method gives an off-line noise free limit cycle signal at high computational cost. Since the noisy output signal is being fed to the relay, it often results in multiple switching. These limitations are taken care of by inserting an adaptive low pass filter in the feedback path during the relay experiment. The new technique is able to estimate the process model parameters accurately even when the process is subjected to the static load disturbance and measurement noise.

1.3.2 Chapter 3

In this chapter, the proposed relay based on-line identification method of chapter 2 is extended for the TITO processes. At first, an on-line identification method for the TITO processes is presented where two PID controllers are connected across the relays in the forward paths to induce the limit cycle output. The proposed method identifies two second order plus delay SISO transfer function models for the TITO process dynamics in the presence of load disturbance and measurement noise. The interaction between the loops affects the accuracy in the identification of the process model. Therefore, the identification method is modified by inserting proportional controllers in the inner feedback loops. The proportional controllers stabilize the process and reduce the loop interactions at the critical frequency thereby increasing the accuracy of the identified models. Further, P_relays based

identification method is proposed for the identification of two SISO transfer function models of the process from a single relay test in the presence of large loop interaction, static disturbance and measurement noise.

1.3.3 Chapter 4

Some controller design methods based on process model parameters are provided in this chapter. Simple PID tuning formulae for stable and unstable FOPDT process models are derived to meet user defined gain and phase margin specifications. Further, the method is extended to design PI-PD controller to improve the control performances. The PD controller in the inner feed back loop plays an important role in stabilizing the open loop processes. A method for finding the parameters of decentralized controllers for a TITO process based on the loop phase and gain margins is also presented. The controller parameters are tuned on-line without disrupting the closed loop operation. The control scheme is modified by inserting proportional controllers in the inner feedback paths to improve performances of the forward path controllers.

1.3.4 Chapter 5

A modified relay (an ideal relay in series with a PI controller of unit proportional gain) based auto-tuning method for PID controller is proposed in this chapter. The method does not require the intermediate stage (identification of process model), improves the describing function approximation and ensures a symmetrical and noise free limit cycle output even in the presence of static load disturbance and measurement noise. In describing function technique, the input to the relay is assumed to be sinusoidal leading to error in the estimation of the critical gain and frequency. In the proposed method, the effect of higher harmonics is reduced due to the integral action in the modified relay. The integral time constant of the PI controller of the modified relay is updated during the auto-tuning test ensuring a minimum loop phase margin of 30^0. Thereafter, the PID controller is designed using the limit cycle output data of the modified relay. The derivative time constant is obtained by maintaining the above mentioned loop phase margin. Minimization of distance of Nyquist curve of the loop transfer function from the imaginary axis of the complex plane gives the proportional gain of the controller.

1.3.5 Chapter 6

Conclusions and some general remarks are given in chapter 6. Also, some ideas about possible future work related to the research are included in this chapter.

1.4 Aim of the Research Work

One of the primary aims of this work is the identification of lower order transfer function models of the stable and unstable processes in the presence of load disturbance and measurement noise. The thesis presents some relay based approaches for the on-line identification of SISO processes using the DF and state space analysis. Then, the on-line identification method using DF analysis is extended for the identification of two SISO transfer function models of TITO processes having various levels of loop interactions. A P_relay based identification scheme for TITO processes is also proposed. The proposed scheme estimates the process model parameters accurately even in the presence of loop interaction and measurement noise. The parameters of the process models are estimated from a single relay test. Another aim of the research work is to design effective and robust PID controllers for the identified models of both SISO and TITO processes. The controller tuning methods using loop gain and phase margin criteria are then proposed for the identified process models. Further, a model-free controller tuning approach is proposed where the controller is tuned based directly on the frequency response information obtained from the relay experiment. The identification and control methods are demonstrated through different simulation results.

Chapter 2

On-line Identification of SISO Processes

2.1 Introduction

Luyben [3] pioneered the use of relay feedback tests and the describing function analysis for system identification. The describing function approximation allows one to identify one point of the process Nyquist curve on the basis of its frequency and amplitude. Then, an equivalent transfer function model of the process is obtained based on the identified point. The describing function technique is used by several authors to identify transfer function models of stable and unstable processes. The accuracy and efficiency of the relay based identification have been improved in [4–14] by reducing high-order harmonic terms or using the Fourier analysis instead of the describing function method. To improve the accuracy of the identification methods, some exact methods such as z-transform method [15], time-domain approach [16], exact waveform method [17], state space approach [18] and using the effect of shape factor [11, 19] are proposed. However, unlike the DF method, the exact methods are not straightforward and are time consuming. It is extremely difficult to obtain simple explicit expressions for the process model parameters by the exact analysis methods.

Although the relay auto-tuning methods have been improved by several authors [4-19], the improvements do not overcome the constraints of the ideal relay based identification discussed in subsection 1.1.1. This chapter presents a number of on-line identification methods that include a relay in parallel with a PID controller in the error path (forward path) to induce symmetrical limit cycle output even in the presence of static load disturbances. The initial settings of the PID controller may be based on the simple prior information about the process or one can use some default settings. However, the initial controller settings should be selected carefully to induce stable limit cycle output. In the proposed work, a method to set the initial PID parameters has been suggested.

Once a parametric model of the process dynamics is obtained, thereafter, the PID controller parameters are updated using the model-based PID tuning formulae derived in chapter 4. One of the proposed identification methods uses a low pass filter in the feedback path that filters out the frequency components much higher than the critical frequency and results in noise-free limit cycle output. The filter time constant is obtained adaptively from the parameters of the limit cycle output. The relay experiment may be re-invoked for retuning purposes as and when changes in set-points or process dynamics take place.

2.2 On-line Identification

2.2.1 Describing Function Analysis

The describing function technique has been widely used to determine the limit cycle and the dynamical behaviour of the processes [71]. The technique has been used in industries for decades and is receiving increasing attention for relay based identification of the industrial processes. The relay induces a permanent oscillation of the process output and the frequency and amplitude of the oscillation are used to identify an equivalent transfer function model of the processes using the describing function analysis [3]. The describing function specifies the change in the amplitude and phase of the fundamental component of the relay output with respects to its input assumed to be a pure sine wave. The principle of identification using a conventional relay that induces limit cycle output Y is shown in Fig. 2.1 where $G(s)$ is the process and N is the ideal relay of height h. In the figure, E and U are the relay input and output signal, respectively. R is the reference or set-point input.

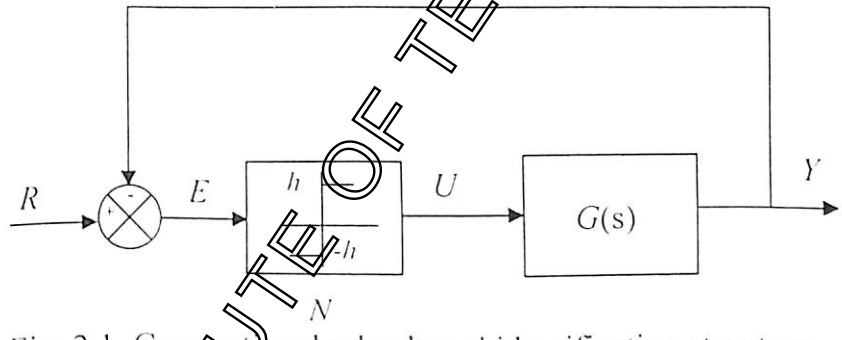

Fig. 2.1. Conventional relay based identification structure

Let $e(t) = A\sin\omega t$, where A is the peak amplitude and ω is the fundamental frequency of the relay input signal. Using the Fourier series expansion, the periodic output $u(t)$ of the relay can be written as

$$u(t) = \sum_{k=1}^{\infty} \mu_{2k-1} \sin(2k-1)\omega t \qquad (2.1)$$

where $\mu_{2k-1} = \dfrac{4h}{\pi(2k-1)}$ are the amplitudes of different frequency components of $u(t)$. The describing function is obtained by considering only the principal harmonic of the relay output signal. Therefore, the relay is approximated by a gain of

$$N = \frac{4h}{\pi A} \tag{2.2}$$

and the limit cycle information is obtained from the intersection of the locus

$$-\frac{1}{N} = -\frac{\pi A}{4h} \tag{2.3}$$

and the Nyquist curve of $G(j\omega)$ as illustrated in Fig. 2.2. The frequency at the intersection is the critical frequency, ω_{cr} and the gain of the relay is called the critical gain, K_{cr}.

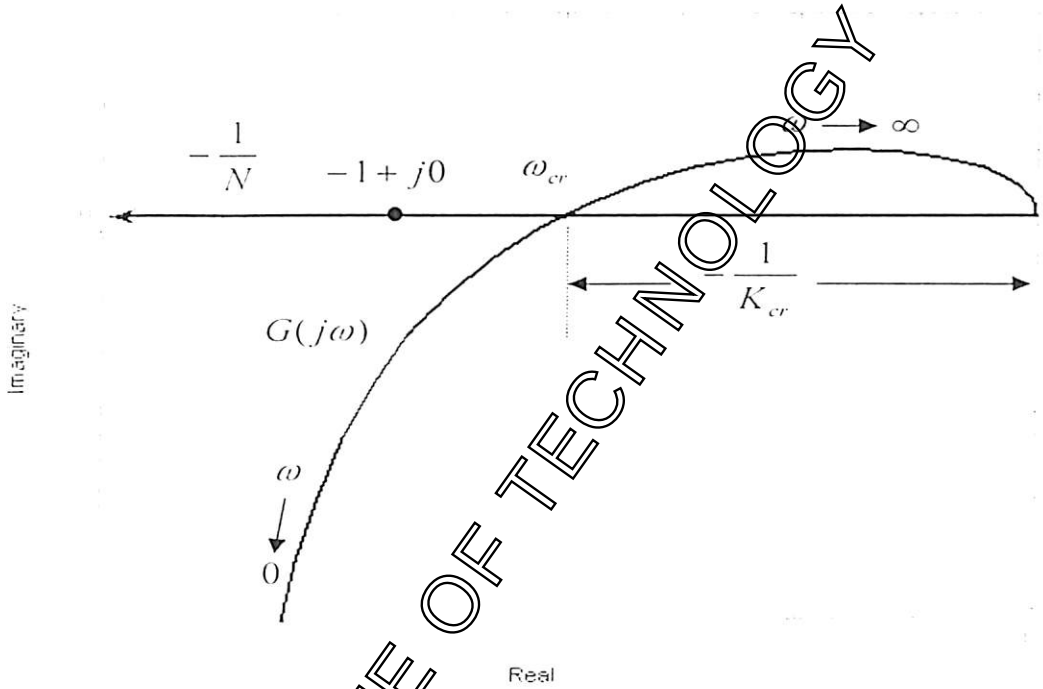

Fig. 2.2. Nyquist curve of $G(j\omega)$ and $-1/N$ locus

The relevant equations at the intersection point are

$$\angle G(j\omega_{cr}) = -\pi \tag{2.4}$$

and

$$K_{cr} = \frac{1}{|G(j\omega_{cr})|} = \frac{4h}{\pi A} \tag{2.5}$$

The parameters of the critical point ω_{cr} and K_{cr} provide valuable information about the magnitude and phase of a process under relay feedback. Using this information, an equivalent transfer function model of the process can be estimated. In practice, the accuracy of these estimates depends on how close the relay induced limit cycle signal is sinusoidal,

since it relates the accuracy of the describing function method in predicting the limit cycle parameters A and $\omega_{cr} = \frac{\pi}{T_{cr}}$ where $2T_{cr}$ is time period of the limit cycle signal.

2.2.1.1 Proposed On-line Identification Structure

The proposed on-line identification structure comprises of an ideal relay in parallel with a PID controller $G_c(s)$ in the error path as shown in Fig. 2.3. It is assumed that the static load disturbance L and the random measurement noise M appear at the process input and output, respectively. The proposed identification method induces the limit cycle output around the set-point. Based on the measurements of the limit cycle output, a stable or unstable FOPDT transfer function model of the process dynamic is identified. The relay height h is non-zero during identification and immediately after the relay test it is set to zero. When the relay height is zero, one obtains a control structure with the PID controller. However, the controller $G_c(s)$ always remains in action.

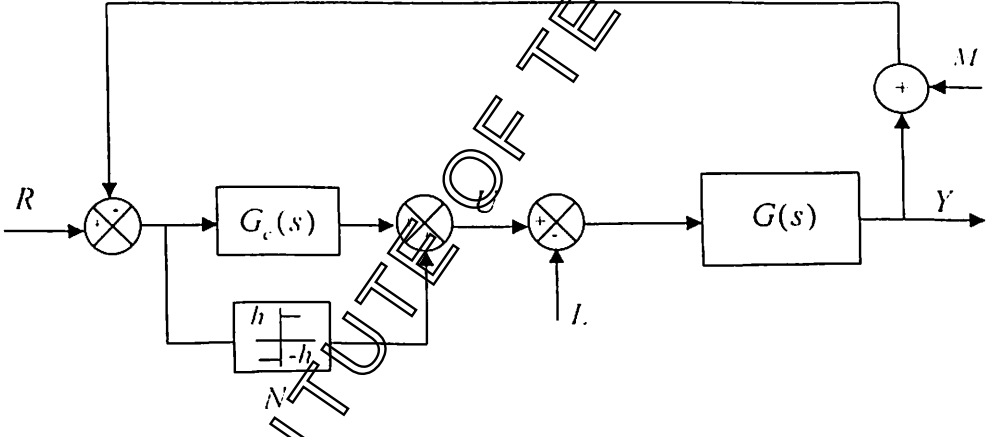

Fig. 2.3. Proposed on-line identification structure with PID controller

2.2.1.2 Identification Procedure

Many industrial processes require designing simple and easy-to-use controllers for their smooth operation. Hence, it is desirable to model these process dynamics by lower order transfer function models and then design simple controllers based on these lower order representations. In this subsection, a first order plus time delay model of process dynamics is obtained using the proposed on-line identification method. Let the process model transfer function has the following typical form

$$G_m(s) = \frac{Ke^{-Ds}}{Ts \pm 1} \tag{2.6}$$

where K, T and D are the steady state gain, time constant and time delay of the process model, respectively. Let the form of the PID controller be

$$G_c(s) = K_c\left(1 + \frac{1}{T_I s} + \frac{T_d s}{\beta T_d s + 1}\right) \tag{2.7}$$

where K_c, T_I, T_d and β are the proportional gain, integral time constant, derivative time constant and derivative filter constant, respectively. Normally, β is very small, so the derivative filter term in (2.7) is neglected in the following for ease in analysis. Fig. 2.4 shows the equivalent representation of the Fig. 2.3. It is apparent from the Fig. 2.4 that the relay sees a fictitious process $\bar{G}(s)(G(s)$ coupled with the inner loop controller $G_c(s))$ in the loop. The process gets stabilizing signal from the inner feedback controller $G_c(s)$ thereby improving its stability during identification. The estimation of the process model parameters is carried out in the following manner.

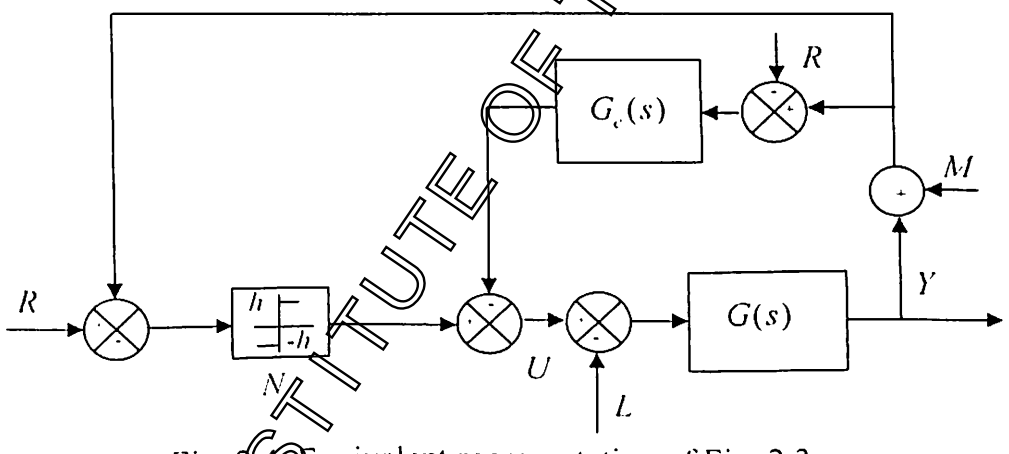

Fig. 2.4. Equivalent representation of Fig. 2.3

Estimation of Steady State Gain (K)

The average value of the process input $u(t)$ is non-zero for non-zero reference input due to the integral action in the controller. So, the steady state gain of the process can be obtained from the ratio of the average values of the process output and input signals. The method ensures accurate estimation of the steady state gain in the presence of measurement noise

and static load disturbance. For some $t > 2T_{cr}$, when steady state limit cycle is produced, let y_{avg} and u_{avg} be the averages of the process output signal $y(t)$ and input signal $u(t)$, respectively, as shown in Fig. 2.5. The average value of the limit cycle output is the set-point value due to the integral action of the PID controller. Therefore, the steady state gain can be estimated as

$$K = \frac{y_{avg}}{u_{avg}} = \frac{2R}{u_{\max} + u_{\min}} \tag{2.8}$$

If average value of the limit cycle output signal is zero when $r(t) = 0$, then a temporal disturbance may be given to the set-point for a short period of time to obtain y_{avg}.

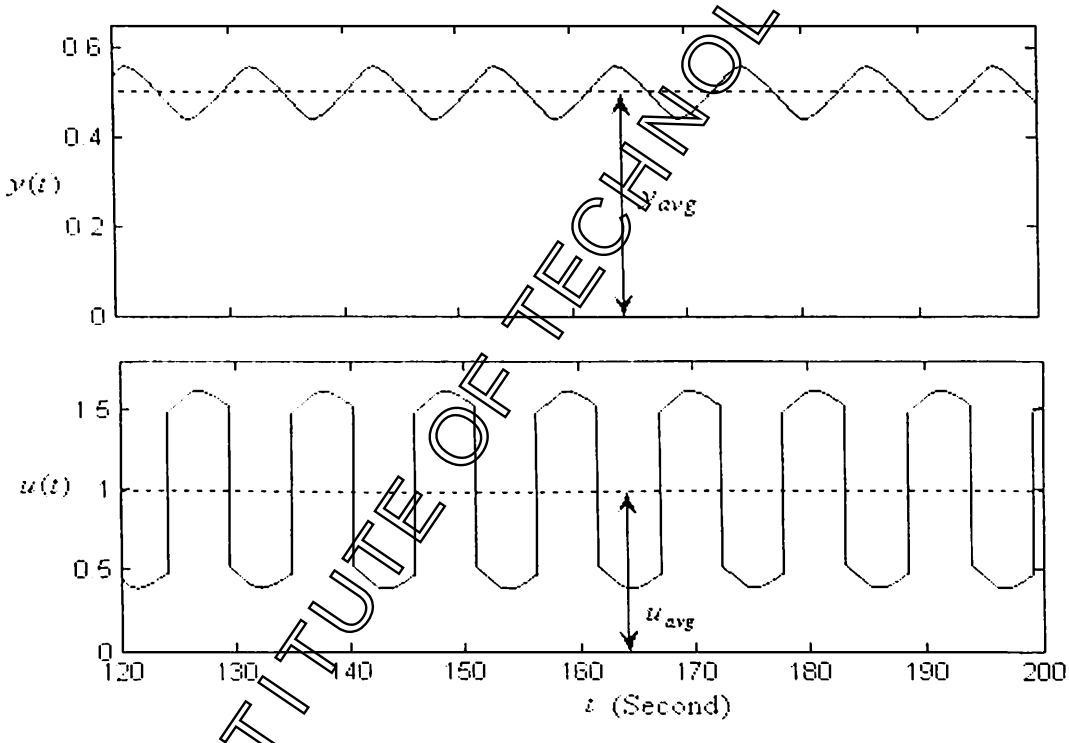

Fig. 2.5. Typical waveforms of $y(t)$ and $u(t)$

Estimation of T and D

From the measurements of A and ω_{cr} of the limit cycle output signal, T and D of the process models can be estimated for any $h \neq 0$. In order for a periodic solution to correspond to a stable limit cycle

$$NG_m(j\omega_{cr}) = -1 \tag{2.9}$$

where

$$\bar{G}_m(j\omega_{cr}) = \frac{G_m(j\omega_{cr})}{1 + G_c(j\omega_{cr})G_m(j\omega_{cr})} \tag{2.10}$$

Note that the oscillation frequency ω_{cr} varies with different controller settings. Then, (2.9) becomes

$$G_m(j\omega_{cr})\left[N + G_c(j\omega_{cr})\right] = -1 \tag{2.11}$$

Substitution of $G_m(j\omega_{cr}), N$ and $G_c(j\omega_{cr})$ in (2.11) gives

$$\frac{Ke^{-j\omega_{cr}D}}{(j\omega_{cr}T \pm 1)}(a_1 + ja_2) = -1 \tag{2.12}$$

where

$$a_1 = \frac{4h}{\pi A} + K_c \text{ and } a_2 = K_c\left(\omega_{cr}T_d - \frac{1}{\omega_{cr}T_I}\right).$$

Equating the magnitude and phase angle of both sides of (2.12), one obtains

$$T = \frac{\sqrt{K^2(a_1^2 + a_2^2) - 1}}{\omega_{cr}} \tag{2.13}$$

for both stable and unstable processes and

$$D = \frac{\pi + \tan^{-1}\left(\frac{a_2}{a_1}\right) - \tan^{-1}(\omega_{cr}T)}{\omega_{cr}} \tag{2.14}$$

for the stable process and

$$D = \frac{\tan^{-1}\left(\frac{a_2}{a_1}\right) + \tan^{-1}(\omega_{cr}T)}{\omega_{cr}} \tag{2.15}$$

for the unstable process.

The steady state gain K of the process model is obtained from (2.8) and the remaining parameters (T, D) of the stable or unstable process model are estimated either from (2.13) and (2.14) or (2.13) and (2.15). The auto-tuning test is carried out in two stages. At first, the initial controller parameters are chosen by the method given below and with these settings, the auto-tuning test is started. Once stable limit cycle is obtained, a FOPDT model of the process is identified based on the limit cycle data. Then, the controller parameters are updated using the model based controller tuning technique presented in chapter 4. The updated controller setting is now used for the second stage of relay test to obtain the final

transfer function model of the process dynamics. However, one may perform more stages of relay test, if necessary, to improve the accuracy of the identification method. Again, the initial stage of the relay test is not required if the initial controller is known a priori. Assuming an initial controller is known, which is true for a process already in operation, the final FOPDT transfer function model is obtained from a single relay test. Another advantage of the tuning scheme is that the relay height can be increased from zero to some acceptable value when the operator requires re-tuning the controller.

The frequency domain estimation error index using the integral of absolute error (IAE) criterion for each of the process models is

$$EE = \int_0^{\omega_{cr}} \left| \frac{G_m(j\omega) - G(j\omega)}{G_m(j\omega)} \right| d\omega \qquad (2.16)$$

where $G(j\omega)$ is the actual process and $G_m(j\omega)$ is the process model. The frequency range for the integration is taken from 0 to ω_{cr}, since that is most important for controller design.

Choice of Initial PID Controller Parameters

The relay induces stable limit cycle output when the fictitious process model $\bar{G}_m(s)$ satisfies (2.9). Using (2.6) and (2.7) and setting $T_d = 0$ and $T_f = 1$, $\bar{G}_m(s)$ can be expressed as

$$\bar{G}_m(s) = \frac{sKe^{-Ds}}{s(Ts \pm 1) + KK_c(s+1)e^{-Ds}} \qquad (2.17)$$

For a small value of K_c, (2.17) becomes

$$\bar{G}_m(s) = \frac{Ke^{-Ds}}{Ts \pm 1} \qquad (2.18)$$

It is evident from (2.18) that a positive value of $\frac{D}{T}$ ensures a limit cycle condition for stable processes whereas for unstable processes $\frac{D}{T}$ should be less than 0.693 [18]. From extensive simulation studies, it has been found that the choice of initial controller parameters

$$K_c = 0.01 - 0.1,\ T_f = 1 \text{ and } T_d = 0 \qquad (2.19)$$

results in a stable limit cycle output for of stable and unstable processes. The above initial choice is suggested for the processes with $KD \le 100$. For higher value of KD, the value of K_c can further be reduced to obtain the stable limit cycle output.

2.2.1.3 Effects of Static Load Disturbance

Static load changes frequently occur during a process operation and load disturbance rejection is a major problem in process control. Generally, conventional relay feedback test with an ideal relay under load disturbance results in an asymmetric limit cycle output. This problem is overcome by our on-line identification method by the forward path PID controller. The transfer function of the closed loop system with respect to the static load disturbance is

$$\frac{Y}{L}(s) = \frac{1}{1/G(s) + N + G_c(s)} \tag{2.20}$$

The steady state value of the output with respect to the static load disturbance becomes zero due to the presence of integral action in the PID controller. Thus, a symmetrical steady state limit cycle output is obtained around the set-point input even in the presence of static load disturbance during the auto-tuning test.

2.2.1.4 Effects of Measurement Noise

Measurement noise is a common problem in almost all process industry. The noisy limit cycle output signal makes it difficult to measure its amplitude and frequency accurately. So, the need arises to recover the smooth signal from the noisy output. The Fourier series based curve fitting with the options of least squares method and trust region algorithm in MATLAB is used in this work to obtain best fit output signal from the noisy one. It has been observed from extensive simulation that the following Fourier series

$$y'(t) = \sum_{k=0}^{8} \zeta_{1k} \cos(k\omega t) + \sum_{k=1}^{8} \zeta_{2k} \sin(k\omega t) \tag{2.21}$$

yields satisfactory results. In (2.21), $y'(t)$ is the best fit output signal, $\zeta_{1k}\ (k = 0,1,...8)$ and $\zeta_{2k}\ (k = 0,1,...8)$ are the Fourier coefficients and ω is the frequency of the recovered output signal.

2.2.1.5 Simulation Results

A stable and two unstable process transfer functions are considered in the examples in this subsection to illustrate the proposed identification method. In the first example, three stages of relay tests are performed. Normally, the second stage relay test yields very much similar

transfer function model parameters compared to the third stage (Table 2.1(a)). Therefore, the auto-tuning test is limited to two stages for all the remaining simulation examples. In all the examples, $K_c = 0.1$, $T_I = 1$ and $T_d = 0$ are chosen for the initial stage of relay tests. The PID controller parameters needed in the subsequent stages of relay test are updated using (4.11) and (4.16-4.17) of subsection 4.4.1 for specified values of the design parameters α, g_m and ϕ_m and using the results of the auto-tuning procedure given in subsection 2.2.1.2. The simulation results are compared with that of the ATV method given by Li et al. [4], the identification methods proposed by Tyagrajan and Yu [11] and Vivek and Chidambaram [13-14]. The accuracy of the identification method is checked by the estimation error index, EE. In this work, the effect of measurement noise on the process model parameters is investigated in simulations by introducing normally distributed random additive noise with zero mean and varying variance, $N(0,\sigma_N^2)$, at the outputs during the relay test thus making the oscillation noisy. The noise power is quantified by SNR (Signal to Noise Ratio) in decibel (dB) which is defined as $\text{SNR} = 10\log(\sigma_y^2/\sigma_N^2)$, where, σ_y^2 is the variance of the output signal and σ_N^2 is the variance of the noise. An ideal relay with height $h = 1$ is considered for all the examples. More examples are given in appendix B1 to highlight the proposed identification method.

Example 2.1

Let us consider a typical second order process [4] $G(s) = \dfrac{e^{-2s}}{(10s+1)(s+1)}$. The relay test is performed and the resulting process model parameters along with the controller parameters are given in Table 2.1(a). The design values $\alpha = 0.2$, $g_m = 3$ and $\phi_m = 60^0$ are used to design the controller required in the second and third stages of the relay test. One is free to choose the design values for satisfactory transient performances. Because of the similar estimated parameters in both the second and third stages (Table 2.1(a)), the process model obtained in the second stage of relay test is considered to be final. The FOPDT model parameters obtained by Li et al.'s method are $K = -0.501$, $T = -5.03$ and $D = 2$. Since the model is not valid, they have recommended a second order plus time delay model for the process dynamics. The method suggested by Vivek and Chidambaram fit the process as a

FOPDT model with parameters $K = 1.03$, $T = 11.98$ and $D = 2.84$. However, their model has an estimation error of 0.0606. The proposed method gives improved parameter estimates in terms of the estimation error index, EE. The Nyquist curves of the actual process and the process models by the proposed method and the method given by Vivek and Chidambaram are shown in Fig. 2.6. It is clear from Fig. 2.6 that the Nyquist curves of the proposed model and actual process are very close to each other, showing that the higher order processes can be approximated by a FOPDT model more accurately using the proposed on-line identification method. To verify the identification method under realistic conditions, the process model parameters are estimated with different levels of measurement noise as given in Table 2.1(b). From Table 2.1(b), it is seen that the processes are identified well by the proposed method even for high level of noise. The largest error in the estimated parameters is 9 % which is within the acceptable limit. The noisy output signal with SNR = 20dB and the recovered signal obtained by using Fourier series based curve fitting method are shown in Fig. 2.7.

Table 2.1(a) Controller and process model parameters for example 2.1

Stage 1	$G_c(s)$	$K_c = 0.4$, $T_I = 1$, $T_d = 0$	
	$G_m(s)$	$K = 1.0$, $T = 10.8176$, $D = 2.8885$	
Stage 2	$G_c(s)$	$K_c = 2.4493$, $T_I = 11.1424$, $T_d = 0.5477$	$EE = 0.0368$
	$G_m(s)$	$K = 1.0$, $T = 11.4341$, $D = 2.8602$	
Stage 3	$G_c(s)$	$K_c = 2.6062$, $T_I = 11.7212$, $T_d = 0.5441$	$EE = 0.0366$
	$G_m(s)$	$K = 1.0$, $T = 11.4673$, $D = 2.8591$	

Table 2.1(b) Estimated parameters and the errors at different noise levels for example 2.1

SNR in dB	K	Error in K	T	Error in T	D	Error in D
No noise	1.0	-	11.4341	-	2.8602	-
30	1.0	0.0	11.4780	0.0009	2.8574	0.0005
20	1.05	0.05	11.5538	0.0075	2.8509	0.0029
10	1.09	0.09	11.7712	0.0262	2.8677	0.0034

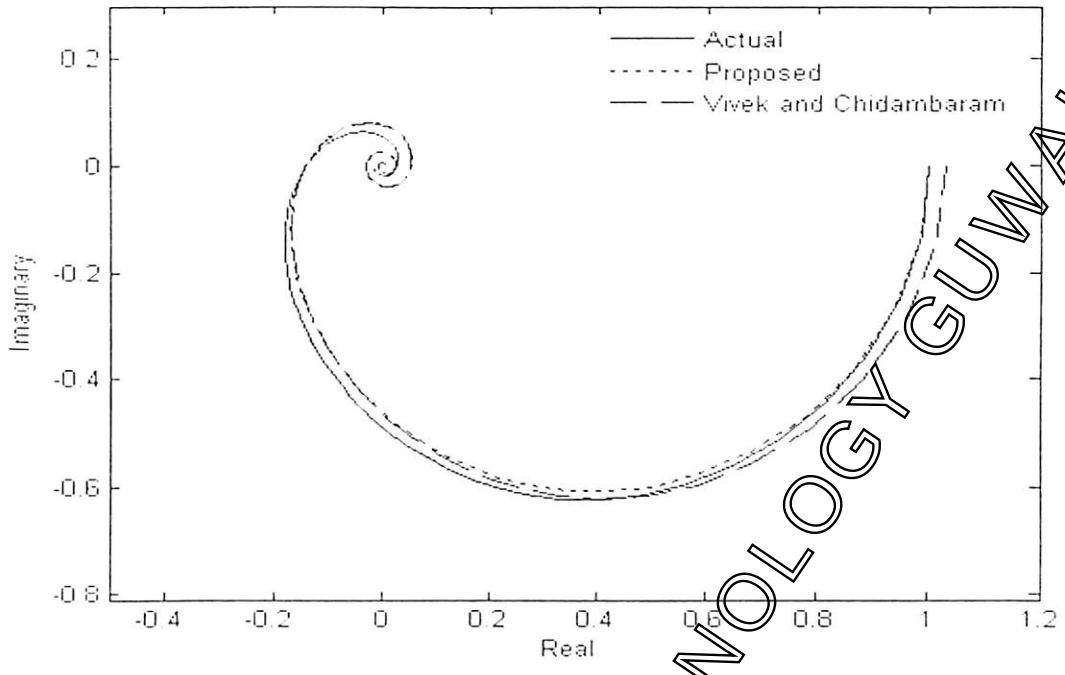

Fig. 2.6. Nyquist curves of process models for example 2.1

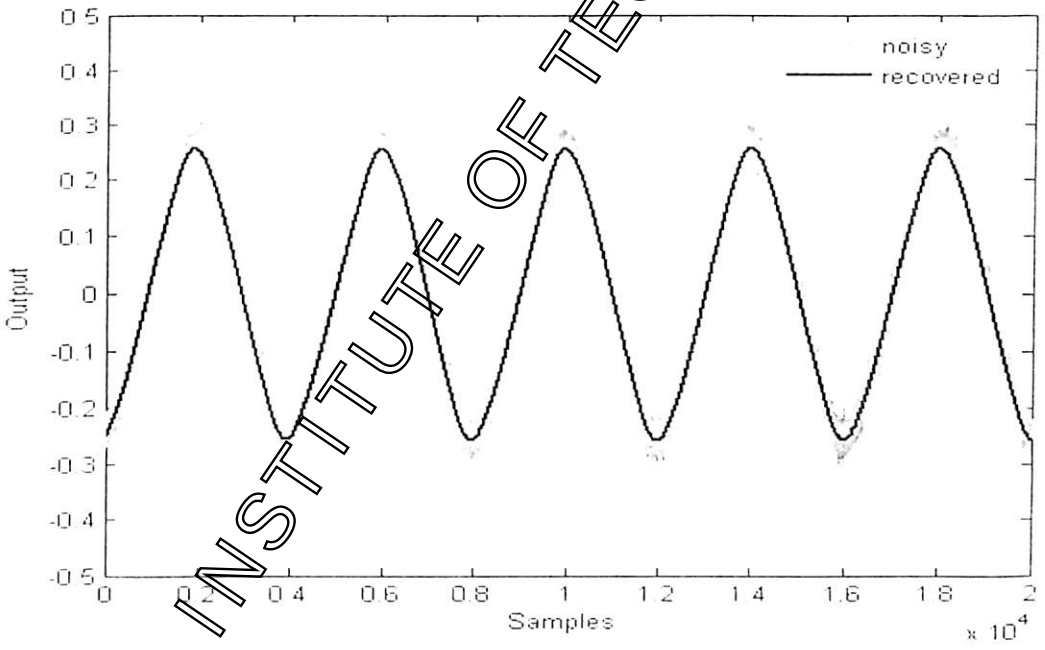

Fig. 2.7. Recovered and noisy output signal with SNR = 20dB for example 2.1

Example 2.2

Consider the open loop unstable process [13]

$$G(s) = \frac{e^{-0.5s}}{(s-1)}$$

The relay test starts with the initial controller $K_c = 0.1$, $T_I = 1$ and $T_d = 0$ and then updates the controller using the design values of $\alpha = 0.9$, $g_m = 5$ and $\phi_m = 45^0$. The controller and the process model parameters along with the estimation error index are given in Table 2.2. The model parameters obtained by the Li et al.'s method [4] and by the Vivek et al.'s method [13] are $K = 0.94$, $T = 0.77$, $D = 0.5$ with $EE = 0.4564$ and $K = 1.0638$, $T = 1.0832$, $D = 0.5127$ with $EE = 0.0825$, respectively. The proposed method identifies the process dynamics more accurately in terms of the estimation error index in comparison to the above discussed methods.

Table 2.2 Controller and process model parameters for example 2.2

Stage 1	$G_c(s)$	$K_c = 0.1, T_I = 1, T_d = 0$	
	$G_m(s)$	$K = 1.0, T = 0.8592, D = 0.5127$	
Stage 2	$G_c(s)$	$K_c = 1.7399, T_I = 3.9790, T_d = 0.4462$	EE=0.0406
	$G_m(s)$	$K = 1.0, T = 0.9912, D = 0.5014$	

Example 2.3

Let us consider a process transfer function possessing one stable pole and one unstable pole [14]

$$G(s) = \frac{e^{0.5s}}{(2s-1)(0.5s+1)}$$

$K_c = 0.1$, $T_I = 1$ and $T_d = 0$ is used in the initial stage of relay test and the design values of $\alpha = 0.85$, $g_m = 5$ and $\phi_m = 45^0$ are used to obtain the controller parameters for the next stage of test. The controller and the process model parameters of both the stages of the relay test are given in Table 2.3. The model parameters obtained by Vivek and Chidambaram's method [14] are $K = 0.7534$, $T = 2.1642$, $D = 0.9951$ with $EE = 0.3524$. The identification method by Tyagarajan and Yu [11] fails to identify a FOPDT model as the estimated values of process steady state gain and time constant become complex. The estimation error index by the proposed method is 0.2760. The Nyquist curves of the actual process and the process models obtained by Vivek and Chidambaram and by proposed

method are given in Fig. 2.8. As seen from the Nyquist curves, the proposed method can estimate the model parameters more accurately than the method given in [14].

Table 2.3 Controller and process model parameters for example 2.3

Stage 1	$G_c(s)$	$K_c = 0.1,\ T_I = 1,\ T_d = 0$	
	$G_m(s)$	$K = 1.0,\ T = 2.3304,\ D = 1.0729$	
Stage 2	$G_c(s)$	$K_c = 2.0853,\ T_I = 11.7183,\ T_d = 0.8410$	EE=0.2760
	$G_m(s)$	$K = 1.0,\ T = 2.6408,\ D = 0.9541$	

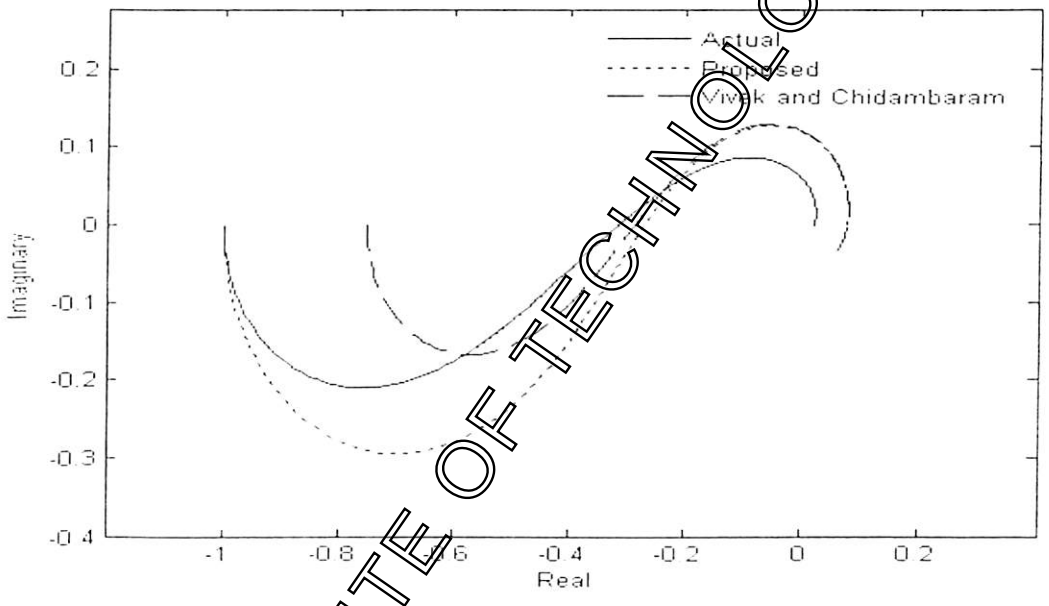

Fig. 2.8. Nyquist curves of process models for example 2.3

2.2.1.6 Special Case

To improve the identification method particularly for unstable process, the structure in Fig 2.3 is modified and given in Fig. 2.9. The modified structure comprises of an ideal relay in parallel with a PI controller in the forward path and a PD controller in the inner feedback path. The relay test induces the limit cycle output. Based on the parameters of the limit cycle output, the process dynamics is identified by a stable or unstable FOPDT model with the transfer function form given in (2.6).

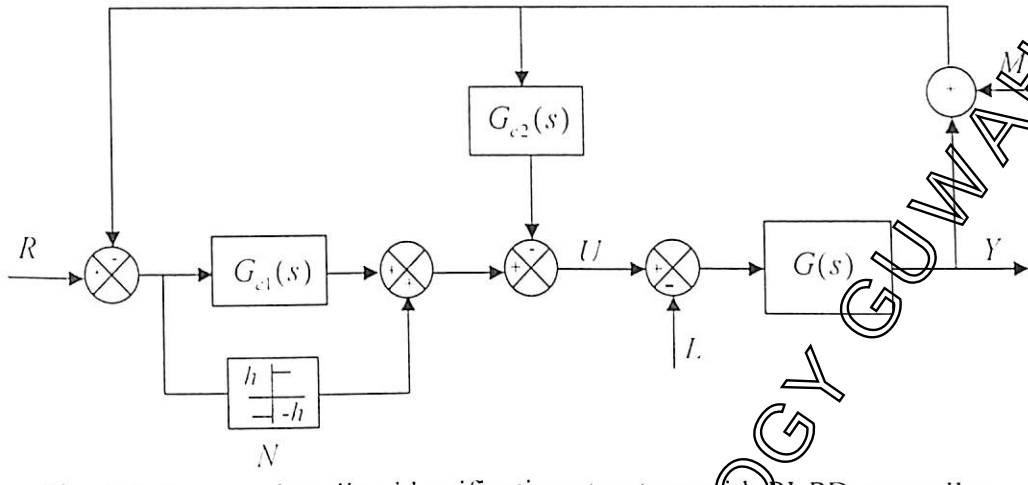

Fig. 2.9. Proposed on-line identification structure with PI-PD controller

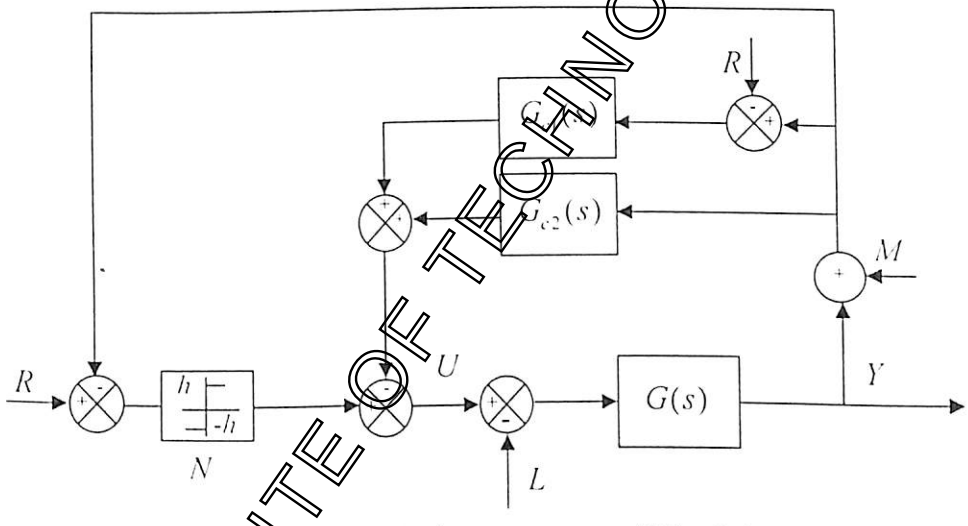

Fig. 2.10. Equivalent structure of Fig. 2.9

The forms of the PI and PD controllers are

$$G_{c1}(s) = K_c\left(1 + \frac{1}{T_i s}\right) \tag{2.22}$$

$$G_{c2}(s) = K_c\left(1 + \frac{T_d s}{1 + \beta T_d s}\right) \tag{2.23}$$

Fig. 2.10 shows the equivalent structure of Fig. 2.9 and depicts how during relay feedback test the process is subjected to the PI and PD controllers in the inner feedback path which can stabilize the stable and unstable processes. During the identification, the PI+PD controller assuming negligible β becomes

$$G_c(s) = G_{c1}(s) + G_{c2}(s) = K_f\left(1 + T_d s\right) + K_c\left(1 + \frac{1}{T_I s}\right) \tag{2.24}$$

The identification is carried out using the procedures given in the subsection 2.2.1.2. The steady state gain K of the process model is obtained from (2.8). The other two unknown parameters of the FOPDT process model are estimated either from (2.13) and (2.14) or (2.13) and (2.15) where, the expressions for a_1 and a_2 are

$$a_1 = \frac{4h}{\pi A} + K_c + K_f \text{ and } a_2 = \omega_{cr} K_f T_d - \frac{K_c}{\omega_{cr} T_I} \tag{2.25}$$

The relay test is carried out in two stages in a similar manner as in subsection 2.2.1.2. In the initial stage of relay test, $K_c = 0.01 - 0.1$ (a value in between 0.01 and 0.1), $T_I = 1$, $K_f = 0$ and $T_d = 0$ are chosen. But, the PI-PD controller parameters are updated at the beginning of the second stage of relay test by using (4.41-4.42), (4.27) and (4.22) of the subsection 4.4.2 for specified values of g_m and ϕ_m.

2.2.1.7 Simulation Results

The identification technique is demonstrated by two examples. For the first example, a second order stable process is considered. The unstable process of the second example possesses a stable pole and an unstable pole. An ideal relay height of $h = 1$ is considered in both the examples.

Example 2.4

Consider the stable process discussed in the example 2.1. The identification test begins with the choice of $K_c = 0.1$, $T_I = 1$, $K_f = 0$ and $T_d = 0$. The controller parameters are updated before the second stage of relay test using the design values of $g_m = 2$ and $\phi_m = 30^0$. Then, using the limit cycle parameters and (2.8), (2.13) and (2.15), process model parameters as given in Table 2.4 are estimated. The EE of the process models by the proposed method is 0.0428 which is slightly more than the EE calculated in example 2.1. However, the method estimates the parameters more accurately compared to the methods discussed in [4] and [13].

Table 2.4 Controller and process model parameters for example 2.4

Stage 1	$G_c(s)$	$K_c = 0.1, T_I = 1, K_f = 0, T_d = 0$	
	$G_m(s)$	$K = 1.0, T = 10.8236, D = 2.8884$	
Stage 2	$G_c(s)$	$K_c = 1.6891, T_I = 1.6184, K_f = 2.7376, T_d = 1.4442$	
	$G_m(s)$	$K = 1.0, T = 11.7301, D = 2.8524$	$EE = 0.0488$

Example 2.5

This example considers the unstable process given in example 2.3. The controller parameters along with the process model parameters for both the stages of the relay test are given in Table 2.5. Gain margin of 4 and phase margin of 60° are used for the controller design for the second stage of relay test. As seen from Tables 2.3 and 2.5, identification based on the modified structure (Fig. 2.9) gives better estimates for the unstable process in comparison to the structure shown in Fig. 2.3.

Table 2.5 Controller and process model parameters for example 2.5

Stage 1	$G_c(s)$	$K_c = 0.1, T_I = 1, K_f = 0, T_d = 0$	
	$G_m(s)$	$K = 1.0, T = 2.3304, D = 1.0729$	
Stage 2	$G_c(s)$	$K_c = 0.5905, T_I = 1.1133, K_f = 2.0843, T_d = 0.5365$	
	$G_m(s)$	$K = 1.0, T = 2.6225, D = 0.9570$	EE=0.2253

2.2.2 State Space Analysis

Relay based identification using approximate describing function method is used widely to obtain model related information of industrial processes. Despite the apparent success in industrial applications, the ideal relay auto-tuning method can in some instances be improved significantly with a more accurate estimate of the model parameters obtained when the procedure is based on exact analysis of the limit cycle rather than the describing function method. The reason is that the estimated ultimate gain and the ultimate frequency derived from the describing function are only an approximation for information at the critical frequency. Several identification methods [15-19] are proposed in literature to identify the process model accurately without using the describing function technique. In

this subsection, state space approach [18] is extended for the on-line identification of stable and unstable processes and exact expressions for the model parameters in term of the limit cycle measurements are derived.

2.2.2.1 Identification Structure

The identification structure given in Fig. 2.3 is redrawn in Fig. 2.11 to make the analysis easier. Two stages of relay test are performed to obtain the process model parameters. The relay test starts with some initial choice of controller parameters as suggested in subsection 2.2.1.2. When a stable limit cycle is obtained, the controller parameters are updated using the model based controller design technique given in subsection 4.4.1. This controller setting is used for the next stage of the relay test. Then, the desired process model is obtained by using the limit cycle parameters obtained from the second stage of relay test.

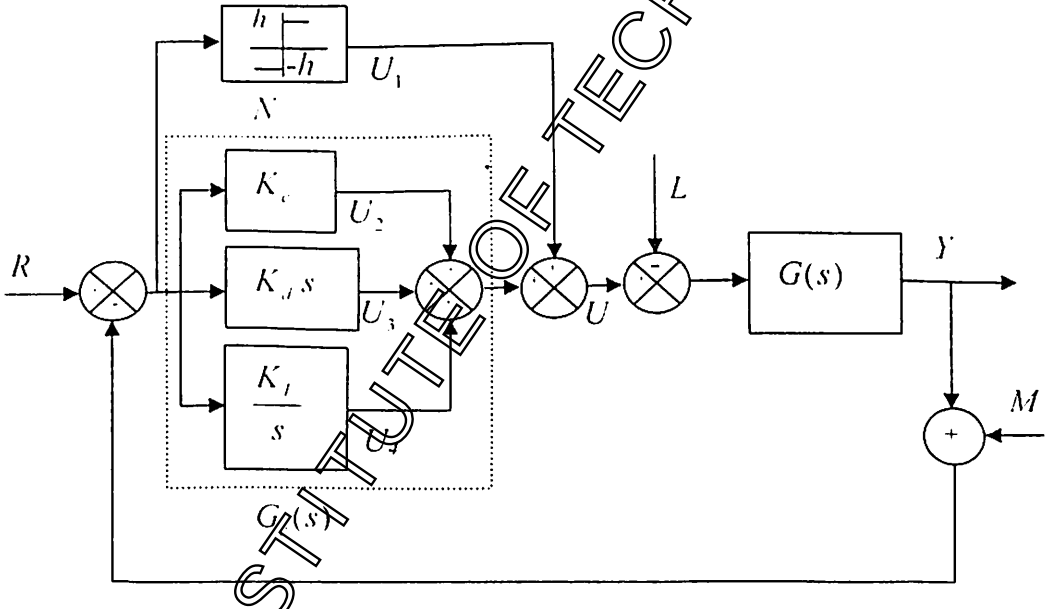

Fig. 2.11 Proposed on-line identification scheme in state space analysis

2.2.2.2 Analytical Expressions

Let the process model transfer function be $G_m(s)$, as given in (2.6) and the controller in (2.7) neglecting β be expressed in the following form

$$G_c(s) = K_c + K_d s + \frac{K_I}{s} \tag{2.26}$$

where $K_d = K_c T_d$ and $K_I = K_c / T_I$. For ease in analysis, the proposed identification structure (Fig. 2.11) can be represented by the configuration given in Fig. 2.4 where the relay is kept in the forward path and the PID controller is coupled with the process. Then, the transfer function of the fictitious process model (which the relay sees) becomes

$$\frac{Y(s)}{U_1(s)} = \bar{G}_m(s) = \frac{G_m(s)}{1 + G_c(s) G_m(s)} \tag{2.27}$$

The static load disturbance is neglected during the analysis. Substitution of (2.6) and (2.26) in (2.27) gives

$$\frac{Y(s)}{U_1(s)} = \frac{K e^{-Ds}}{Ts \pm 1 + KK_c e^{-Ds} + KK_d s e^{-Ds} + \dfrac{KK_I e^{-Ds}}{s}} \tag{2.28}$$

Cross multiplication and inverse Laplace transform of (2.28) gives

$$\dot{y}(t) = \lambda y(t) - K\lambda u_1(t-D) + KK_c \lambda y(t-D) + KK_I \lambda \int_0^t y(t-D)\,dt + KK_d \lambda \dot{y}(t-D) \tag{2.29}$$

where $\lambda = \mp \dfrac{1}{T}$. The above delayed differential equation when represented in state space form becomes

$$\dot{x}(t) = Ax(t) + b_1 u_1(t-D) + b_2 u_2(t-D) + b_3 u_3(t-D) + b_4 u_4(t-D) \tag{2.30}$$

$$y(t) = x(t) \tag{2.31}$$

where $A = \lambda$, $b_1 = -K\lambda$, $b_2 = KK_c\lambda$, $b_3 = KK_d\lambda$, $b_4 = KK_I\lambda$, $u_1(t-D) = \pm h$, $u_2(t-D) = y(t-D)$, $u_3(t-D) = \dot{y}(t-D)$ and $u_4(t-D) = \int_0^t y(t-D)\,dt$. In the state model (2.30), it is assumed that the four inputs to the process contribute the limit cycle output. Let the peak amplitude A occurs at time t_p of the limit cycle output. During the half period of the process output, the relay provides two piecewise constant input signals to the process as shown in Fig. 2.12. Therefore, the output waveform analysis is carried out for the time interval $0 \le t \le D$ and $D < t \le T_{cr}$. Majhi and Atherton [18] derived the expressions for the output equation of a FOPDT process model for the interval $0 \le t \le D$ and $D < t \le T_{cr}$ as

$$y(t) = \pm Kh(1 - e^{\lambda t}) \tag{2.32}$$

and

$$y(t) = \pm Kh(2e^{\lambda(t-D)} - e^{\lambda t} - 1), \tag{2.33}$$

respectively.

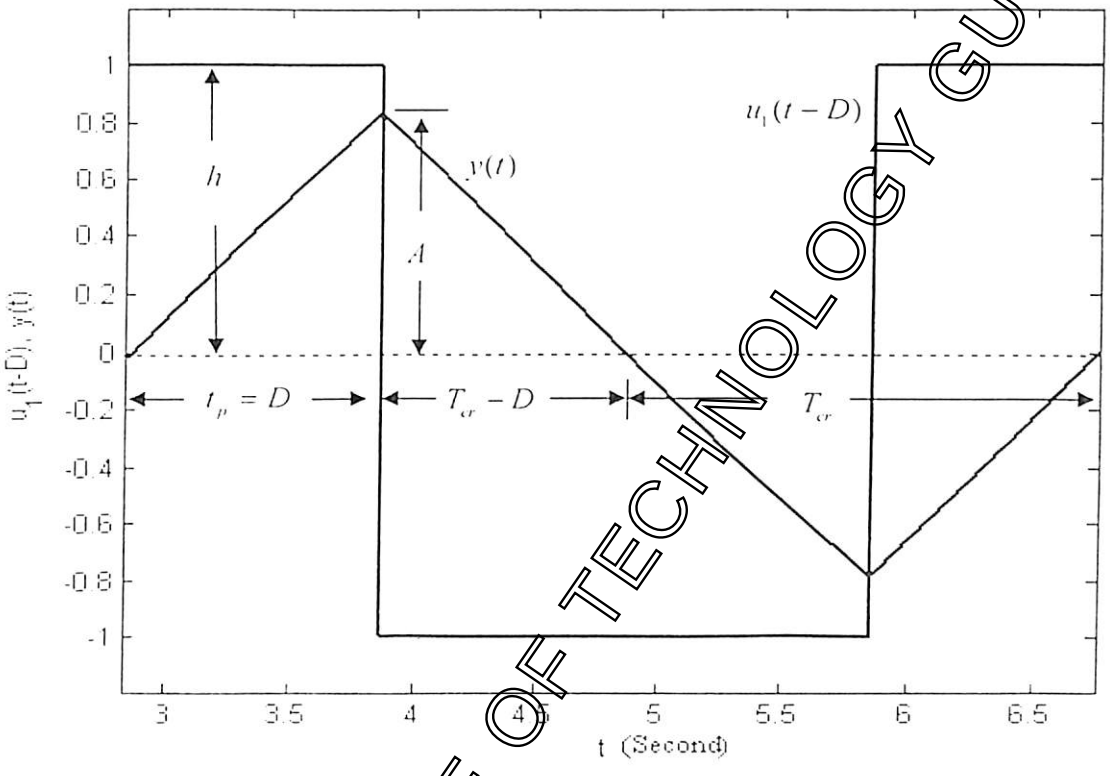

Fig. 2.12 Process and relay output signals

Similarly, with the help of (2.32), (2.33) and using the method discussed in [18], the solution of (2.30) for $0 \le t \le D$ and $D < t \le T_{cr}$ gives

$$y(t) = Kh(1 - e^{\lambda t})\left(\pm 1 - K_p - \frac{KK_I}{\lambda} - \frac{KK_I e^{-\lambda D}}{\lambda}\right)$$

$$- K^2 ht(K_d\lambda + K_d\lambda^2 + K_I)e^{\lambda(t-D)} - K^2 K_I ht \tag{2.34}$$

$$y(t) = e^{\lambda(t-D)}x(D) + Kh(1 - e^{\lambda(t-D)}) + K^2 K_I h\left[(t-D) + \frac{(1 - e^{\lambda(t-D)})(2 - e^{\lambda D})}{\lambda}\right]$$

$$+ K^2 h(K_d\lambda + K_d\lambda^2 + K_I)\left[(t-D)(2e^{\lambda(t-D)} - e^{\lambda t}) + \frac{(1 - e^{\lambda(t-D)})}{\lambda}\right] \tag{2.35}$$

The relay gives symmetrical limit cycle only when the following condition is satisfied

$$y(0) = -y(T_{cr}) = 0 \tag{2.36}$$

Looking at the Fig. 2.12, one can write

$$t_p = D \tag{2.37}$$

Substituting (2.37) in (2.34) or (2.35), the expression for the peak amplitude is obtained as

$$A = Kh(1 - e^{\lambda D})(\pm 1 - KK_c) - K^2 h\left[K_c \lambda D + K_d \lambda^2 D + K_I (2D - \frac{2}{\lambda}\sinh \lambda D)\right] \tag{2.38}$$

From (2.35) and (2.36), we get

$$e^{\lambda(T_{cr}-D)}x(D) \mp Kh(1 - e^{\lambda(T_{cr}-D)}) + K^2 K_I h\left[(T_{cr} - D) + \frac{(1 - e^{\lambda(T_{cr}-D)})(2 - e^{\lambda D})}{\lambda}\right]$$

$$+ K^2 h(K_c \lambda + K_d \lambda^2 + K_I)\left[(T_{cr} - D)(2e^{\lambda(T_{cr}-D)} - e^{\lambda T_{cr}}) + \frac{(1 - e^{\lambda(T_{cr}-D)})}{\lambda}\right] = 0 \tag{2.39}$$

The time delay of the process is obtained from (2.37). The other parameters λ (or T) and K can be determined from the simultaneous solution of (2.38) and (2.39).

2.2.2.3 Simulation Results

The proposed on-line auto-tuning method is illustrated by considering a stable and an unstable FOPDT processes in this subsection. For both the processes, the relay experiments are conducted with PID initial controllers with the parameters $K_c = 0.1$, $T_I = 1$ and $T_d = 0$. The controller parameters are updated in the beginning of the next stage of relay test using (4.11) and (4.16-4.17) of subsection 4.4.1 for some user defined values of α, g_m and ϕ_m. The process time delay is obtained from (2.37). Once the time delay, D, is obtained, the other process model parameters are estimated by solving the nonlinear equations (2.38-2.39) using the nonlinear equation solver routine of MATLAB.

Example 2.6

Let us consider a typical FOPDT order process

$$G(s) = \frac{e^{-2s}}{10s + 1}$$

The auto-tuning test is carried out in two stages and the limit cycle parameters of the second stage of relay test yield the final transfer function model of the process. The design values of $\alpha = 0.2$, $g_m = 4$ and $\phi_m = 45^0$ are used to update the controller needed for the second

stage of relay test . The limit cycle measurements, controller and process model parameters along with the estimation error index are given in Table 2.6 (a). The estimation error index is estimated using (2.16) to check the exactness of the identification method. The proposed on-line identification method (using DF analysis) discussed in subsection 2.2.1.2 gives the model parameters $K = 1$, $T = 8.89$ and $D = 2.0003$ with the estimation error index 0.0814. The identification method proposed by Li et al. [4] gives $K = 0.988$, $T = 9.02$ and $D = 2.0$ with the estimation error 0.1383. The estimation error index by the present method is 0.0271, showing excellent improvements over the identification methods using the DF analysis. As mentioned in subsection 2.2.1.2, random noise is next added to the process output during the relay tests. The estimated process model parameters and the respective estimation errors at different noise levels are tabulated in Table 2.6 (b). The noisy output signal with SNR = 20 dB and the recovered signal waveforms are given in Fig. 2.13. The tabular values show sufficiently low estimation errors by the state space based identification in the face of additive measurement noise.

Table 2.6(a) Controller, limit cycle and process model parameters for example 2.6

Stage 1	$G_c(s)$	$K_c = 0.1,\ T_I = 1,\ T_d = 0$	
	Limit cycle parameters	$T_{cr} = 3.6878, t_p = 2.0009, A = 0.1838$	
	$G_m(s)$	$K = 1.0255, T = 10.4063, D = 2.0009$	
Stage 2	$G_c(s)$	$K_c = 2.3912,\ T_I = 5.0846,\ T_d = 0.3687$	$EE = 0.0271$
	Limit cycle parameters	$T_{cr} = 3.4848, t_p = 2.0005, A = 0.2141$	
	$G_m(s)$	$K = 1.0449, T = 10.1377, D = 2.0005$	

Table 2.6(b) Estimated parameters and the errors at different noise levels for example 2.6

SNR in dB	K	Error in K	T	Error in T	D	Error in D
No noise	1.0449	-	10.1377	-	2.0005	-
30	1.0705	0.0245	10.9765	-0.0827	1.9915	0.0047
20	1.0718	0.0257	10.9822	0.0833	1.9915	0.0047
10	1.1123	0.0645	11.2345	0.1082	1.9502	0.0252

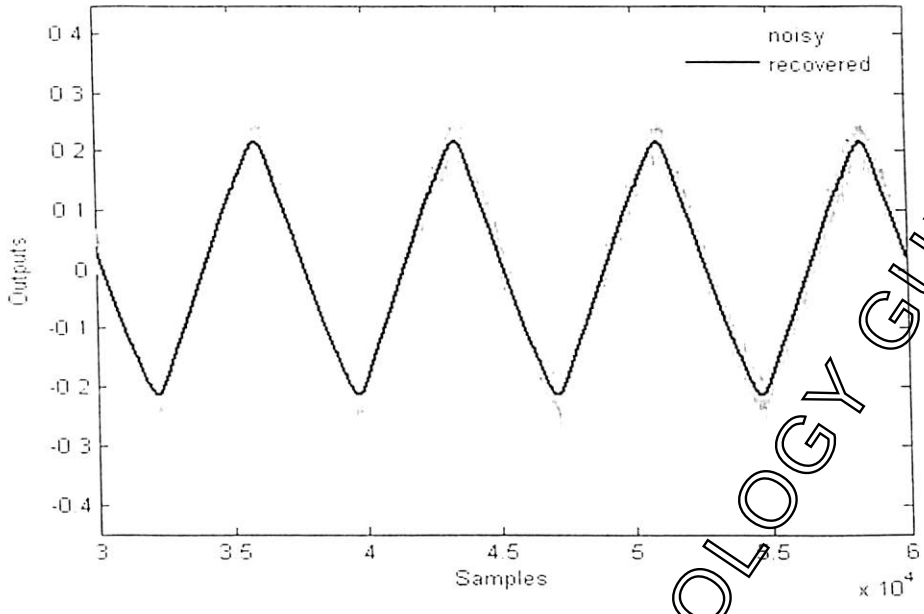

Fig. 2.13. Recovered and noisy output signal with SNR =20dB for example 2.6

Example 2.7

Consider the first order unstable process of example 2.2. Table 2.7 lists the limit cycle parameters, the controller and process model parameters. The controller required for the second stage is designed by using the design values $\alpha = 0.9$, $g_m = 5$ and $\phi_m = 45^0$. Again, the present method gives less estimation error index ($EE = 0.0382$) as compared to the describing function method (example 2.2) which resulted in $EE = 0.0406$.

Table 2.7 Controller, limit cycle and process model parameters for example 2.7

Stage 1	$G_c(s)$	$K_c = 0.1,\ T_I = 1,\ T_d = 0$	
	Limit cycle parameters	$T_{cr} = 1.5911,\ t_p = 0.5001,\ A = 0.6813$	
	$G_m(s)$	$K = 1.001,\ T = 0.9843,\ D = 0.5001$	
Stage 2	$G_c(s)$	$K_c = 2.1914,\ T_I = 4.6176,\ T_d = 0.4061$	$EE = 0.038$
	Limit cycle parameters	$T_{cr} = 0.8440, t_p = 0.5001, A = 1.1513$	
	$G_m(s)$	$K = 1.001, T = 0.9892, D = 0.5002$	

2.2.2.4 Special Case

To identify stable processes which can efficiently be represented by lower order transfer function models, a PI controller in parallel with the relay (setting $T_d = 0$ in Fig. 2.11) is suggested. The expressions for the model parameters are obtained by substituting $T_d = 0$ in (2.38) and (2.39). Several examples are given below to illustrate exactness of the identification method.

Example 2.8

This example considers the first order process of example 2.6. The controller parameters, the limit cycle measurements and the process model parameters in both the stages of relay test are given in Table 2.8. The controller required in the second stage of relay test is designed by using $g_m = 4$ and $\phi_m = 45^0$. It is observed from Table.2.8 that the maximum estimation error index is 0.0168 which is less than the estimation error index obtained in example 2.6.

Table 2.8 Controller, limit cycle and process model parameters for example 2.8

Stage 1	$G_c(s)$	$K_c = 0.1,\ T_I = 1$	
	Measured parameters	$T_{cr} = 5.6878, t_p = 2.0009, A = 0.1838$	
	$G_m(s)$	$K = 1.0255, T = 10.4063, D = 2.0009$	
Stage 2	$G_c(s)$	$K_c = 1.2216,\ T_I = 6.1779$	$EE = 0.0168$
	Measured parameters	$T_{cr} = 3.7178, t_p = 2.0009, A = 0.2107$	
	$G_m(s)$	$K = 1.0203, T = 10.1656, D = 2.0009$	

Example 2.9

The transfer function of a FOPDT process is given as

$$G(s) = \frac{e^{-0.5s}}{(0.5s+1)^4}$$

Table 2.9 shows values of the limit cycle measurements, the controller and the process model parameters for both the stages of relay test. Once again, the maximum estimation error index is found to be 0.0017. The gain and phase margin values of 3 and 60^0 are used to design the PI controller necessary for performing the second stage test.

Table 2.9 Controller, limit cycle and process model parameters for example 2.9

Stage 1	$G_c(s)$	$K_c = 0.1,\ T_I = 1$	
	Measured parameters	$T_{cr} = 0.6799, t_p = 0.3999, A = 0.4467$	
	$G_m(s)$	$K = 1.0001, T = 0.7997, D = 0.3999$	
Stage 2	$G_c(s)$	$K_c = 1.0471,\ T_I = 0.8375$	$EE = 0.0017$
	Measured parameters	$T_{cr} = 0.7503, t_p = 0.4001, A = 0.5475$	
	$G_m(s)$	$K = 1.0001, T = 0.7998, D = 0.4001$	

Example 2.10

One of the important issues in industry is the path-tracking (PT) problem of a mobile robot, which is concerned with the ability to drive it autonomously as close as possible to a previously defined reference path. This path is usually specified as either a sequence of consecutive reference points or by a set of geometrical primitives such as straight lines or arcs of circumferences. Many approaches have been tested for the PT problem using PI/PID controller and reported in the literature [26-28]. The PI/PID controller is designed based on the model of the kinematics of a mobile robot. But, the external load disturbances create problems during the path tracking. Therefore, an on-line identification of the model of the robot kinematics is required for a smooth path tracking. In this example, we use the on-line identification method discussed in subsection 2.2.2.4 for the path tracking of a mobile robot. Consider the process dynamics of a mobile robot [26]

$$G(s) = \frac{e^{-0.2s}}{s}$$

The controller, the limit cycle parameters and process model parameters are given in Table 2.10. A PI controller is designed by taking $g_m = 3.5$ and $\phi_m = 60^0$ at the beginning of the second stage of the relay test. As the dynamics of the robot is integrating in nature and the process model is first order, the estimation error is evaluated in the frequency range $[0.1\omega_{cr}\ \ \omega_{cr}]$. It is clear from Table 2.10 that the estimation error is high if the integrating model is identified as a FOPDT model. Simulation results show that the PI controller designed for the process model gives satisfactory path tracking of the mobile robot compared to some other methods reported in the literature [26-28].

Table 2.10 Controller, limit cycle and process model parameters for example 2.10

Stage 1	$G_c(s)$	$K_c = 0.1,\ T_I = 1$	
	Measured parameters	$T_{cr} = 0.4025,\ t_p = 0.2004,\ A = 0.2026$	
	$G_m(s)$	$K = 42.6134,\ T = 42.5621,\ D = 0.2004$	
Stage 2	$G_c(s)$	$K_c = 2.0877,\ T_I = 2.0899$	$EE = 0.2074$
	Measured parameters	$T_{cr} = 0.4015,\ t_p = 0.2009,\ A = 0.2531$	
	$G_m(s)$	$K = 20.8068,\ T = 20.2840,\ D = 0.2009$	

The on-line identification procedure for FOPDT processes using the exact state space analysis method has been presented in the subsection 2.2.2. The simulation examples show that the relay in parallel with the PI controller is sufficient to estimate transfer function model of a process having first order dynamics. This section highlights the complexities of the state space based exact analysis technique. The method is subjected to increased computational burden due to the set of nonlinear equations one needs to solve.

2.3 Design of Adaptive Noise Filter

Measurement noise falling into the high frequency range of the signal spectrum is a common problem that arises during the process identification. Since the identification is carried out at loop critical frequency, a low pass filter (Noise filter) that filters out the frequencies much higher than the critical frequency is inserted in the feedback path as shown in Fig. 2.14. The filter time constant is obtained adaptively from the limit cycle output as described below.

2.3.1 Estimation of Noise Filter Time Constant

Let the transfer function of the noise filter be

$$G_f(s) = \frac{1}{T_f s + 1} \tag{2.40}$$

Since the identification is carried out at the loop critical frequency (ω_{cr}), the cut-off frequency (ω_0) of the filter can be chosen as

$$\omega_0 \geq \omega_{cr} \tag{2.41}$$

In this work, ω_0 is chosen as ω_{cr}. Therefore, the expression for the filter time constant becomes

$$T_f = \frac{1}{\omega_{cr}} \tag{2.42}$$

The filter time constant T_f is updated adaptively from the limit cycle output data in the following manner.

$$T_f(n) = \frac{1}{\omega(n-1)} \tag{2.43}$$

where n and $n-1$ denote the data for the present and previous test period, respectively. The filter time constant is updated every period by using (2.43) until a stable limit cycle is obtained. Once the limit cycle is stable, the final value of T_f that satisfies (2.42) is estimated.

2.3.2 Estimation of Process Model Parameters

Fig. 2.14 shows the proposed on-line identification scheme where a relay coupled with a PID controller in the forward path and a noise filter in the feedback path are placed. The three parameters of the assumed FOPDT process model given in (2.6) are obtained using the parameters of the filtered limit cycle output signal $y'(t)$. Obviously, the noise filter helps in estimating the model parameters accurately even in the presence of measurement noise.

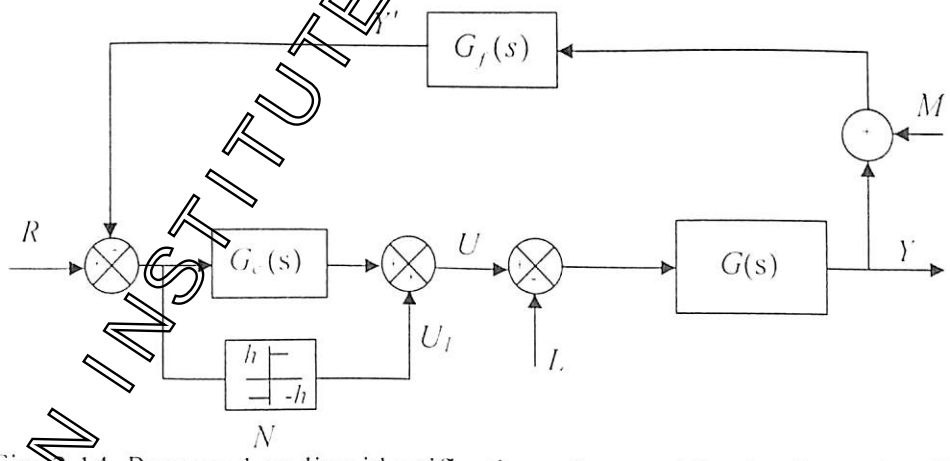

Fig. 2.14. Proposed on-line identification scheme with adaptive noise filter

The steady state gain of the process (K) is obtained during the relay test using (2.8). The procedure to obtain the other two parameters (T and D) of the process model is given below. In order to get a stable limit cycle

$$N\bar{G}_m(j\omega_{cr}) = -1 \tag{2.44}$$

where

$$\bar{G}_m(j\omega_{cr}) = \frac{G_f G_m(j\omega_{cr})}{1 + G_f G_m G_c(j\omega_{cr})} \tag{2.45}$$

Then, (2.44) becomes

$$G_f G_m(j\omega_{cr})\left[N + G_c(j\omega_{cr})\right] = -1 \tag{2.46}$$

Using (2.6), (2.7) and (2.40) in (2.46) gives

$$\frac{Ke^{j\omega_{cr}D}}{(j\omega_{cr}T_f + 1)(j\omega_{cr}T \pm 1)}(a_1 + ja_2) = -1 \tag{2.47}$$

The expressions for a_1 and a_2 are the same as given in the subsection 2.2.1.2. Equating the magnitude and phase of both sides of (2.47), one obtains

$$T = \frac{1}{\omega_{cr}}\sqrt{\frac{K^2(a_1^2 + a_2^2)}{\omega_{cr}^2 T_f^2 + 1}} - 1 \tag{2.48}$$

for both stable and unstable processes and

$$D = \frac{\pi + \tan^{-1}\left(\frac{a_2}{a_1}\right) - \tan^{-1}(\omega_{cr}T) - \tan^{-1}(\omega_{cr}T_f)}{\omega_{cr}} \tag{2.49}$$

for the stable process and

$$D = \frac{\tan^{-1}\left(\frac{a_2}{a_1}\right) + \tan^{-1}(\omega_{cr}T) - \tan^{-1}(\omega_{cr}T_f)}{\omega_{cr}} \tag{2.50}$$

for the unstable process. Therefore, the process model parameters (T and D) are obtained either from (2.48) and (2.49) or (2.48) and (2.50). Unlike the situation for a stable process, the unstable process does not always experience a limit cycle condition. Again, the noise filter in the feedback path gives a phase lag of 45^0 at the critical frequency and destabilizes the closed loop system. Hence, it is necessary to tune the initial PID controller parameters judiciously so that the fictitious process model $\bar{G}_m(s)$ given in (2.45) satisfies (2.44) and induces stable limit cycle output. The procedure to obtain the initial PID parameters is described below. Neglecting the derivative filter constant, the PID controller given in (2.7) can be written as

$$G_c(s) = K_c'\left(1 + \frac{1}{T_I' s}\right)(1 + T_d' s) \tag{2.51}$$

with the relationships

$$K_c = K_c'\left(1 + \frac{T_d'}{T_I'}\right) \tag{2.52}$$

$$T_I = T_I'\left(1 + \frac{T_d'}{T_I'}\right) \tag{2.53}$$

$$T_d = \frac{T_d'}{\left(1 + \dfrac{T_d'}{T_I'}\right)} \tag{2.54}$$

Assuming,

$$T_d' = T_I \tag{2.55}$$

and using the Taylor series expansion for the exponential term, $\bar{G}_m(s)$ can be expressed as

$$\bar{G}_m(s_n) = \frac{KT_{In}' s_n e^{-D_n s_n}}{(T_{In} s_n + 1)\left[(T_{In}' - KK_c' T_{In}' D_n)s_n^2 + (KK_c' T_{In}' - KK_c' D_n \pm T_{In}')s_n + KK_c'\right]} \tag{2.56}$$

where $D_n = \frac{D}{T}$, $s_n = Ts$, $e^{-D_n s_n} = 1 - D_n s_n$, $T_{In} = \frac{T_I}{T}$ and $T_{In}' = \frac{T_I'}{T}$. The subscript n stands for the normalization. Let

$$K_c' = \frac{1}{KD_n} \tag{2.57}$$

Substitution of (2.57) in (2.56) gives

$$\bar{G}_m(s_n) = \frac{KT_{In}' D_n s_n e^{-D_n s_n}}{(T_{In} s_n + 1)\left[(T_{In}' \pm T_{In}' D_n - D_n)s_n + 1\right]} \tag{2.58}$$

For a large value of $(T_{In}' \pm T_{In}' D_n - D_n)$, $\bar{G}_m(s_n)$ can be reduced to

$$\bar{G}_m(s_n) = \frac{K' e^{-D_n s_n}}{(T_{In} s_n + 1)} \tag{2.59}$$

where $K' = \dfrac{KT_{In}' D_n}{(T_{In}' \pm T_{In}' D_n - D_n)}$ (2.60)

It has been found from extensive simulation that the value of $(T_{In}' \pm T_{In}' D_n - D_n)$ can be

assumed as $\frac{10}{T}$ which gives

$$T'_m = \frac{10 + TD_n}{T(1 \pm D_n)} \tag{2.61}$$

It is apparent from (2.61) that a positive value of D_n ensures a limit cycle for stable processes and a value of $D_n < 1$ for unstable processes. The approximation of time delay using Taylor series expansion for unstable processes is appropriate as the normalized time delay is less than unity. In the case of a stable process with high normalized time delay, the approximation is crude. However, the overall performances due to the controller settings are satisfactory even if the normalized time delay is high.

Choice of Initial Controller

In the beginning of the relay test, the choice of controller parameters is most important as the information about the process dynamics is unknown. Poor choice of initial controller may not yield limit cycle output. Once limit cycle output is obtained, the controller parameters are updated using the expressions given in (2.55), (2.57) and (2.61). Assuming a small value of K'_c, (2.56) can be expressed as

$$\bar{G}_m(s_n) = \frac{Ke^{-D_n s_n}}{(T_m s_n + 1)(s_n \pm 1)} \tag{2.62}$$

Therefore, a positive value of D_n ensures a limit cycle for a stable process whereas for an unstable process $D_n \le 0.693 - \ln(T_m + 1)$ [40]. So, the value of the filter time constant should be less than unity to obtain limit cycle condition. From the extensive simulation studies, the initial controller parameters for the initial relay test for stable processes are suggested as $K'_c = 0.01 - 0.1$, $T'_d = T_f = \omega_{cr}$ and $T_I = 1$. The values of T'_d and T_f are updated adaptively during the relay test using (2.43). However, $K'_c = 0.01 - 0.1$, $T'_I = 1$ and $T'_d = T_f = 0.1$ are chosen for unstable processes that restricts D_n to 0.5977 so as to ensure limit cycle output. It is found from the simulation results and from (2.58) that the suggested initial setting of the controller is applicable for the processes with $KD \le 100$. For higher value of KD, the value of K'_c can further be reduced to obtain stable limit cycle.

2.3.3 Simulation Results

This subsection considers a second order stable process and an unstable process possessing one stable pole and one unstable pole to illustrate the identification method. The results are compared with the identification methods using DF given in subsection 2.2.1 which shows improved results over some recent identification methods reported in the literature. To induce the limit cycle, a relay height $h = 1$ is used in both the examples.

Example 2.11

Consider the second order stable process of example 2.1. The initial controller parameters $K_c' = 0.1$, $T_i' = 1$ and $T_d' = T_i = \omega_{cr}$ are used in the initial stage of relay test and updated before beginning of the second stage using the expressions (2.55), (2.57) and (2.61). Four cycles of the noisy signal ($y(t)$ having SNR = 20 dB) and the filtered limit cycle outputs ($y'(t)$) obtained at the end of the second stage of relay test are shown in Fig. 2.15.

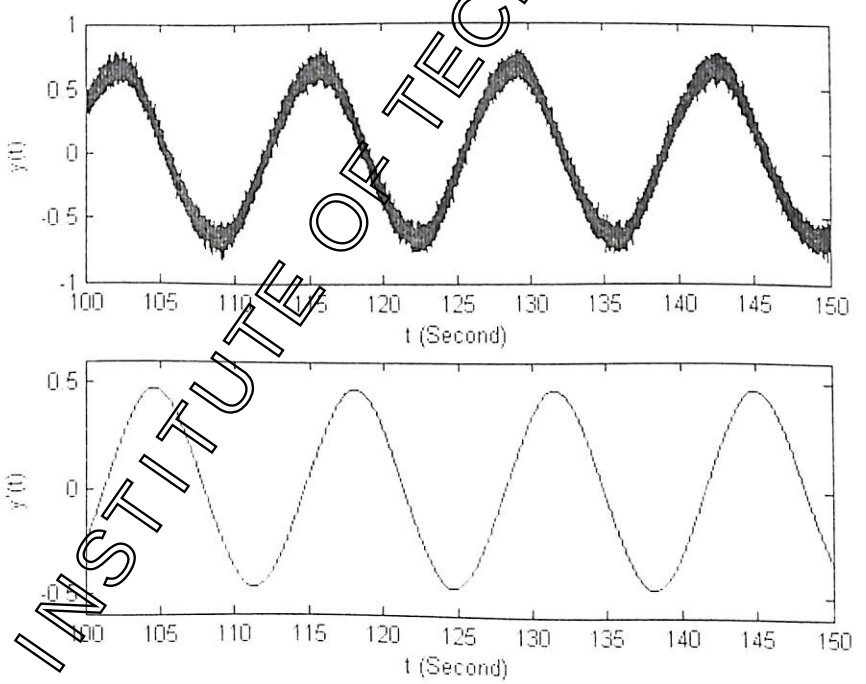

Fig. 2.15. Noisy and filtered limit cycle outputs for example 2.11

The updated values of the filter time constant are 2.9151 and 2.1403 in the first and second stage of the relay tests, respectively. Table 2.11 gives the controller and the process model parameters along with the estimation error index. The Nyquist curves of the process model and the original process are shown in Fig. 2.16 and they are very close to each other near to

-180^0, showing the accuracy of the identification method in the presence of measurement noise. The *EE* of the process model for the same process estimated in example 2.1 is 0.0368. One can conclude from the *EE* values of both the examples that the process can be approximated as a FOPDT model using the proposed on-line identification method.

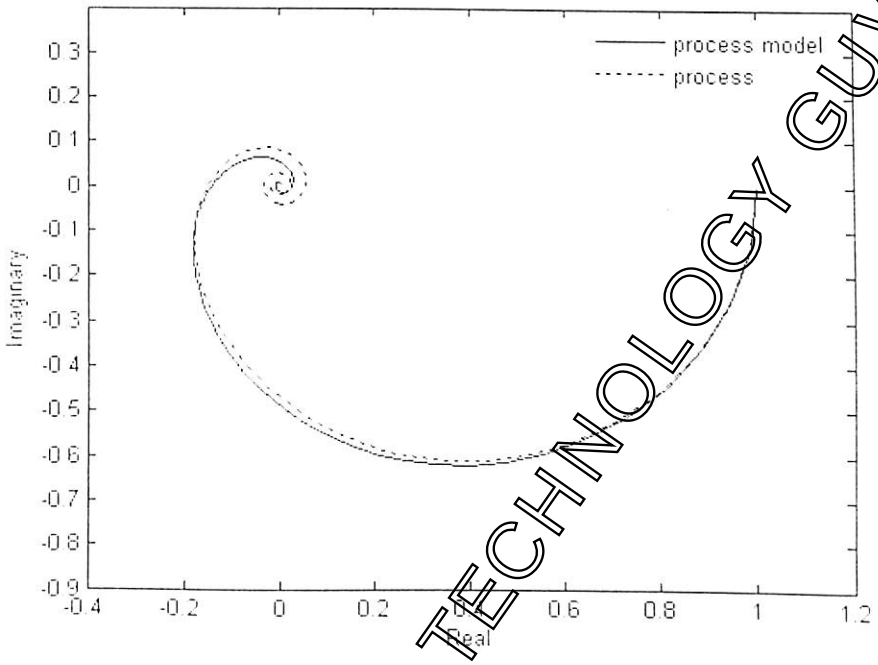

Fig. 2.16. Nyquist curves of process and process model for example 2.11

Table 2.11 Controller and process model parameters for example 2.11

Stage 1	$G_c(s)$	$K_c' = 0.1,\ T_I' = 1,\ T_d' = 2.9151$	
	$G_m(s)$	$K = 1.0,\ T = 10.3208,\ D = 2.9846$	
Stage 2	$G_c(s)$	$K_c' = 3.4580,\ T_I' = 10.0720,\ T_d' = 2.1403$	$EE = 0.0201$
	$G_m(s)$	$K = 1.0, T = 11.0299, D = 2.8951$	

Example 2.12

This example considers the unstable process of example 2.3. The controller settings used in the first stage of relay test are $K_c' = 0.1$, $T_I' = 1$ and $T_d' = T_f = 0.1$. A random noise of variance 0.0364, which results in a noisy signal of SNR = 20 dB, is injected at the limit

cycle output during the relay test. The updated value of the filter time constant in the second stage is 1.0644. The controller parameters and the estimated model parameters are given in Table 2.12. The *EE* in the second stage of relay test is 0.034 whereas the method in subsection 2.2.1 finds a process model for which *EE* = 0.2760. It shows that the proposed noise filter method obtains superior estimates of the model parameters in the presence of measurement noise.

Table 2.12 Controller and process model parameters for example 2.12

Stage 1	$G_c(s)$	$K_c' = 0.1, T_i' = 1, T_d' = 0.1$	
	$G_m(s)$	$K = 1.0, T = 2.2505, D = 1.1187$	
Stage 2	$G_c(s)$	$K_c' = 2.0116, T_i' = 22.1097, T_f' = 1.0644$	$E = 0.034$
	$G_m(s)$	$K = 1.0, T = 2.2638, D = 1.0217$	

2.4 Conclusions

In this chapter, three new on-line identification methods for stable and unstable SISO processes are proposed. In subsection 2.2.1, the describing function analysis is used for the identification method and simple expressions to estimate the FOPDT process model parameters are derived. The method estimates the model parameters with less estimation error compared to some recent identification methods available in the literature [4, 11, 13 and 14]. Further, the on-line identification structure (relay with the PID controller) is modified in subsection 2.2.1.6 (relay with the PI-PD controller) to improve accuracy of the identification method. The modified identification structure gives significantly more accurate estimates of the model parameters particularly for unstable processes.

An exact method using the state space analysis is proposed for the on-line identification of stable and unstable processes in subsection 2.2.2. The advantage of this method is that it does not require any approximation like the DF to estimate the model parameters. It is shown in simulation examples that the exact identification method gives better estimates than the describing function method. However, one has to solve a set of nonlinear equations simultaneously to identify a parametric model of the process dynamics. This limitation of the exact method compels one to use the DF based analysis.

The static load disturbance during the on-line identification is successfully removed due to the continuous action of the integral controller in the loop. Smooth limit cycle is obtained from the noisy one using the Fourier series based curve fitting method. The on-line identification method is further improved by inserting an adaptive noise filter in the feedback path. The filter time constant is updated adaptively during the relay test. The method is able to estimate the model parameters accurately even in the presence of static load disturbance and measurement noise. All the proposed techniques possess practically useful and desirable characteristics than many conventional/modified relay based identification methods available in the literature.

Chapter 3

Identification of TITO Processes

3.1 Introduction

Identification of TITO processes is more difficult due to the interaction between the loops. For easier field implementation, it is desirable to identify two SISO transfer function models of the TITO process. Many methods have been presented in the literature for the identification of TITO processes [45-58] by using a single relay or sequential operations of relays or by decentralized relay.

This chapter proposes new identification methods for TITO processes. The methods overcome some constraints of the conventional relay auto-tuning techniques available in the literature. In section 3.2, we propose an on-line identification method where a pair of relay-controller (relay in parallel with a PID controller) is used for identification of two SISO second order plus delay process transfer function models of the TITO process. A modified identification method is given in subsection 3.2.2 by introducing proportional controllers in the inner feedback loop. The proportional controller stabilizes the process and reduces the interaction between the loops. In section 3.3, we propose a new structure for the identification of a TITO process. In the structure, two preload relays are inserted in the error paths and two integral filters are used in the feedback paths. The method ensures a smooth limit cycle of the TITO process in the presence of measurement noise and loop interaction of various magnitudes. The concluding remarks to the methods are given in section 3.4.

3.2 On-line Identification of TITO Processes

3.2.1 Identification with PID Controllers

3.2.1.1 Identification Structure

Fig. 3.1 shows the on-line identification structure for a TITO process. It comprises of an ideal relay in parallel with a PID controller in the error path of each loop. The proposed relay identification method induces the limit cycle outputs Y_1 and Y_2 around the set-points R_1 and R_2, respectively. Based on the measurements of the limit cycle outputs, two SISO transfer function models of the process dynamics are identified. The relay heights h_1 and h_2 are non-zero during identification and these values are set to zero after the relay test for normal closed loop operation. The PID controllers in the loop are able to reject the effect of static load disturbance during the identification. As shown in the figure, the static load

disturbances L_1 and L_2 and random measurement noises M_1 and M_2 appear at the inputs of the process $G(s)$ and output of the sensors, respectively.

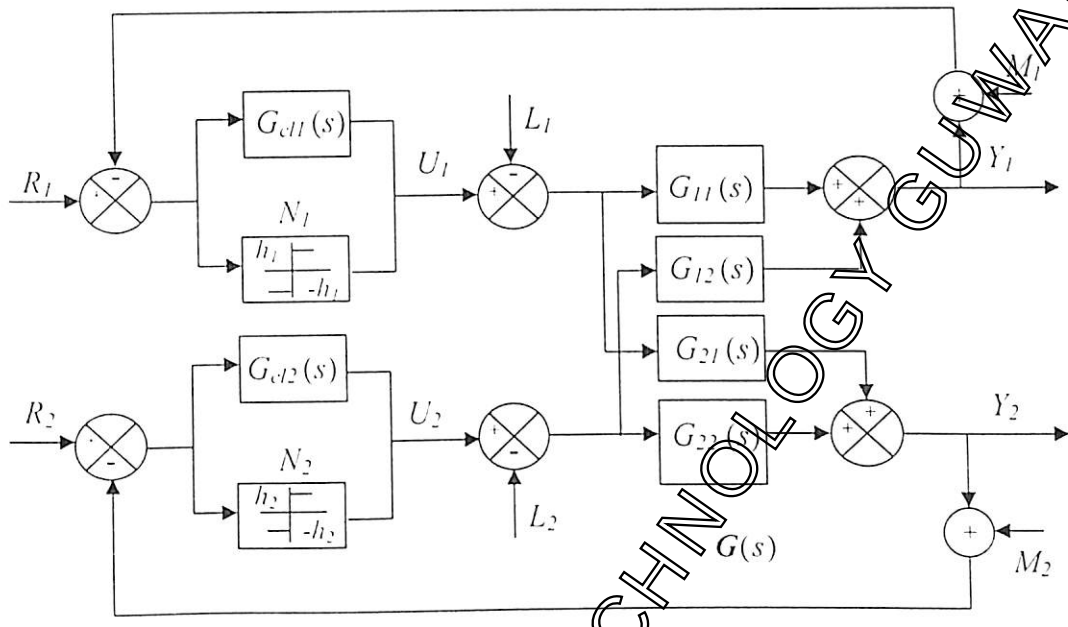

Fig. 3.1. Proposed on-line identification structure for a TITO process

3.2.1.2 Identification Procedure

The equivalent of the proposed identification structure (shown in Fig. 3.1) is redrawn in Fig. 3.2. It is apparent from Fig. 3.2 that the controllers are in the inner feedback paths and help in stabilizing the process during the identification. Attempt is made in this subsection to identify two SISO second order plus time delay transfer function models of the TITO process from the relay experiments. Let the model transfer matrix be

$$\boldsymbol{G}_m(s) = \begin{bmatrix} G_{m1}(s) & 0 \\ 0 & G_{m2}(s) \end{bmatrix} \tag{3.1}$$

which possesses the SISO transfer function models as given below

$$G_{mi}(s) = \frac{K_i e^{-D_i s}}{(T_i s + 1)^2} \qquad \forall \quad i = 1, 2 \tag{3.2}$$

where K_i, T_i and D_i are the process model parameters to be estimated.

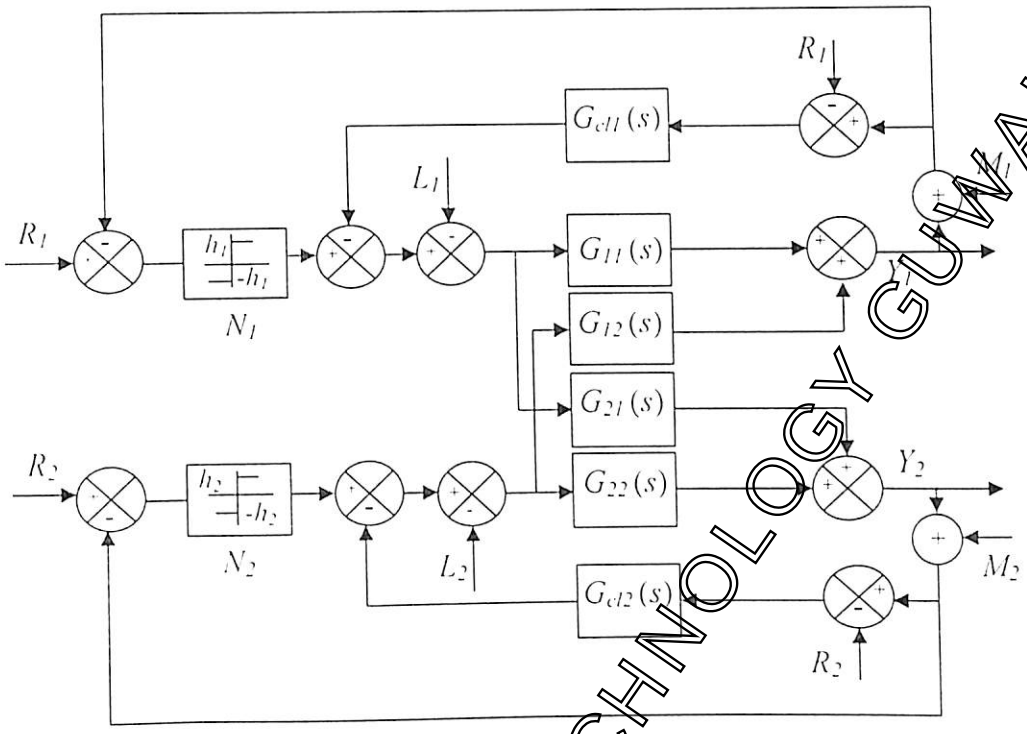

Fig. 3.2. Equivalent representation of the structure of Fig. 3.1

Let $\boldsymbol{G}_{cl}(s) = \begin{bmatrix} G_{cl1}(s) & 0 \\ 0 & G_{cl2}(s) \end{bmatrix}$ be the PID controller matrix where

$$G_{cli}(s) = K'_{ci}\left(1 + \frac{1}{T'_{Ii}s}\right)\left(1 + \frac{T'_{di}s}{1 + \beta_i T'_{di}s}\right) \qquad \forall\ i = 1, 2 \tag{3.3}$$

In the above expression, β_i is the derivative filter constant of the i^{th} loop and neglected in the following for ease in analysis. Similarly, let the describing function matrix be

$$N = \begin{bmatrix} N_1 & 0 \\ 0 & N_2 \end{bmatrix} \tag{3.4}$$

where N_1 and N_2 are the gains of the ideal relays of loop 1 and 2, respectively. The estimation of process model parameters is carried out in the following manner.

Estimation of Steady State Gains (K_i)

The philosophy of estimation of the steady state gain for the SISO process described in subsection 2.2.1.2 is extended for the TITO process. For $t > 2T_{cr}$, when steady state limit cycle is obtained around the set-points, the average values of the process inputs (u^1_{1avg} and u^1_{2avg}) and the process outputs (y^1_{1avg} and y^1_{2avg}) are measured. Then, a temporal disturbance is given to one of the set-points or reference inputs for a short duration and the corresponding average values u^2_{1avg}, u^2_{2avg}, y^2_{1avg} and y^2_{2avg} are measured. If the limit cycles occur around zero ($r_i(t) = 0$), two temporal disturbances may be given to measure the average values of the process inputs and outputs. Then, the steady state gains are estimated by the relations

$$\left.\begin{aligned} K_1 &= \frac{\chi}{(u^1_{1avg}.y^2_{2avg} - u^2_{1avg}.y^2_{1avg})(u^1_{1avg}u^2_{2avg} - u^2_{1avg}u^1_{2avg})} \\ K_2 &= \frac{\chi}{(u^2_{2avg}.y^1_{1avg} - u^1_{2avg}.y^1_{2avg})(u^1_{1avg}u^2_{2avg} - u^2_{1avg}u^1_{2avg})} \end{aligned}\right\} \qquad (3.5)$$

where

$$\chi = (u^2_{2avg}.y^1_{1avg} - u^1_{2avg}.y^1_{2avg})(u^1_{1avg}.y^2_{2avg} - u^2_{1avg}.y^2_{1avg}) - (u^1_{1avg}.y^1_{2avg} - u^2_{1avg}.y^1_{1avg})(u^2_{2avg}.y^1_{1avg} - u^1_{2avg}.y^2_{2avg}).$$

Detailed derivation of the expressions given in (3.5) is presented in Appendix A.

Estimation of Process Model Parameters

It is assumed that both the loops under limit cycle condition have the same frequencies. The peak amplitudes A_i and critical frequency ω_{cr} of the limit cycle outputs are measured. The describing function of the ideal relays for each loop is given by

$$N_i = \frac{4h_i}{\pi A_i} \qquad \forall i = 1,2 \qquad (3.6)$$

The auto-tuning test results in stable limit cycle outputs for any $h_1 / h_2 \neq 0$ when

$$N\bar{G}_m(j\omega_{cr}) = -I \qquad (3.7)$$

where

$\bar{G}_m(j\omega_{cr}) = \left[I + G_m G_{cl}(j\omega_{cr}) \right]^{-1} G_m(j\omega_{cr})$ and I is the identity matrix.

Then, (3.7) becomes

$$G_{mi}(j\omega_{cr})(N_i + G_{ch}(j\omega_{cr})) = -1 \qquad \forall\ i = 1,2 \tag{3.8}$$

Using (3.2), (3.3) and (3.6) in (3.8), we obtain

$$\frac{K_i e^{-j\omega_{cr}D_i}}{(1+j\omega_{cr}T_i)^2}(a_{1i} + a_{2i}) = -1 \tag{3.9}$$

where

$$a_{1i} = \frac{4h_i}{\pi A_i} + K'_{ci}\left(1 + \frac{T'_{di}}{T'_{Ii}}\right) \tag{3.10}$$

$$a_{2i} = K'_{ci}\left(\omega_{cr}T'_{di} - \frac{1}{\omega_{cr}T'_{Ii}}\right) \tag{3.11}$$

Equating the magnitudes of both sides of (3.9), one obtains

$$\omega_{cr}T_i = \sqrt{K_i\sqrt{a_{1i}^2 + a_{2i}^2} - 1} \tag{3.12}$$

Similarly, equating the phase angles of both sides of (3.9) gives

$$\omega_{cr}T_i = \pi + \tan^{-1}\left(\frac{a_{2i}}{a_{1i}}\right) - 2\tan^{-1}(\omega_{cr}T_i) \tag{3.13}$$

Then, (3.12-3.13) gives the expressions for the transfer function model parameters as

$$T_i = \frac{\sqrt{K_i\sqrt{a_{1i}^2 + a_{2i}^2} - 1}}{\omega_{cr}} \tag{3.14}$$

$$D_i = \frac{\pi + \tan^{-1}\left(\frac{a_{2i}}{a_{1i}}\right) - 2\tan^{-1}(\omega_{cr}T_i)}{\omega_{cr}} \tag{3.15}$$

Two stages of relay tests are performed to estimate the process model parameters. In the first stage of relay test, the initial controller parameters for each loop are set in a similar manner as given in the subsection 2.2.1.2. Once stable limit cycle outputs are obtained, two temporal SISO models of the TITO process are identified using the limit cycle parameters and the expressions given in (3.5) and (3.14-3.15). Thereafter, the controller parameters are updated using (4.44) and (4.58-4.59) of chapter 4 for specified values of loop gain margins (g_{mi}) and phase margins (ϕ_{mi}), where the subscript $i = 1, 2$. The second stage of relay test is

performed using the above controller settings to obtain the final SISO transfer function process models of the TITO process.

3.2.1.3 Load Disturbance Rejection

The output of a TITO process for a step load disturbance is

$$Y(s) = \left[I + NG(s) + G_{cl} G(s) \right]^{-1} G(s) L(s) \tag{3.16}$$

The presence of the controllers in the loops during identification results in zero steady state value of the outputs to the step load disturbance inputs implying symmetrical steady state limit cycle outputs around the set-points. This ensures accurate estimates of the limit cycle parameters under static load disturbances.

3.2.1.4 Measurement Noise

To measure the amplitudes and the loop frequency accurately, the smooth signals from the noisy outputs are recovered using the technique discussed in subsection 2.2.1.4. The best fit outputs for the TITO process can be expressed as

$$y_i'(t) = \sum_{k_i=0}^{8} \zeta_{1k_i} \cos(k_i \omega t) + \sum_{k_i=0}^{8} \zeta_{2k_i} \sin(k_i \omega t) \tag{3.17}$$

where, $y_i'(t)$ is the recovered output for the i^{th} $(i = 1,2)$ loop, ζ_{1k_i} $(k_i = 0,1,...8)$ and ζ_{2k_i} $(k_i = 0,1,...8)$ are the Fourier coefficients and ω is the frequency of the recovered outputs.

3.2.1.5 Simulation Results

To illustrate the methodology discussed in the preceding subsections, two examples are presented here. One more example is given in appendix B.1 for further illustration. The auto-tuning test starts with the choice of $K_{ci}' = 0.1$, $T_{Ii}' = 1$ and $T_{di}' = 0$. The final model of the process is obtained using the procedure given in the subsection 3.2.1.2. The effect of measurement noise on the process model parameters is investigated in simulations by introducing normally distributed random additive noise with zero mean and varying variances $M_i(0, \sigma_M^2)$, at the outputs during the relay tests thus making the oscillations noisy. The relay test is performed with $h_1 = h_2 = 1$.

Example 3.1

Consider a TITO process [62] with the transfer matrix

$$G(s) = \frac{1}{den(s)} \begin{bmatrix} (1.5s+1) & 0.2(0.75s+1) \\ 0.6(0.75s+1) & 0.8(1.2s+1) \end{bmatrix}$$

where $den(s) = (1+s)(1+2s)^2(1+0.5s)$. The gain margin of 2, phase margin of 45^0 and the derivative filter constant of 0.01 are used for both the loops to design the PID controllers for the second stage of relay test. The process model parameters along with the controller parameters are given in Table 3.1(a). Similar relay tests are performed with additive noise of various σ_N^2 such that the SNR varies from 10 dB to 30 dB. The estimated parameters (T_1, T_2, D_1 and D_2) with different noise levels and their respective errors are given in Table 3.1 (b). The recovered and noisy outputs signals with SNR = 20 dB are shown in Fig. 3.3. From the results, it is seen that the process is identified very well by the proposed method although it is subjected to high level of noise. The largest errors in the estimated parameters T_i and D_i are 0.18 % and 0.78 %, respectively which are within the acceptable limit.

Table 3.1 (a) Controller and process model parameters for example 3.1

	Loop 1	Loop 2
Stage 1	$K'_{c1} = 0.1,\ T'_{I1} = 1,\ T'_{d1} = 0$	$K'_{c2} = 0.1,\ T'_{I2} = 1,\ T'_{d2} = 0$
	$K_1 = 0.849,\ T_1 = 1.6698,\ D_1 = 0.4370$	$K_2 = 0.678,\ T_2 = 1.5343,\ D_2 = 0.4272$
Stage 2	$K'_{c1} = 3.5298,\ T'_{I1} = 1.5711,\ T'_{d1} = 1.6698$	$K'_{c2} = 3.7481,\ T'_{I2} = 1.5343,\ T'_{d2} = 1.5343$
	$K_1 = 0.849,\ T_1 = 1.8790,\ D_1 = 0.3422$	$K_2 = 0.678,\ T_2 = 1.7573,\ D_2 = 0.3271$

Table 3.1 (b) Estimated parameters and the errors at different noise levels for example 3.1

SNR in dB	Loop1				Loop2			
	T_1	Error in T_1	D_1	Error in D_1	T_2	Error in T_2	D_2	Error in D_2
No noise	1.8790	Nil	0.3422	Nil	1.7573	Nil	0.3271	Nil
30 dB	1.8792	-0.0011	0.3421	0.0002	1.7573	0.0	0.3270	0.0002
20 dB	1.8767	0.0013	0.3428	- 0.0018	1.7563	0.0005	0.3267	0.0004
10 dB	1.8759	0.0018	0.3432	-0.0029	1.7558	0.0005	0.3245	0.0078

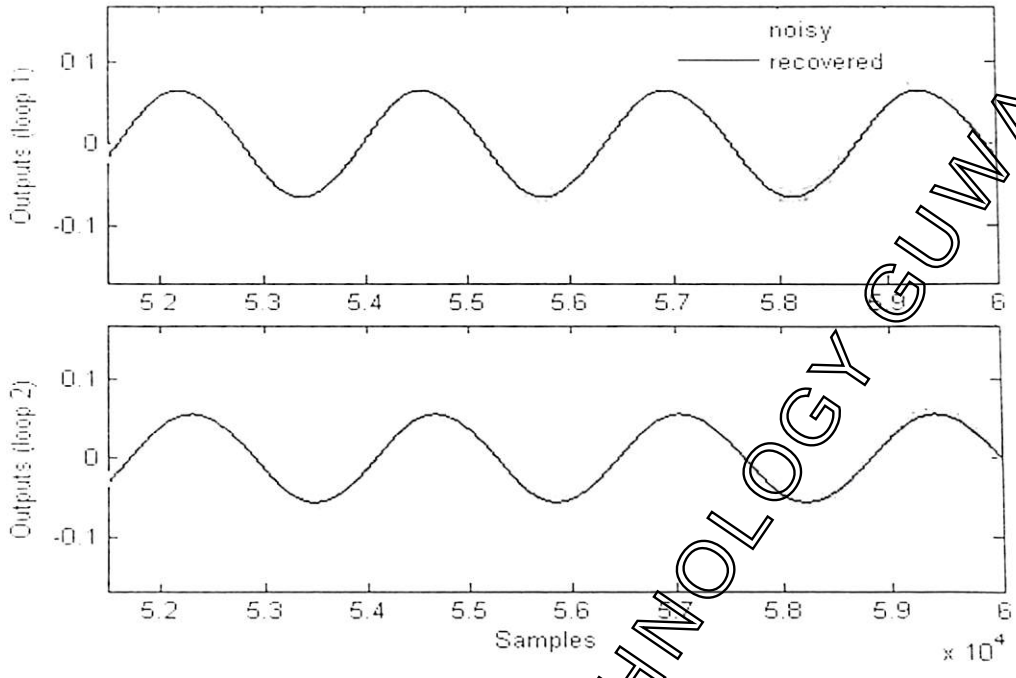

Fig. 3.3. Recovered and noisy output signals with SNR=20dB for example 3.1

Example 3.2

Let the transfer matrix of a TITO process [62] be

$$G(s) = \frac{1}{den(s)}\begin{bmatrix} 1 & \dfrac{-2.4}{1+0.5s} \\ \dfrac{0.5}{1+0.1s} & 1 \end{bmatrix}$$

where $den(s) = (1+0.1s)(1+0.2s)$. The estimated process model and the controller parameters for both the stages of relay tests are given in Table 3.2. The design values $g_m = 2$ and $\phi_m = 45^0$ are used to calculate the controller settings required for the second stage of the relay test.

Table 3.2 Controller and process model parameters for example 3.2

	Loop 1	Loop 2
Stage 1	$K'_{c1} = 0.1,\ T'_{I1} = 1,\ T'_{d1} = 0$	$K'_{c2} = 0.1,\ T'_{I2} = 1,\ T'_{d2} = 0$
	$K_1 = 2.1923,\ T_1 = 0.3342,\ D_1 = 0.0399$	$K_2 = 2.1923,\ T_2 = 0.3342,\ D_2 = 0.0399$
Stage 2	$K'_{c1} = 2.9868, T'_{I1} = 0.3348, T'_{d1} = 0.3342$	$K'_{c2} = 2.9868, T'_{I2} = 0.3348, T'_{d2} = 0.3342$
	$K_1 = 2.1925, T_1 = 0.4119, D_1 = 0.0419$	$K_2 = 2.1925,\ T_2 = 0.4119, D_2 = 0.0419$

3.2.2 Identification with PID-P Controllers

3.2.2.1 Identification Structure

Fig. 3.4 shows the identification and control structure for the TITO processes. In the structure, two PID controllers across the relays in the forward paths and two proportional controllers of gains $K_{bi}(\forall\, i=1,2)$ in the inner feedback paths are connected to induce the limit cycle outputs. The main aim of the inner feedback proportional controllers is to improve the stability margin of the open loop processes and also to reduce the interaction between the loops.

3.2.2.2 Reduction of Loop Interaction

This subsection explains how the inner feedback proportional controllers are able to reduce the loop interaction. Let the fictitious process $P(s)$ be the TITO process coupled with the inner feedback controllers. From Fig. 3.4 (setting the load disturbance and measurement noise to zero), one obtains

$$P(s)=\begin{bmatrix}1+K_{b1}G_{11}(s) & K_{b2}G_{12}(s)\\ K_{b1}G_{21}(s) & 1+K_{b2}G_{22}(s)\end{bmatrix}^{-1}\begin{bmatrix}G_{11}(s) & G_{12}(s)\\ G_{21}(s) & G_{22}(s)\end{bmatrix}=\begin{bmatrix}P_{11}(s) & P_{12}(s)\\ P_{21}(s) & P_{22}(s)\end{bmatrix} \tag{3.18}$$

where

$$P_{11}(s)=\frac{G_{11}(s)+K_{b2}\left(G_{11}G_{22}(s)-G_{12}G_{21}(s)\right)}{1+K_{b1}G_{11}(s)+K_{b2}G_{22}(s)+K_{b1}K_{b2}\left(G_{11}G_{22}(s)-G_{12}G_{21}(s)\right)} \tag{3.19}$$

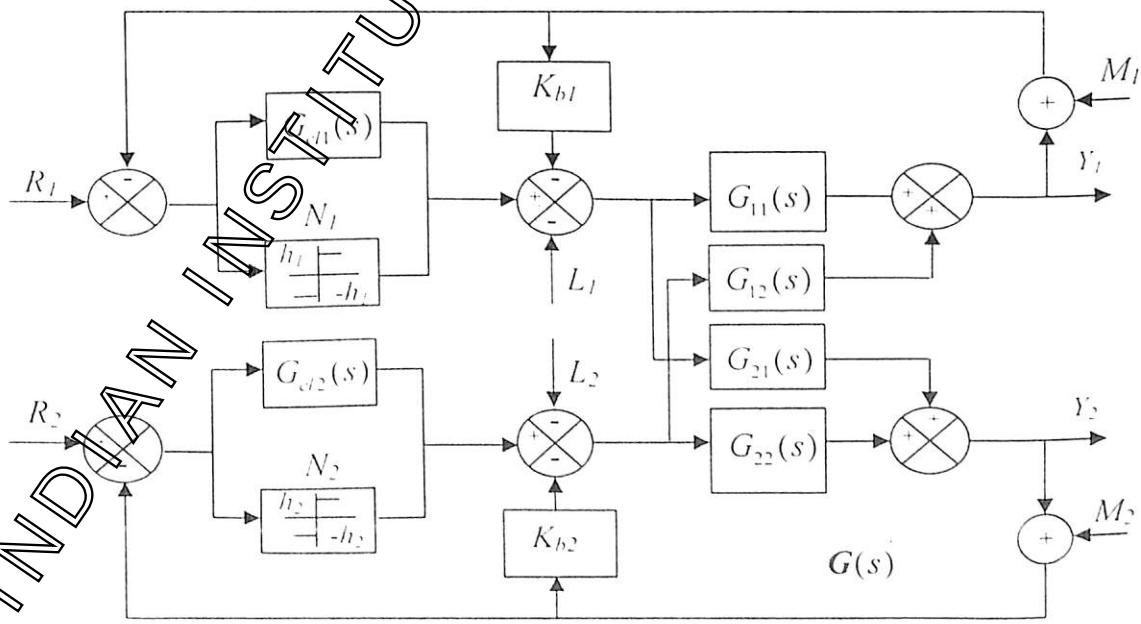

Fig. 3.4. Proposed on-line identification structure for a TITO process with PID-P controller

$$P_{12}(s) = \frac{G_{12}(s)}{1 + K_{h1}G_{11}(s) + K_{h2}G_{22}(s) + K_{h1}K_{h2}\left(G_{11}G_{22}(s) - G_{12}G_{21}(s)\right)} \tag{3.20}$$

$$P_{21}(s) = \frac{G_{21}(s)}{1 + K_{h1}G_{11}(s) + K_{h2}G_{22}(s) + K_{h1}K_{h2}\left(G_{11}G_{22}(s) - G_{12}G_{21}(s)\right)} \tag{3.21}$$

$$P_{22}(s) = \frac{G_{22}(s) + K_{h1}\left(G_{11}(s)G_{22}(s) - G_{12}G_{21}(s)\right)}{1 + K_{h1}G_{11}(s) + K_{h2}G_{22}(s) + K_{h1}K_{h2}\left(G_{11}G_{22}(s) - G_{12}G_{21}(s)\right)} \tag{3.22}$$

Assuming $K_{h1} = K_{h2} = K_h$, the above expressions at steady state are reduced to

$$P_{11}(0) = \frac{K_{11} + K_h(K_{11}K_{22} - K_{12}K_{21})}{1 + K_hK_{11} + K_hK_{22} + K_h^2(K_{11}K_{22} - K_{12}K_{21})} \tag{3.23}$$

$$P_{12}(0) = \frac{K_{12}}{1 + K_hK_{11} + K_hK_{22} + K_h^2(K_{11}K_{22} - K_{12}K_{21})} \tag{3.24}$$

$$P_{21}(0) = \frac{K_{21}}{1 + K_hK_{11} + K_hK_{22} + K_h^2(K_{11}K_{22} - K_{12}K_{21})} \tag{3.25}$$

$$P_{22}(0) = \frac{K_{22} + K_h(K_{11}K_{22} - K_{12}K_{21})}{1 + K_hK_{11} + K_hK_{22} + K_h^2(K_{11}K_{22} - K_{12}K_{21})} \tag{3.26}$$

where $K_{ij} = G_{ij}(0)$ for all $i = 1, 2$ and $j = 1, 2$. It is clear from (3.23-3.26) that for TITO processes with $(K_{11}K_{22} - K_{12}K_{21}) > 0$, the off-diagonal elements of the fictitious model $\boldsymbol{P}(s)$ at steady state are reduced if the values of K_{h1} and K_{h2} are increased which indicates that the loop interactions can be reduced at steady state. However, the identification is carried out at critical frequency. Therefore, it is required to reduce the interaction at critical frequency to increase the accuracy of the identification. Palmor et. al's technique [53] is used to verify how the proposed method helps in the reduction of the loop interactions at critical frequency. The loop interaction is measured in terms of the critical gains and steady state gains by their method. The condition for the limit cycle oscillation for a TITO process can be written as

$$\boldsymbol{P}\ \boldsymbol{N}'(j\omega_{cr})\,\boldsymbol{e} = -\boldsymbol{e} \tag{3.27}$$

where $\boldsymbol{N}'(j\omega_{cr}) = \boldsymbol{N} + \boldsymbol{G}_{cl}(j\omega_{cr})$ and $\boldsymbol{e}$ is the input error signal vector. Assuming the limit cycles of the loops are at the same frequency (ω_{cr}), the input error signal vector elements can be expressed as

$$e_1 = P_{11}N_1'(j\omega_{cr})e_1 + P_{12}N_2'(j\omega_{cr})e_2 \tag{3.28}$$

$$-e_2 = P_{21}N_1'(j\omega_{cr})e_1 + P_{22}N_2'(j\omega_{cr})e_2 \tag{3.29}$$

Setting $e = \left[A_1\cos(\omega_{cr}t) \quad A_2\cos(\omega_{cr}t+\theta)\right]^T$, where θ is the phase difference between the loops and referring [62], we can find the approximate relationship between K_{1cr} and K_{2cr} as

$$\frac{K_{1cr}}{K_{2cr}} = \frac{P_{21}(0)\dfrac{h_1}{h_2} + P_{22}(0)}{P_{11}(0) + P_{12}(0)\dfrac{h_2}{h_1}} \tag{3.30}$$

where $K_{icr} = \left|N_i + G_{ch}(j\omega_{cr})\right|$ is the critical gain of i^{th} loop. If the terms $P_{12}(0)$ and $P_{21}(0)$ are assumed to be very small for the suitable choice of K_{h1} and K_{h2}, (3.30) is reduced to

$$\frac{K_{1cr}}{K_{2cr}} \approx \frac{P_{22}(0)}{P_{11}(0)} \tag{3.31}$$

According to Palmor et al.'s method [53], the loop interaction can be measured by an error as

$$\text{Error} = \left|\varphi - \varphi_d\right| \tag{3.32}$$

where φ is defined by

$$\varphi = \tan^{-1}\left(\frac{K_{2cr}P_{22}(0)}{K_{1cr}P_{11}(0)}\right) \tag{3.33}$$

and $\varphi_d = 45^0$. Substitution of (3.31) in (3.33) gives

$$\varphi = 45^0 \tag{3.34}$$

It is clear from (3.32) and (3.34) that the loop interaction becomes zero if $P_{12}(0) = P_{21}(0) = 0$. Therefore, the loop interaction can be reduced with proper selection of the gain of the inner feedback proportional controllers. If the effect of the diagonal elements of the fictitious process $P(s)$ is reduced, the TITO process can be identified by two independent SISO transfer function models accurately.

3.2.2.3 Identification Procedure

Two SISO second order plus time delay transfer function models of the TITO process are identified from the relay test using the procedure given in subsection 3.2.1.2. The PID controller (3.3) required during the identification is assumed as

$$G_{ci}(s) = K_{ci}\left(1 + \frac{1}{T_{Ii}s} + \frac{T_{di}s}{1+\beta_i T_{di}s}\right) \tag{3.35}$$

with the relationships (neglecting β_i)

$$K_{ci} = K'_{ci}\left(1 + \frac{T'_{di}}{T'_{Ii}}\right) \tag{3.36}$$

$$T_{Ii} = T'_{Ii}\left(1 + \frac{T'_{di}}{T'_{Ii}}\right) \tag{3.37}$$

$$T_{di} = \frac{T'_{di}}{\left(1 + \frac{T'_{di}}{T'_{Ii}}\right)} \tag{3.38}$$

Then, the process model parameters (K_i, T_i and D_i) are obtained from (3.5), (3.14) and (3.15) with the modification in the expressions of a_{1i} as

$$a_{1i} = \frac{4h_i}{\pi A_i} + K_{bi} + K_{ci} \tag{3.39}$$

Once, the process model parameters are identified, the controller parameters can be obtained using the expressions given in subsection 4.5.2.

3.2.2.4 Simulation Results

Example 3.3

Consider the TITO process [63]

$$\boldsymbol{G}(s) = \begin{bmatrix} \dfrac{22.89e^{-0.2s}}{1+4.572s} & \dfrac{-11.64e^{-0.4s}}{1+1.807s} \\ \dfrac{4.689e^{-0.2s}}{1+2.174s} & \dfrac{5.80e^{-0.4s}}{1+1.801s} \end{bmatrix}$$

The time scales are in hours, so it is a quite slow process. Further, the process is not diagonally dominant. Hence, accurate SISO models of the process need to be identified for satisfactory closed loop performance. The relay test is performed with $h_1 = h_2 = 0.1$. The controller parameters are assumed as $K_{ci} = 0.01$, $T_{Ii} = 1$, $T_{di} = 0$ and $K_{bi} = 0$ in the first stage of the relay test. However, the controller parameters are updated at the beginning of

the next stage of relay test using the expressions derived in subsection 4.5.2 with the design values $g_m = 4$ and $\phi_m = 45^0$. The chosen value of $K_{b1} = 0.2$ is within the suggested range as explained in subsection 4.5.2. The controller parameters along with the estimated model parameters are given in Table 3.3(a). Table 3.3 (b) gives the critical gains, critical frequencies and the errors for different values of K_{b1} and K_{b2} with the controller settings given in Table 3.3 (a). It is apparent from the last column of Table 3.3 (b) that the error which measures the loop interaction decreases for higher values of K_{b1} and K_{b2}. The controller performances for the process model are shown in the subsection 4.5.2.

Table 3.3 (a) Controller and process model parameters for example 3.3

	Loop 1	Loop 2
Stage 1	$K_{c1} = 0.01,\ T_{I1} = 1,\ T_{d1} = 0,\ K_{b1} = 0$	$K_{c2} = 0.01,\ T_{I2} = 1,\ T_{d2} = 0,\ K_{b2} = 0$
	$K_1 = 32.274,\ T_1 = 1.2623,\ D_1 = 0.1604$	$K_2 = 8.176,\ T_2 = 0.6789,\ D_2 = 0.2864$
Stage 2	$K_{c1} = 0.3160,\ T_{I1} = 1.7596,$ $T_{d1} = 0.3567,\ K_{b1} = 0.2$	$K_{c2} = 0.2616,\ T_{I2} = 1.1428,$ $T_{d2} = 0.2756,\ K_{b2} = 0.2$
	$K_1 = 32.273,\ T_1 = 1.2690,\ D_1 = 0.2042$	$K_2 = 8.178,\ T_2 = 0.5781,\ D_2 = 0.2667$

Table 3.3(b) Critical gains, critical frequency and errors for example 3.3

K_{b1}	K_{b2}	$P_{11}(0)$	$P_{22}(0)$	K_{1cr}	K_{2cr}	ω_{cr}	$\lvert\varphi-\varphi_d\rvert$ in °
0.0	0.0	22.8900	5.8000	0.8002	0.7775	4.0459	31.1694
0.1	0.1	7.2485	4.2724	0.7324	0.6855	4.0343	16.1102
0.2	0.2	4.2411	3.0403	0.6628	0.5934	4.0255	12.3097
0.3	0.3	2.9883	2.3426	0.5882	0.5019	4.0197	11.2189

3.3 Identification of TITO Processes using P_relay

3.3.1 Identification Structure

The proposed identification structure comprises of two P_relays in the forward paths and two adaptive integral filters, $G_{lf}(s) = \frac{k_I}{s}$, in the feedback paths as shown in Fig. 3.5. The P_relay is made up of an ideal relay and a proportional gain connected in parallel to yield a robust performance [10]. The method ensures smooth limit cycle measurements of the TITO process $G(s)$ in the presence of measurement noise and loop interaction of various magnitudes.

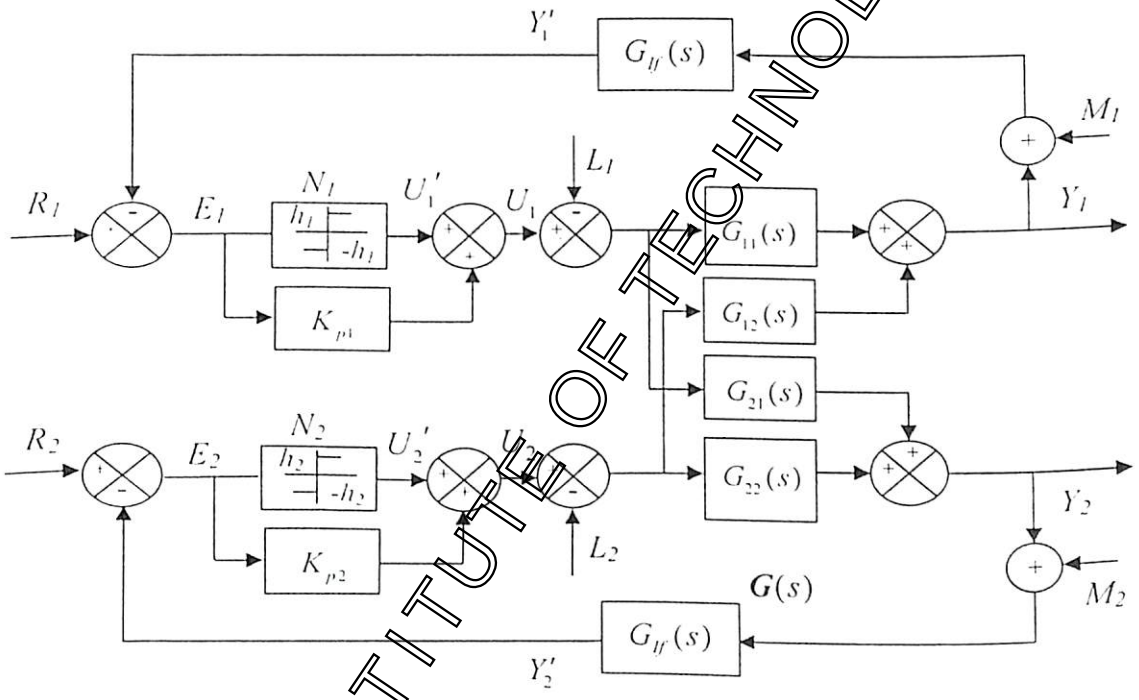

Fig. 3.5. Proposed identification structure using P_relay

The static load disturbances and random measurement noises appear at the inputs and outputs of the process, respectively. The value of the proportional gains of the P_relay is chosen using the method given in [10]. The selection procedure for the gain of the integral filter k_I is described in the following subsection. $G_{lf}(s)$ filters out noise and enables one to obtain accurate limit cycle measurements. Based on the measurements of the filtered limit cycle outputs, a two-by-two diagonal transfer function matrix model of the TITO process dynamics is identified.

3.3.2 Measurement Noise and Load Disturbance

The identification of the process is carried out at the critical frequency while the measurement noise is of high frequency. Therefore, an integral filter, which is a low pass filter, is inserted in the feedback path that attenuates the high frequency components of the noisy output signal. The cut-off frequency of the integral filter is

$$\omega_0 = \sqrt{2}\, k_I \tag{3.40}$$

As the identification is carried out at critical frequency, the cut-off frequency is chosen as

$$\omega_0 \geq \omega_{cr} \tag{3.41}$$

Therefore, it is easy to write

$$k_I = \frac{\gamma\, \omega_{cr}}{\sqrt{2}} \tag{3.42}$$

where $\gamma \geq 1$. As the bandwidth of the integral filter increases with the increased values of γ, therefore, the suggested range of γ values for noise free limit cycle outputs is $1 \leq \gamma \leq 10$. The value of k_I is updated during the relay test with the following adaptive law

$$k_I(n) = \frac{\gamma\, \omega(n-1)}{\sqrt{2}} \tag{3.43}$$

where n and $n-1$ denote the data for the present test period and the previous test period, respectively. To begin with, $k_I(0) = 0.01$ is chosen and thereafter, its value is updated every period using the formula given in (3.43).

The influence of static load disturbance during identification is overcome by using the method suggested by Majhi [25].

3.3.3 Reduction of Loop Interaction

The relay identification of TITO process exhibits a variety of behaviors under relay feedback control due to the loop interactions. With the proposed identification method, the effect of loop interactions in the TITO processes during identification is reduced. This allows one to analyze the loops independently. For ease in analysis, Fig. 3.5 can be reduced to an equivalent configuration having ideal relays in the forward path in series with the fictitious process $\boldsymbol{P}(j\omega)$ as shown in Fig. 3.6.

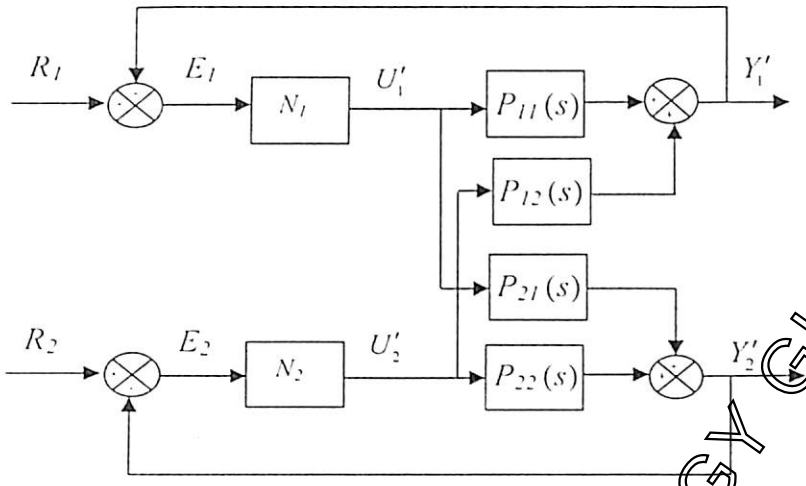

Fig. 3.6. Equivalent configuration of Fig. 3.5

If K_{pi} is the proportional gain of the P_relay of i^{th} loop, $\boldsymbol{P}(j\omega)$ can be written as

$$\boldsymbol{P}(j\omega)=\begin{bmatrix} P_{11}(j\omega) & P_{12}(j\omega) \\ P_{21}(j\omega) & P_{22}(j\omega) \end{bmatrix} \tag{3.44}$$

where

$$\left.\begin{aligned} P_{11}(j\omega)&=\frac{G_{II}G_{11}(j\omega)+K_{p2}G_{II}^2(j\omega)\left(G_{11}G_{22}(j\omega)-G_{12}G_{21}(j\omega)\right)}{1+K_{p1}G_{II}G_{11}(j\omega)+K_{p2}G_{II}G_{22}(j\omega)+K_{p1}K_{p2}G_{II}^2(j\omega)\left(G_{11}G_{22}(j\omega)-G_{12}G_{21}(j\omega)\right)}\\ P_{12}(j\omega)&=\frac{G_{II}G_{12}(j\omega)}{1+K_{p1}G_{II}G_{11}(j\omega)+K_{p2}G_{II}G_{22}(j\omega)+K_{p1}K_{p2}G_{II}^2(j\omega)\left(G_{11}G_{22}(j\omega)-G_{12}G_{21}(j\omega)\right)}\\ P_{21}(j\omega)&=\frac{G_{II}G_{21}(j\omega)}{1+K_{p1}G_{II}G_{11}(j\omega)+K_{p2}G_{II}G_{22}(j\omega)+K_{p1}K_{p2}G_{II}^2(j\omega)\left(G_{11}G_{22}(j\omega)-G_{12}G_{21}(j\omega)\right)}\\ P_{22}(j\omega)&=\frac{G_{II}G_{22}(j\omega)+K_{p1}G_{II}^2(j\omega)\left(G_{11}G_{22}(j\omega)-G_{12}G_{21}(j\omega)\right)}{1+K_{p1}G_{II}G_{11}(j\omega)+K_{p2}G_{II}G_{22}(j\omega)+K_{p1}K_{p2}G_{II}^2(j\omega)\left(G_{11}G_{22}(j\omega)-G_{12}G_{21}(j\omega)\right)} \end{aligned}\right\} \tag{3.45}$$

At very low frequency, (3.45) can be approximated as

$$\left.\begin{aligned} P_{11}(j\omega)&=\frac{1}{K_{p1}},\quad P_{22}(j\omega)=\frac{1}{K_{p2}}\\ P_{12}(j\omega)&=\frac{j\omega}{k_f}\frac{G_{12}(j\omega)}{K_{p1}K_{p2}\left(G_{11}G_{22}(j\omega)-G_{12}G_{21}(j\omega)\right)}\\ P_{21}(j\omega)&=\frac{j\omega}{k_f}\frac{G_{21}(j\omega)}{K_{p1}K_{p2}\left(G_{11}G_{22}(j\omega)-G_{12}G_{21}(j\omega)\right)} \end{aligned}\right\} \tag{3.46}$$

It is apparent from (3.46) that the diagonal elements of the fictitious process $P(j\omega)$ is decoupled completely at steady state ($\omega = 0$) and the coupling increases with the increase in ω as the magnitude of the off diagonal elements of $\boldsymbol{P}(j\omega)$ increases. However, the coupling can be reduced by the choice of a large value of k_I. It is straight forward to see that the closed loop transfer matrix can be described by

$$\boldsymbol{P}_{cl}(j\omega) = \begin{bmatrix} P_{cl11}(j\omega) & P_{cl12}(j\omega) \\ P_{cl21}(j\omega) & P_{cl22}(j\omega) \end{bmatrix} \quad \text{where}$$

$$\left.\begin{aligned} P_{cl11}(j\omega) &= \frac{N_1 P_{11}(j\omega) + N_1 N_2 \left(P_{11}P_{22}(j\omega) - P_{12}P_{21}(j\omega)\right)}{1 + N_1 P_{11}(j\omega) + N_2 P_{22}(j\omega) + N_1 N_2 \left(P_{11}P_{22}(j\omega) - P_{12}P_{21}(j\omega)\right)} \\ P_{cl12}(j\omega) &= \frac{N_2 P_{12}(j\omega)}{1 + N_1 P_{11}(j\omega) + N_2 P_{22}(j\omega) + N_1 N_2 \left(P_{11}P_{22}(j\omega) - P_{12}P_{21}(j\omega)\right)} \\ P_{cl21}(j\omega) &= \frac{N_1 P_{21}(j\omega)}{1 + N_1 P_{11}(j\omega) + N_2 P_{22}(j\omega) + N_1 N_2 \left(P_{11}P_{22}(j\omega) - P_{12}P_{21}(j\omega)\right)} \\ P_{cl22}(j\omega) &= \frac{N_2 P_{22}(j\omega) + N_1 N_2 \left(P_{11}P_{22}(j\omega) - P_{12}P_{21}(j\omega)\right)}{1 + N_1 P_{11}(j\omega) + N_2 P_{22}(j\omega) + N_1 N_2 \left(P_{11}P_{22}(j\omega) - P_{12}P_{21}(j\omega)\right)} \end{aligned}\right\} \tag{3.47}$$

For $|\omega| \le \omega_c$, when $|P_{11}P_{22}(j\omega)| >> |P_{12}P_{21}(j\omega)|$, (3.47) can be reduced to

$$\left.\begin{aligned} P_{cl11}(j\omega) &= \frac{N_1 P_{11}(j\omega)}{1 + N_1 P_{11}(j\omega)} \\ P_{cl12}(j\omega) &= \frac{N_2 P_{12}(j\omega)}{\left(1 + N_1 P_{11}(j\omega)\right)\left(1 + N_2 P_{22}(j\omega)\right)} \\ P_{cl21}(j\omega) &= \frac{N_1 P_{21}(j\omega)}{\left(1 + N_1 P_{11}(j\omega)\right)\left(1 + N_2 P_{22}(j\omega)\right)} \\ P_{cl22}(j\omega) &= \frac{N_2 P_{22}(j\omega)}{1 + N_2 P_{22}(j\omega)} \end{aligned}\right\} \tag{3.48}$$

The diagonal elements of $\boldsymbol{P}_{cl}(j\omega)$ given in (3.48) imply that one can analyze the individual loop independently and identify two SISO transfer function models of the TITO process. The off diagonal elements of $\boldsymbol{P}_{cl}(j\omega)$ give the magnitude of interactions due to the identification of the two SISO transfer function models. The interaction magnitudes can be reduced by choosing a large k_I.

3.3.4 Estimation of Process Model Parameters

In this subsection, two second order transfer function models of the TITO processes are estimated based on the limit cycles data. The process model transfer matrix (3.1) is identified in the following manner.

Estimation of Steady State Gains (K_i)

For $t > 2T_{cr}$ when steady state limit cycle is obtained around the set-points, the average values of the process inputs in conjunction with the integral filter ($\overline{u}^1_{1avg}$ and $\overline{u}^1_{2avg}$) and the filtered sensor outputs (y'^1_{1avg} and y'^1_{2avg}) are measured. Then, a temporal disturbance is given to one of the set-point or reference input for a short period and the respective average values $\overline{u}^2_{1avg}$, $\overline{u}^2_{2avg}$, y'^2_{1avg} and y'^2_{2avg} are measured. If the limit cycles occur around zero ($r_i(t) = 0$), two temporal disturbance may be given to measure the average values of the process inputs and outputs. Then the steady state gains are estimated as

$$\left.\begin{aligned} K_1 &= \frac{\overline{\chi}}{(\overline{u}^1_{1avg}.y'^2_{2avg} - \overline{u}^2_{1avg}.y'^2_{1avg})(\overline{u}^1_{1avg}\overline{u}^2_{2avg} - \overline{u}^2_{1avg}\overline{u}^1_{2avg})} \\ K_2 &= \frac{\overline{\chi}}{(\overline{u}^2_{2avg}.y'^1_{1avg} - \overline{u}^1_{2avg}.y'^1_{2avg})(\overline{u}^1_{1avg}\overline{u}^2_{2avg} - \overline{u}^2_{1avg}\overline{u}^1_{2avg})} \end{aligned}\right\} \quad (3.49)$$

where

$$\overline{\chi} = (\overline{u}^2_{2avg}.y'^1_{1avg} - \overline{u}^1_{2avg}.y'^1_{2avg})(\overline{u}^1_{1avg}.y'^2_{2avg} - \overline{u}^2_{1avg}.y'^2_{1avg}) - (\overline{u}^1_{1avg}.y'^1_{2avg} - \overline{u}^2_{1avg}.y'^1_{1avg})(\overline{u}^2_{2avg}.y'^1_{1avg} - \overline{u}^1_{2avg}.y'^2_{2avg}).$$

The detailed derivation of the expressions given in (3.49) is given in Appendix B.

Estimation of T_i and D_i

From the measurement of A_i and ω_{cr} of the limit cycle output signals, T_i and D_i of the process models can be estimated for any $h_1 / h_2 \neq 0$. Two SISO models can be identified independently from the loop limit cycle outputs as explained in subsection 3.3.3. Looking at the expressions given in (3.44-3.45) and (3.48), the equivalent SISO models of the diagonal elements of $\boldsymbol{P}(j\omega)$ can be assumed as

$$\overline{P}_{ii}(j\omega) = \frac{G_{mi}G_{ii}(j\omega)}{1 + K_{ij}G_{mi}G_{ij}(j\omega)} \quad \forall\ i = 1, 2 \quad (3.50)$$

where, G_{mi} are the SISO models of the TITO process as given in (3.2). Then, the diagonal elements of the closed loop transfer function $\boldsymbol{P}_{cl}(j\omega)$ can be written as

$$\bar{P}_{cli}(j\omega) = \frac{N_i G_{mi} G_{Ii}(j\omega)}{1 + (N_i + K_{pi}) G_{mi} G_{Ii}(j\omega)} \quad \forall\ i = 1, 2 \tag{3.51}$$

In order for a periodic solution to correspond to stable limit cycles

$$G_{mi} G_{Ii}(j\omega_{cr}) \{ N_i + K_{pi} \} = -1 \tag{3.52}$$

Using (3.2) in (3.52), one obtains

$$\frac{K_I K_{cri} e^{-j\left(\frac{\pi}{2} + \omega_{cr} D_i\right)}}{(j\omega_{cr} T_i + 1)^2} = -1 \tag{3.53}$$

where $K_{cri} = (N_i + K_{pi}) k_I / \omega_{cr}$. Equating the magnitude and phase on both sides of (3.53), it is easy to obtain

$$\left.\begin{aligned} T_i &= \frac{\sqrt{K_I K_{cri} - 1}}{\omega_{cr}} \\ D_i &= \frac{\frac{\pi}{2} - 2\tan^{-1}(\omega_{cr} T_i)}{\omega_{cr}} \end{aligned}\right\} \tag{3.54}$$

Thus, the TITO process dynamics is identified by a diagonal transfer function matrix.

3.4.5 Simulation Results

Two examples are considered in this subsection to illustrate the proposed identification method. Also, the method proposed by Palmor et al. [53] has been considered for comparison study. The critical gains and the critical frequency estimated by Palmor et al.'s method are at negligible loop interaction. Hence, a diagonal process model is identified by the use of the critical gain and the critical frequency for comparison study. The decoupler obtained by Wang et al.'s method [51] is used to decouple the process assuming that the full matrix transfer function model of the process dynamic is known or identified accurately. $\gamma = 1$ is chosen to obtain update value of k_I during the identification. The value of the proportional gains of the P_relay is chosen as $0.3/k_i$ in both the examples. The effect of measurement noise (M_i) on the process model parameters is investigated by introducing

normally distributed random additive noise with zero mean and varying variance, σ_M^2 at the sensors output during the relay test thus making the limit cycles noisy.

Example 3.4

Consider the Wood-Berry binary distillation column process [53] with transfer matrix

$$G(s)=\begin{bmatrix} \dfrac{12.8e^{-s}}{(16.7s+1)} & \dfrac{-18.9e^{-3s}}{(21s+1)} \\ \dfrac{6.6e^{-7s}}{(10.9s+1)} & \dfrac{-19.4e^{-s}}{(14.4s+1)} \end{bmatrix}$$

It is a typical TITO process with strong interaction and significant time delays. The relay test starts with the parameters $h_1=0.3$, $h_2=-0.3$ and $k_I=0.01$. The height of relay in the second loop is negative because $G_{22}(0)$ is negative. With the help of (3.43), the value of k_I is updated as 0.0912. The modified relay test gives $|P_{11}P_{22}(j\omega_{cr})|=672$ and $|P_{12}P_{21}(j\omega_{cr})|=351$. Hence two SISO transfer function models of the TITO process can be identified using the proposed method. Random noise M_1 and M_2 having variances $\sigma_{M1}^2=0.495$ and $\sigma_{M2}^2=0.641$ respectively, are added to the sensors output during the relay test to make the limit cycle outputs noisy. The noisy limit cycle outputs and the denoised limit cycle outputs (at the integral filter output terminals) resulting from the test are shown in Fig. 3.7. The shape of the noisy and denoised outputs is different because of the integral filters in the feedback paths. Using (3.49), the steady state gains $K_1=6.32$ and $K_2=-9.61$ are estimated during the relay test. The process model parameters T_1, T_2, D_1 and D_2 are estimated from the denoised limit cycle outputs. The identified process transfer function matrix is

$$G_m(s)\big|_{\omega_{cr}=1.0472}=\begin{bmatrix} \dfrac{6.32e^{-3.0833s}}{(1+5.1522s)^2} & 0 \\ 0 & \dfrac{-9.61e^{-5.0000s}}{(1+3.8694s)^2} \end{bmatrix}$$

Using the critical gains and critical frequency estimated by Palmor et al.'s method, the process is identified as

$$G_m(s)\big|_{\text{Palmor et al.}} = \begin{bmatrix} \dfrac{6.32e^{-2.7496s}}{(1+2.5444s)^2} & 0 \\ 0 & \dfrac{-9.61e^{-2.7768s}}{(1+2.5098s)^2} \end{bmatrix}$$

The decoupler obtained by Wang et al.'s method gives

$$G_m(s)\big|_{\text{Wang et al.}} = \begin{bmatrix} \dfrac{12.8e^{-s}}{(16.7s+1)} - \dfrac{6.43(14.4s+1)e^{-7s}}{(10.9s+1)(21s+1)} & 0 \\ 0 & \dfrac{-19.4e^{-s}}{(14.4s+1)} + \dfrac{9.745(16.7s+1)e^{-9s}}{(10.9s+1)(21s+1)} \end{bmatrix}$$

Using the third order Pade approximation for time delay, the Nyquist curves of the diagonal elements are shown in Fig. 3.8. The Nyquist curves of the process models obtained by the proposed method, Palmor et al.'s method and Wang et al.'s method are shown in Fig. 3.8 for comparison study. It is clear from Fig. 3.8 that the Nyquist curves of the process model by the proposed identification method is very close to the Nyquist curves of the process model obtained by using Wang et al.'s decoupler, thereby, indicating the accuracy of the proposed identification method. The frequency responses of the diagonal elements of $P(j\omega)$ upto ω_{cr} for $\gamma = 1, 2, 3, 4$ and 5 are given in Fig. 3.9 to evaluate the magnitude of the loop interaction. The maximum interaction at the critical frequency is 24.82 which decreases further with higher values of γ.

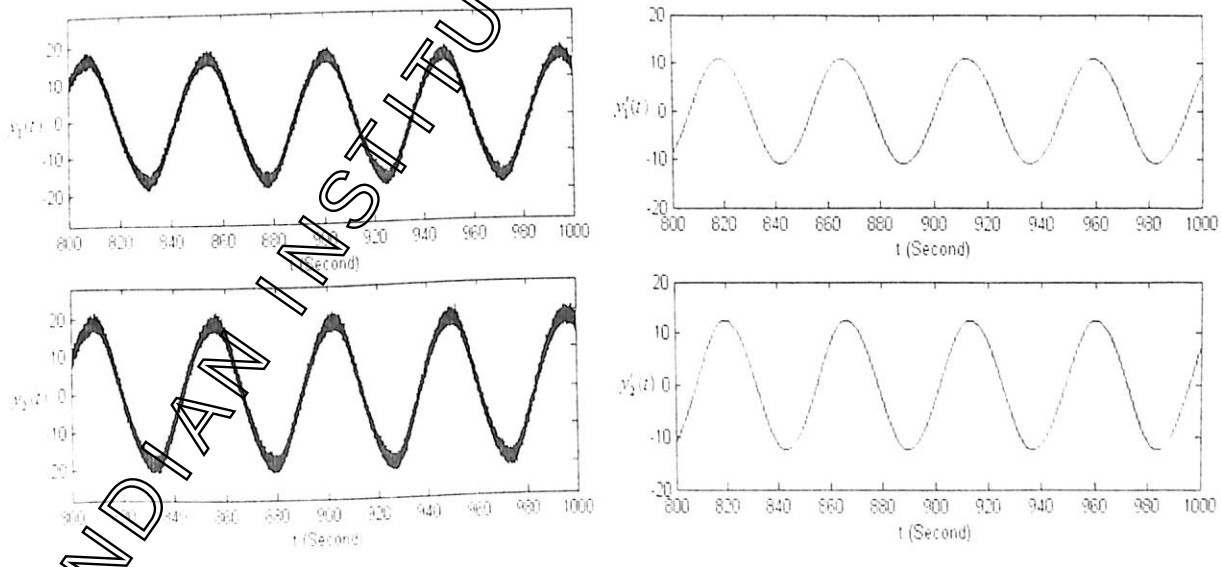

Fig. 3.7. Noisy and filtered limit cycle outputs for example 3.4

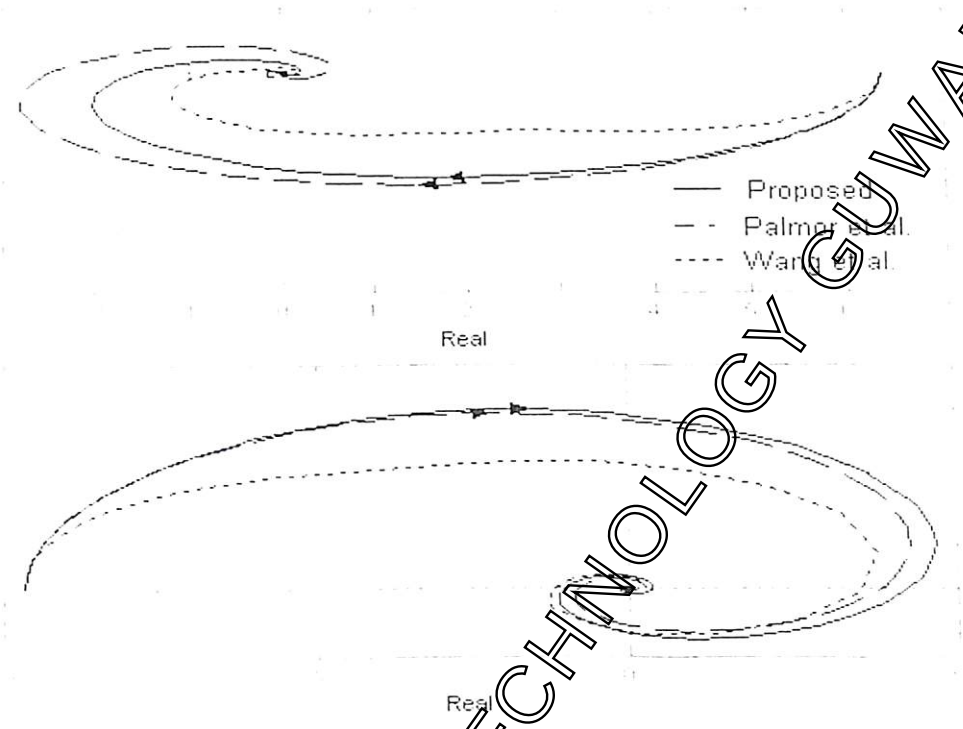

Fig. 3.8. Nyquist curves of process models for example 3.4

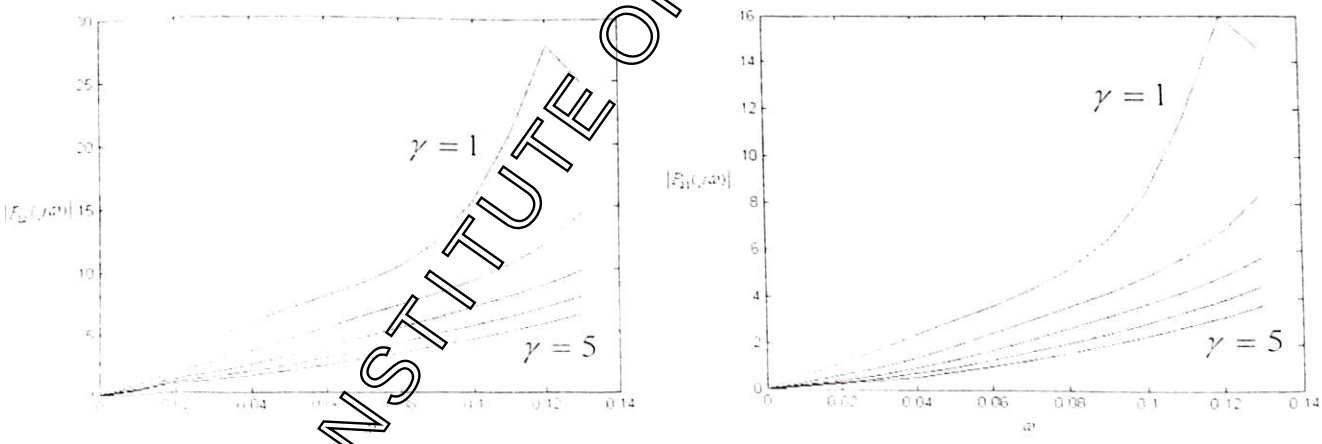

Fig. 3.9. Frequency responses of the diagonal elements of $\boldsymbol{P}(j\omega)$ for example 3.4

Example 3.5

Consider the model of methanol-ethanol distillation column [53] which has large interactions between the loops. The transfer matrix of the process is given as

$$G(s)=\begin{bmatrix}\dfrac{0.471e^{-s}}{(30.7s+1)^2} & \dfrac{0.495e^{-2s}}{(28.5s+1)^2}\\ \dfrac{0.749e^{-1.7s}}{(57s+1)^2} & \dfrac{-0.832e^{-s}}{(50.5s+1)^2}\end{bmatrix}$$

The relay test starts with $h_1=0.5$, $h_2=-0.5$ and $k_I=0.01$. However, k_I is updated as 0.00874 during the relay test. The output signals are corrupted with the addition of $M_1(0,\sigma_M^2=0.495\times10^{-3})$ and $M_2(0,\sigma_M^2=0.1448\times10^{-2})$ during the relay test. The noisy and denoised limit cycle outputs are shown in Fig. 3.10. The steady state gains K_1 and K_2 are estimated as 0.9167 and -1.6193, respectively.

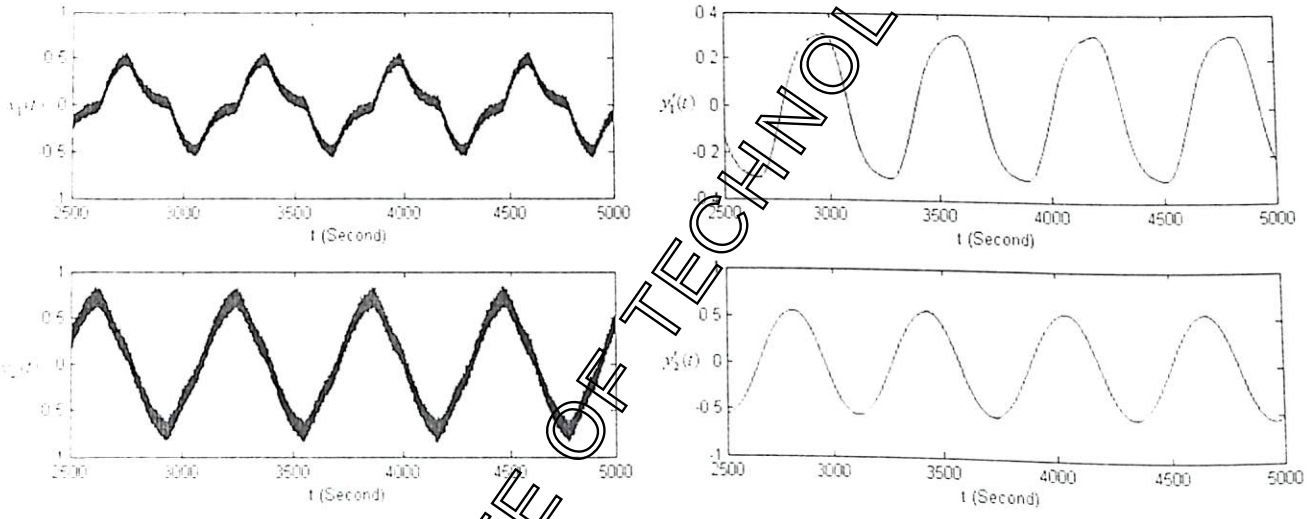

Fig. 3.10. Noisy and filtered limit cycle outputs for example 3.5

Measurements from the denoised limit cycle outputs results in the process dynamic model

$$G_m(s)\big|_{\text{Proposed}}=\begin{bmatrix}\dfrac{0.9167e^{-14.6173s}}{(1+84.8506s)^2} & 0\\ 0 & \dfrac{-1.6193e^{-11.2549s}}{(1+87.8339s)^2}\end{bmatrix}$$

The critical gains and critical frequency obtained by Palmor et al.'s method give

$$G_m(s)\big|_{\text{Palmor et al.}}=\begin{bmatrix}\dfrac{0.9167e^{-9.3521s}}{(1+52.3138s)^2} & 0\\ 0 & \dfrac{-1.6193e^{-9.2713s}}{(1+52.7973s)^2}\end{bmatrix}$$

The diagonal elements of the process model by using Wang et al.'s decoupler are given as

$$G_m(s)\big|_{\text{Wang et al}} = \begin{bmatrix} \dfrac{0.471e^{-s}}{(30.7s+1)^2} + \dfrac{0.4456(50.5s+1)^2 e^{-2.7s}}{(57s+1)^2(28.5s+1)^2} & 0 \\ 0 & \dfrac{-0.832e^{-s}}{(50.5s+1)^2} - \dfrac{0.7872(30.7s+1)^2 e^{-2.7s}}{(57s+1)^2(28.5s+1)^2} \end{bmatrix}$$

Third order Pade approximation is used for the time delays associated with the process models. The Nyquist curves of the diagonal elements obtained after decoupling, that obtained by the proposed method and Palmor et al.'s critical point estimation method are given in Fig. 3.11.

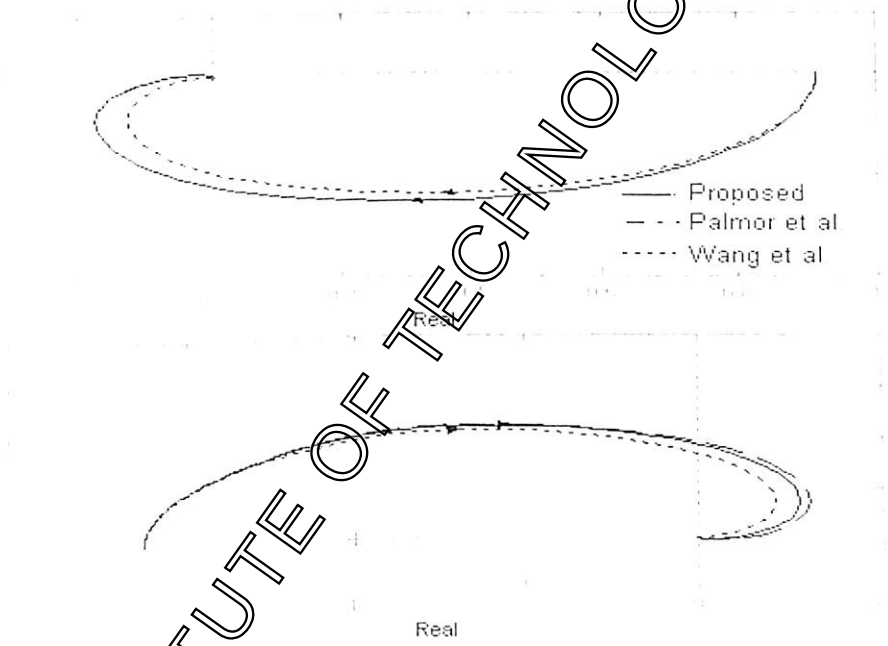

Fig. 3.11. Nyquist curves of process models for example 3.5

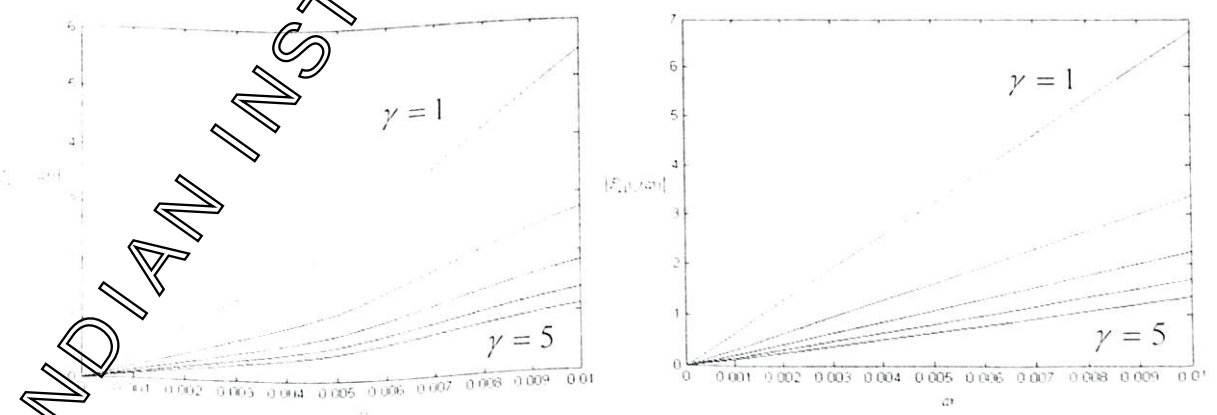

Fig. 3.12. Frequency responses of the diagonal elements of $P(j\omega)$ for example 3.5

It is observed from Fig. 3.11 that the Nyquist curve of the proposed process model once again tracks the decoupled process more accurately in comparison to Palmor et al.'s method. The frequency responses of the diagonal elements of $P(j\omega)$ upto ω_{γ} for $\gamma = 1, 2, 3, 4$ and 5 are given in Fig. 3.12 which shows a maximum interaction of value 6.62 at the critical frequency.

3.4 Conclusions

A relay based on-line identification method for the TITO processes is presented in the subsection 3.2.1. The proposed method requires no prior knowledge of the process and can identify equivalent second order plus delay SISO transfer function models of the process in the presence of load disturbance and measurement noise. A modification of the identification method is given in the subsection 3.2.2 by inserting proportional controllers in the inner feedback loops. The proportional controllers stabilize the process and reduce the loop interaction at critical frequency thereby increasing the accuracy of the process model. A P_relay based identification method is proposed in section 3.3 for the identification of diagonal transfer function models of the TITO process from a single relay test in the presence of large loop interaction and measurement noise. The novelty of the proposed approach is that it successfully reduces the loop interactions and can cope with the presence of measurement noise during the process identification. Most importantly, the steady state gains of the transfer function models are estimated in a simple manner.

Chapter 4

Model Based Controller Design

4.1 Introduction

Conventional PID controllers are still used extensively in industry in spite of the development of many control techniques owing to their simplicity and robustness. Several methods are available in the literature for controlling of single input single output processes [23-44] and two input two output processes [59-69]. However, the controller design based on the gain and phase margins criteria are found to be robust. The idea of controller design for SISO and TITO processes based on loop phase and gain margin was proposed in 1995 [31] and in 1997 [59], respectively. In this chapter, the phase and gain margin criteria is used to design the SISO controllers for the identified transfer function models of SISO and TITO processes.

Different controller configurations of a feedback loop control system are given in section 4.2. Section 4.3 gives some ideas of the performance description of a control system. In Subsection 4.4.1, we use the loop phase and gain margin philosophy to obtain the expressions for the PID controller parameters for both the stable and unstable FOPDT processes. The equations for the controller settings are simple in terms of the model parameters. However, the PID controller gives excessive overshoot, particularly for servo problem. To minimize the overshoot, two degree of freedom controllers [40-44] are used. In subsection 4.4.2, we use the two-degree-of-freedom PI-PD configuration where the PD controller is used to stabilize the process and the PI controller for overall performance improvement. The SISO controller tuning formulae are extended for the decentralized controller design of TITO processes in section 4.5 followed by conclusions in section 4.6.

4.2 Controller Configurations

The basic control system can be represented by the block diagram shown in Fig. 4.1. In the figure, U and Y represent the control signal and the controlled variable, respectively. The design objective of the basic control system involves the determination of the control signal over the prescribed time interval so that design objectives are satisfied. Many of the conventional design methods for control systems rely on the fixed design configurations. The designer decides the basic configuration of the overall system and the place where the controller is to be positioned. Thereafter, the parameters of the controller are designed based

on the process dynamics. The commonly used system configurations with controller compensation are described briefly as follows.

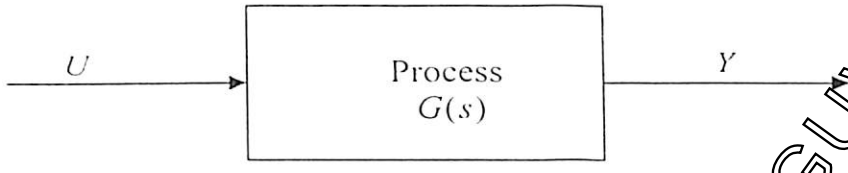

Fig. 4.1. Basic control system

Series Compensation

Fig. 4.2 shows the most commonly used system configuration. In the configuration, the controller is placed in series with the process in the forward path. PI, PID, phase lead and lag type controllers are usually used with this series compensation configuration.

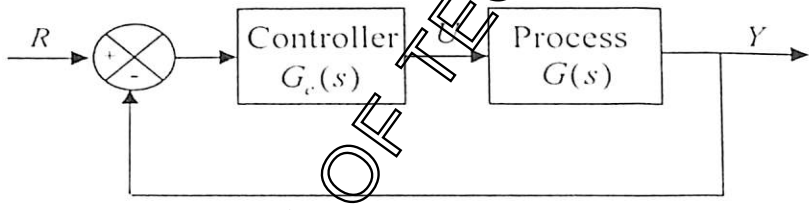

Fig. 4.2. Series compensation

Feedback Compensation

The controller is placed in the feedback path as shown in Fig. 4.3 and the scheme is called feedback compensation. A phase lead type controller can be used with this configuration.

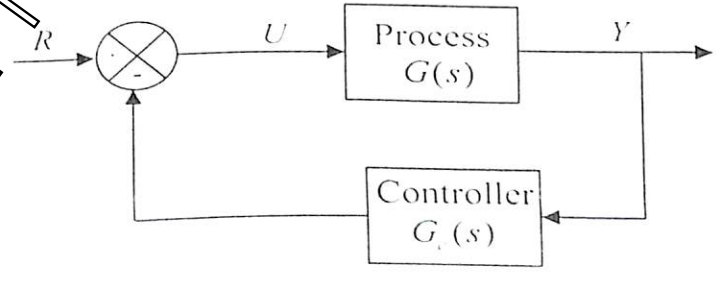

Fig. 4.3. Feedback compensation

Series-Feedback Compensation

Fig. 4.4 shows the series-feedback configuration for which series and feedback controllers are used. The feedback controller is placed in the inner feedback path and the series controller is connected in series with the process in the forward path. PI-D, PID-P and PI-PD controllers are the best examples for this configuration.

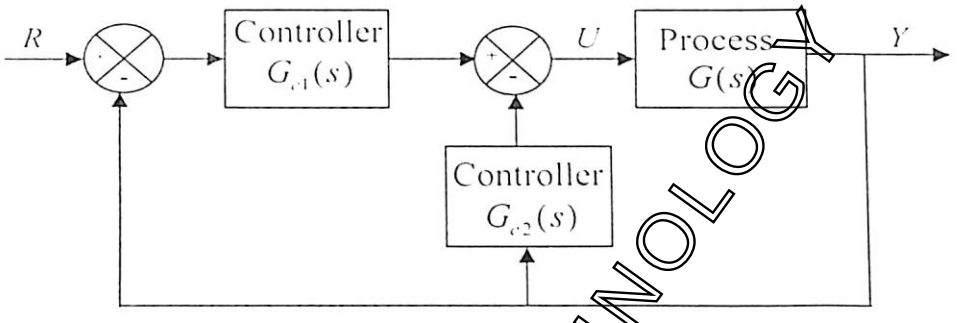

Fig. 4.4. Series-feedback compensation

Series Compensation with the set-point filter

In this compensation, controllers are placed in the reference path and in the forward path in series with the process as shown in Fig. 4.5. The reference path controller ($G_{c1}(s)$) does not affect the roots of the characteristic equation of the system. This is also called set-point weighted compensation. Any of PI, PID, phase lead and lag compensators can be used in this scheme.

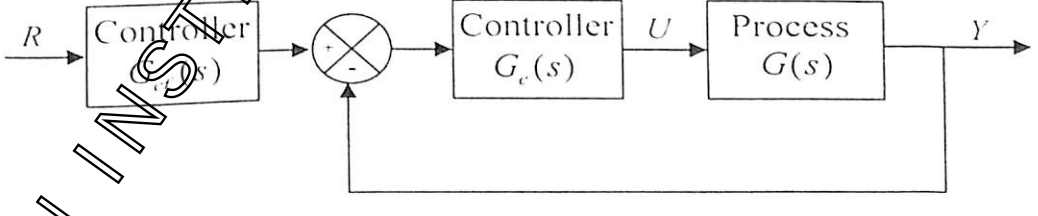

Fig. 4.5. Series compensation with the set-point filter

The compensation schemes shown in Figs. 4.2 and 4.3 have one degree of freedom in that there is only one controller in each system, even though the controller may have more than one parameter that can be varied. The disadvantage of the one degree of freedom controller

is that the performance criteria that can be realized are limited. For example, if a system is to be designed to achieve a certain amount of relative stability, it may have poor sensitivity to parameter variations. Again, if the roots of the characteristic equation are selected to provide a certain amount of relative damping, the maximum overshoot of step response may still be excessive, owing to the zeros of the closed loop transfer function [70]. The compensation schemes shown in Figs. 4.4 and 4.5 have two degrees of freedom.

4.3 Performance Description of a Control System

To analyze and design a control system, the required performance of the control system must be defined and measured. Then the system parameters are adjusted to provide the desired response based on the required performance of the control system. As the control systems are inherently dynamic, their performance is often specified in terms of their step response. The transient response is the response that disappears with time and the steady state response is that which exists at time $t \to \infty$. The performance of the system can be readily improved by inserting a controller in a suitable location within the structure of the system. Since the controller design is directly related to the desired performance of the control system, a brief description of the time and frequency performance measure is given below.

Time domain performance measure

The time domain performance is normally obtained from the response of the process to a test signal. The standard test input signals are step input, ramp input, pulse input and sinusoidal input. In this section, the most commonly used step input is considered for performance measure because it yields very useful information about the process dynamics. The step response of a typical under damped closed loop system is shown in Fig. 4.6. The time domain performance measures of a closed loop system are usually given in terms of maximum overshoot (os) which occurs at peak time (t_p), settling time (t_s), rise time (t_r) and steady state error (e_{ss}). These five quantities give a direct measure of the behavior of a control system to a unit step input. In practice, the system output is usually required to follow the input as closely as possible which ideally means zero steady state error and small rise time, settling time and percentage of overshoot.

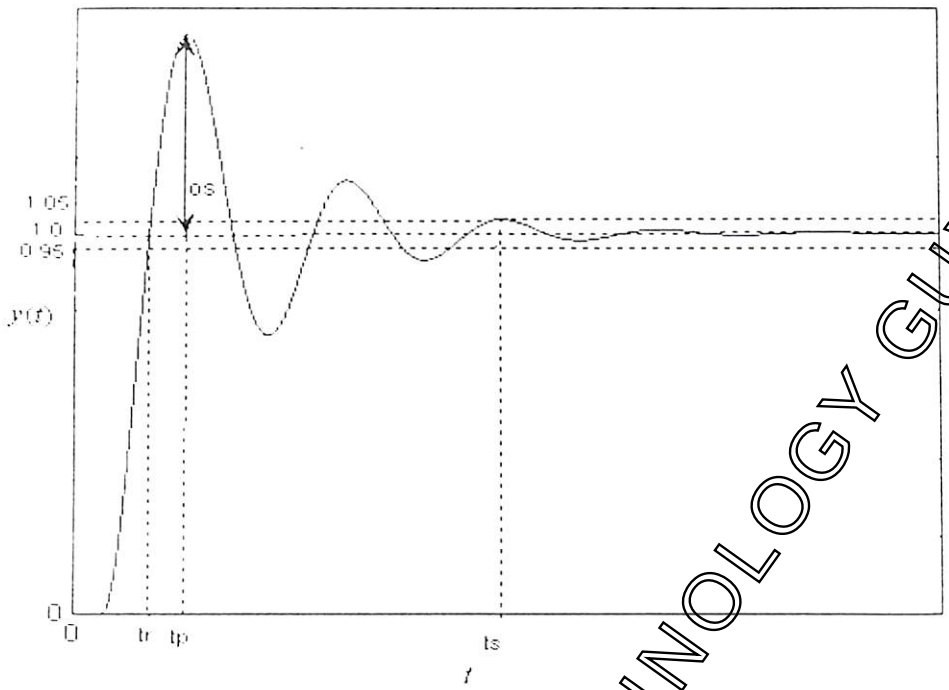

Fig. 4.6. A typical closed loop output response to step input

Frequency domain performance measure

A very practical and important alternative approach for the analysis and design of a system in the time domain is the frequency response method. The frequency response of a system indicates the magnitude and phase relationship between the sinusoidal input and the steady state output of the process. In steady state, the sinusoidal input to a linear process generates sinusoidal response of the same frequency as the input signal, but with different amplitude and phase. Fig. 4.7 illustrates a typical frequency response gain and phase characteristic of a process. In the design of linear control system using frequency domain method, the performance of a system can be identified using the appropriate performance measure such as the phase margin (ϕ_m), gain margin (g_m), resonant peak and bandwidth. In this chapter, the phase margin and gain margin criteria are used to design the controller. Another important characteristic of a frequency response measure of a system is the critical point. The critical point is the point where the Nyquist curve intersects the $-1+j0$ point in the negative real axis. This point yields the critical gain, K_{cr} and the critical frequency, ω_{cr}. These two values are used in chapter 5 to tune a PID controller.

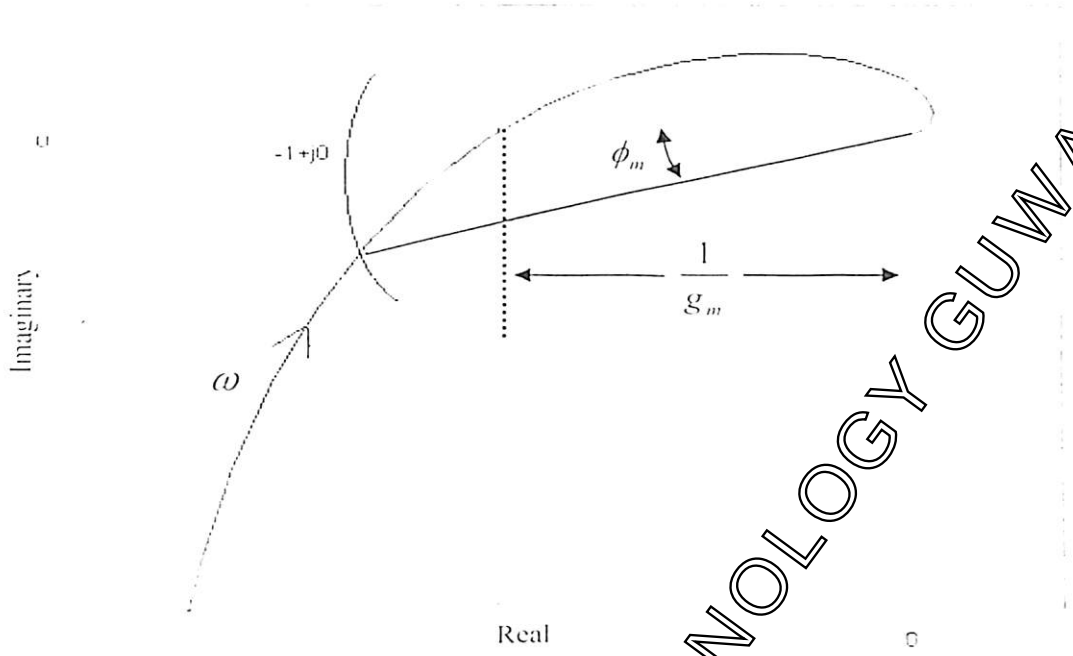

Fig. 4.7. Nyquist curve of a process

4.4 Controller Design for SISO Processes

4.4.1 PID Controller

PID controller is the combination of proportional (P), integral (I) and derivative (D) controllers. The proportional controller with increased gain typically increases the speed of response but, at the same time, yields a much larger overshoot. Especially for higher order processes, large value of proportional gain causes instability. For most control systems, there is an upper limit of the proportional gain in order to achieve a well damped stable response. Again, the limit may still yield certain steady state error. So, an integral term is added to the controller to improve the steady state accuracy of response. Now, the controller becomes the PI type and it reduces the steady state error to zero, but this benefit typically comes at the cost of a worse transient response. To eliminate this problem, a derivative action is required in the controller. Further, the derivative action can be used for the stabilization of the process. So, the control signal is the combination of the weighted error, the time integral of the error and the time rate change of the error. The derivative part of the controller usually improves the system's dynamic performance, but at the same time increases the gain at high frequencies. Therefore, the high frequency noise effects are

increased by the derivative term. To eliminate this problem, a filter is used with the derivative action of the controller.

The dynamics of many processes can be described adequately by stable or unstable FOPDT process models. Several methods for tuning of PID controller for stable and unstable processes are available in literature. Ho et al. [31] designed a PI controller for FOPDT process using loop phase and gain margins. They required solving four design equations of loop gain and phase margin criteria to obtain two unknown controller parameters because of the presence of other two unknown parameters, gain and phase crossover frequencies in the design equations. To design a PID controller for FOPDT process, it is required to solve four equations to obtain five unknown parameters. So, we design the derivative time constant from the process time delay. Thereafter, the other controller parameters are obtained using the design equations of loop gain and phase margin criteria. In this subsection, the expressions for the parameters of PID controller are derived in terms of process model parameters and user defined loop gain and phase margins. The series form of PID controller given in (2.51) is considered in this subsection.

4.4.1.1 Estimation of Controller Parameters

Using the identification method discussed in chapter 2, a FOPDT transfer function model (2.6) of the process is identified. Based on the process model parameters, the PID controller is designed using the phase and gain margin criteria. The open loop transfer function in Fig. 2.3 (setting the relay heights to zero and using (2.6) and (2.51)) can be written as

$$G_m G_c(s) = \frac{KK_c'(1+T_i's)(1+T_d's)e^{-Ls}}{T_i's(Ts+1)} \tag{4.1}$$

Let the phase crossover and gain crossover frequencies of the loop transfer function be ω_p and ω_g, respectively. Similarly, let ϕ_m and g_m be the phase and gain margins. From the definition of phase margin and gain margin, the following set of equations are obtained

$$\left|G_m G_c(j\omega_g)\right| = 1 \tag{4.2}$$

$$\left|G_m G_c(j\omega_p)\right| = \frac{1}{g_m} \tag{4.3}$$

$$\pi + \arg\left(G_m G_c(j\omega_g)\right) = \phi_m \tag{4.4}$$

$$\pi + \arg\left(G_m G_c(j\omega_p)\right) = 0 \tag{4.5}$$

Using (4.1) in (4.2-4.5), we obtain

$$KK_c' = \omega_g T_l' \sqrt{\frac{\omega_g^2 T^2 + 1}{(\omega_g^2 T_l'^2 + 1)(\omega_g^2 T_d'^2 + 1)}} \tag{4.6}$$

$$g_m KK_c' = \omega_p T_l' \sqrt{\frac{\omega_p^2 T^2 + 1}{(\omega_p^2 T_l'^2 + 1)(\omega_p^2 T_d'^2 + 1)}} \tag{4.7}$$

$$\pm\frac{\pi}{2} + \tan^{-1}(\omega_g T_l') + \tan^{-1}(\omega_g T_d') \mp \tan^{-1}\omega_g T - D\omega_g = \phi_m \tag{4.8}$$

$$\pm\frac{\pi}{2} + \tan^{-1}(\omega_p T_l') + \tan^{-1}(\omega_p T_d') \mp \tan^{-1}\omega_p T - D\omega_p = 0 \tag{4.9}$$

The above equations (4.6-4.9) can not be solved analytically in easy way because of the presence of the arctangent function. The following approximation [59] is considered for the arctangent function.

$$\tan^{-1} x = \begin{cases} \dfrac{\pi x}{4} & \text{for } 0 \le |x| \le 1 \\ \dfrac{\pi}{2} - \dfrac{\pi}{4x} & \text{for } |x| \ge 1 \end{cases} \tag{4.10}$$

Let us choose

$$T_d' = \alpha D \tag{4.11}$$

where $0 \le \alpha \le 1$. Assuming the values of $\omega_p T_d'$ and $\omega_g T_d'$ are less than one and that of $\omega_p T_l'$, $\omega_g T_l'$, $\omega_p T$ and $\omega_g T$ greater than one, (4.6-4.9) can be written as

$$KK_c' = \omega_g T \tag{4.12}$$

$$g_m KK_c' = \omega_p T \tag{4.13}$$

$$\frac{\pi}{2} - \frac{\pi}{4\omega_g T_l'} \pm \frac{\pi}{4\omega_g T} - \omega_g D\left(1 - \frac{\pi\alpha}{4}\right) = \phi_m \tag{4.14}$$

$$\frac{\pi}{2} - \frac{\pi}{4\omega_p T_l'} \pm \frac{\pi}{4\omega_p T} - \omega_p D\left(1 - \frac{\pi\alpha}{4}\right) = 0 \tag{4.15}$$

Finally, simultaneous solution of (4.12-4.15) gives

$$K_c' = \left(\frac{C_1}{K}\right)\left(\frac{T}{D}\right) \tag{4.16}$$

$$T_I' = \frac{T}{C_2\left(\frac{T}{D}\right) \pm 1} \tag{4.17}$$

where

$$C_1 = \frac{2\phi_m + \pi(g_m - 1)}{0.5(g_m^2 - 1)(4 - \pi\alpha)} \tag{4.18}$$

$$C_2 = 2g_m C_1\left(1 - \frac{0.5 g_m C_1 (4 - \pi\alpha)}{\pi}\right) \tag{4.19}$$

For a given process model (K, T, D) and user specifications (g_m, ϕ_m), the PID controller parameters (K_c', T_I', T_d') are estimated using (4.11) and (4.16-4.17). Thereafter, the PID controller parameters K_c, T_I and T_d are obtained using the expressions given in (2.52-2.54). The range of gain and phase margin of the compensated system is suggested as $g_m \geq 2$, $\phi_m \geq 30$ [31].

4.4.1.2 Simulation Results

In this subsection, three different typical processes have been considered. At first, a FOPDT model of the process dynamics is estimated by using the method given in subsection 2.2.1.2. Then, the PID controller parameters K_c, T_I and T_d are obtained from (4.11), (4.16-4.17) and (2.52-2.54) for the process model with the choice of the design parameters α, g_m and ϕ_m. The derivative filter constant β is taken as 0.01 in all the examples. The first two examples consider typical stable processes. The last one considers an unstable process. The process model parameters and the PID controller parameters for the above processes are tabulated in Table 4.1. For comparison of results, the controller settings presented by Padma Sree et al. [34], Visioli [35], Wang et al. [37] and Huang et al. [38] are considered. The controller performance for a high-order process is illustrated in appendix B2 and compared with the Leva et al.'s auto-tuning method [79].

Example 4.1

Consider a stable FOPDT process $G(s) = \frac{e^{-0.5s}}{(s+1)}$ [34]. The specifications for the controller design are set as $\alpha = 0.35$, $g_m = 3.0$ and $\phi_m = 60^0$. The controller parameters obtained for the process model are given in Table 4.1. The PID settings by Padma Sree et al.'s method are $K_c = 2.5$, $T_I = 1.25$, $T_d = 0.2167$. Wang et al.'s IMC method which is based on numerical optimization technique gives $K_c = 1.7137$, $T_I = 1.0154$, $T_d = 0.1669$ and the derivative filter time constant of value 0.01856. Fig. 4.8 (a) shows the comparisons of the closed loop output responses to unit step input and step load disturbance of magnitude 0.5 applied at $t = 8$ second for all the controller settings. The proposed method shows improved set-point response and acceptable disturbance rejection in comparison to the other two methods. The robustness of the controller is evaluated by perturbing the values of time delay, steady state gain and time constant of the process by $\pm 10\%$ whereas the controller settings used are for the nominal process. Fig. 4.8 (b), 4.8 (c) and 4.8 (d) show the closed loop responses for the process with variations in process parameters. The performances under the model parameter uncertainty by the proposed method are better than that of Padma Sree et al.'s and Wang et al.'s method.

Table 4.1 Actual process, process model parameters and PID controller parameters

Examples	Processes	Process model parameters			PID Controller parameters		
		K	T	D	K_c	T_I	T_d
1	$\frac{e^{-0.5s}}{(s+1)}$	1.0	0.9996	0.5000	1.6972	1.1600	0.1486
2	$\frac{e^{-2s}}{(10s+1)(s+1)}$	1.0	11.4341	2.8602	3.8578	8.2268	1.5922
3	$\frac{e^{0.5s}}{(s-1)}$	1.0	0.9912	0.5014	2.1720	3.3925	0.2735

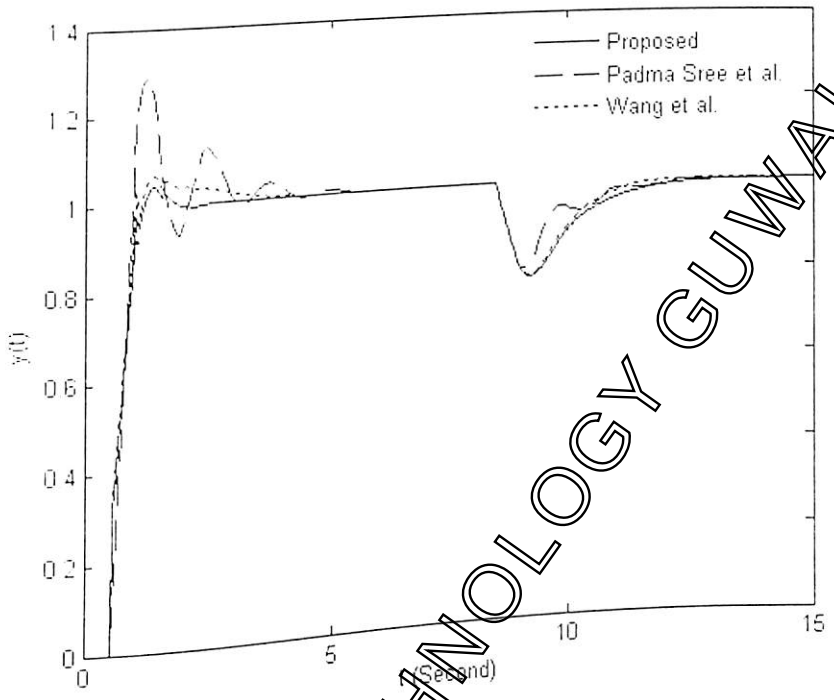

Fig. 4.8 (a). Closed loop responses to step input and load disturbance for example 4.1

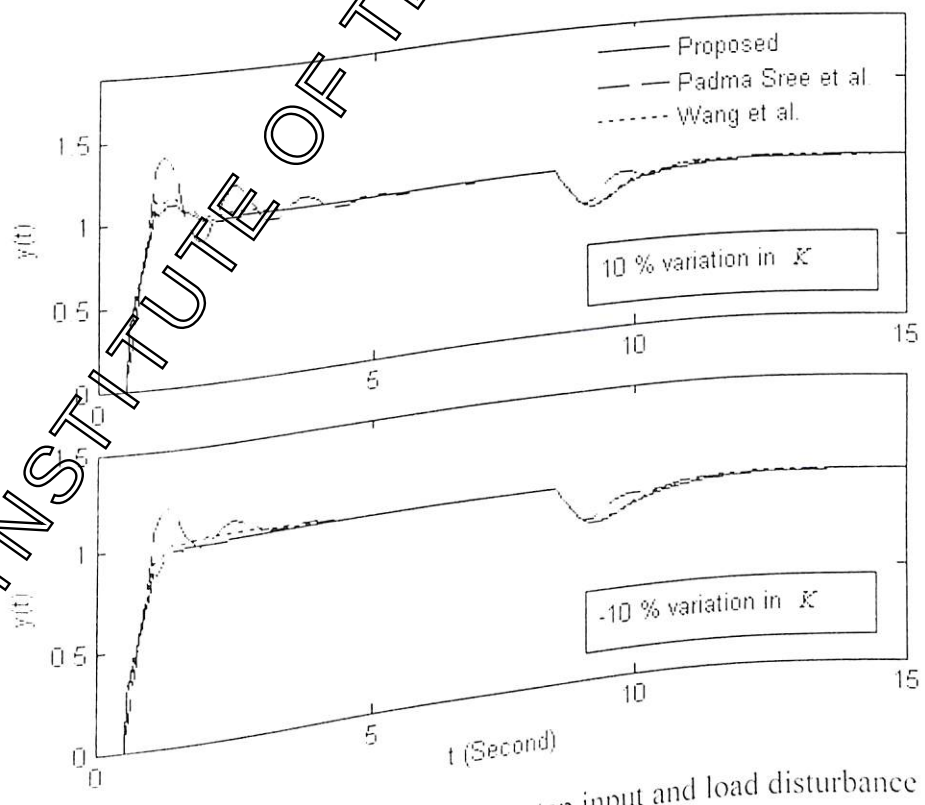

Fig. 4.8 (b). Closed loop responses to step input and load disturbance with $\pm 10\%$ variation in K for example 4.1

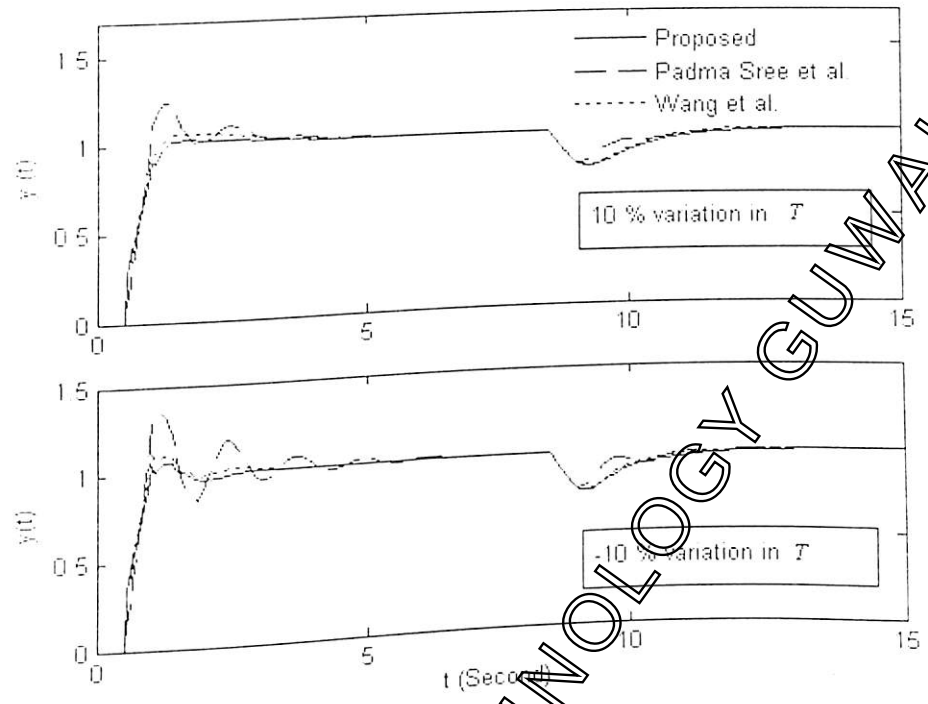

Fig. 4.8 (c). Closed loop responses to step input and load disturbance with ±10% variation in T for example 4.1

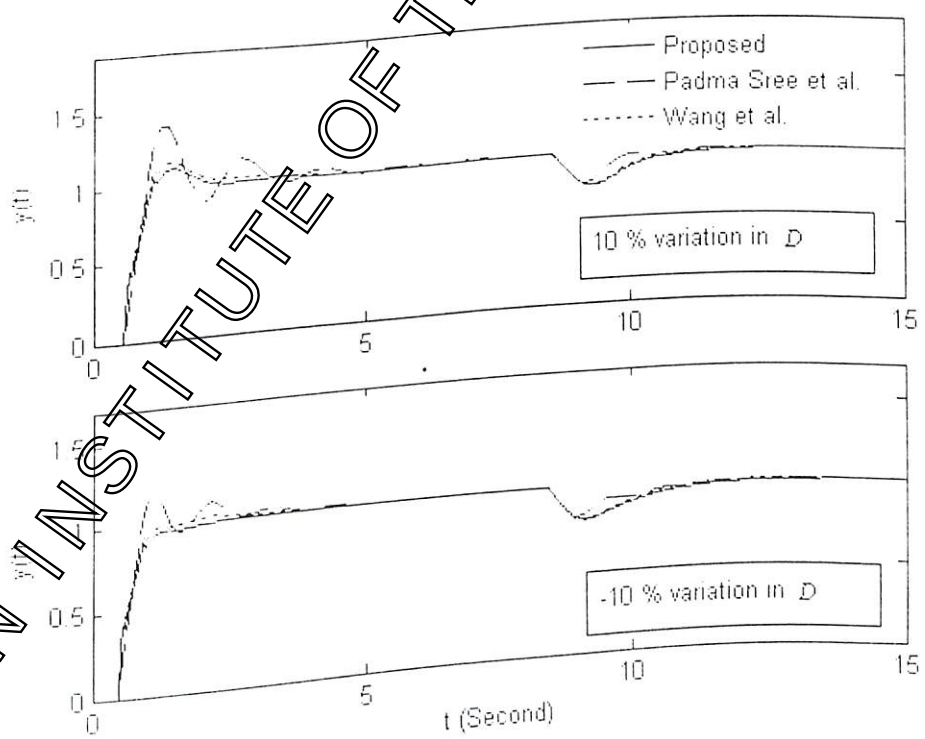

Fig. 4.8 (d). Closed loop responses to step input and load disturbance with ±10% variation in D for example 4.1

Example 4.2

Consider the second order process of example 2.1. The controller parameters for the identified FOPDT model are obtained using the design specifications $\alpha = 0.75$, $g_m = 5$, $\phi_m = 60^0$ and are given in Table 4.1. For comparison, the PID controller design method by Padma Sree et al. is considered for the process model parameters given in Table 4.1 for the second order process. The PID parameters by their method are $K_c = 1.3096$, $T_I = 4.7836$, $T_d = 0.7970$ and $\beta = 0.01$. The closed loop output responses for both the methods are given in Fig. 4.9. The results show that the proposed method gives satisfactory controller performance as compared to their method.

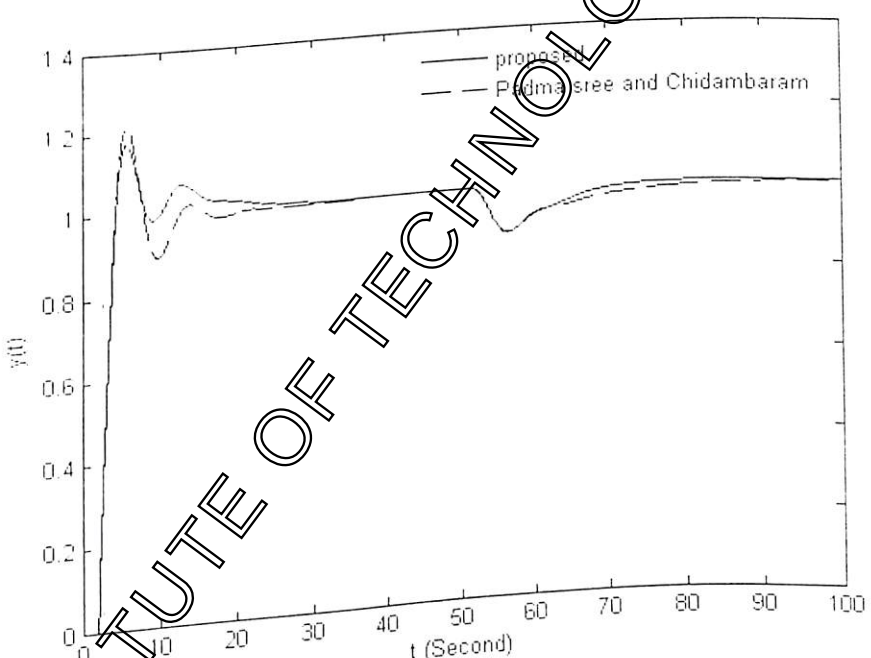

Fig. 4.9 Closed loop responses to step input and load disturbance for example 4.2

Example 4.4

The unstable FOPDT process of example 2.2 is considered here. The FOPDT model identified in subsection 2.2.1.2 along with the PID controller parameters estimated using $\alpha = 0.6$, $g_m = 4.6$ and $\phi_m = 60$ are given in Table 4.1. For performance comparison, we use the controller settings suggested by Padma Sree et al. [34], Visioli [35] and Huang et al. [38]. The controller settings by Padma Sree et al. are $K_c = 2.1934$, $T_I = 2.7792$, $T_d = 0.2561$; by Visioli are $K_c = 2.4976$, $T_I = 2.8879$, $T_d = 0.2901$ and that proposed by

Huang et al. are $K_c = 2.142$, $T_I = 2.9087$, $T_d = 0.1603$. The control performances of all the methods for both the set-point change and the step load disturbance of magnitude 0.5 are shown in Fig. 4.10. The proposed method shows improved control performances in terms of the overshoot, speed of response and settling time.

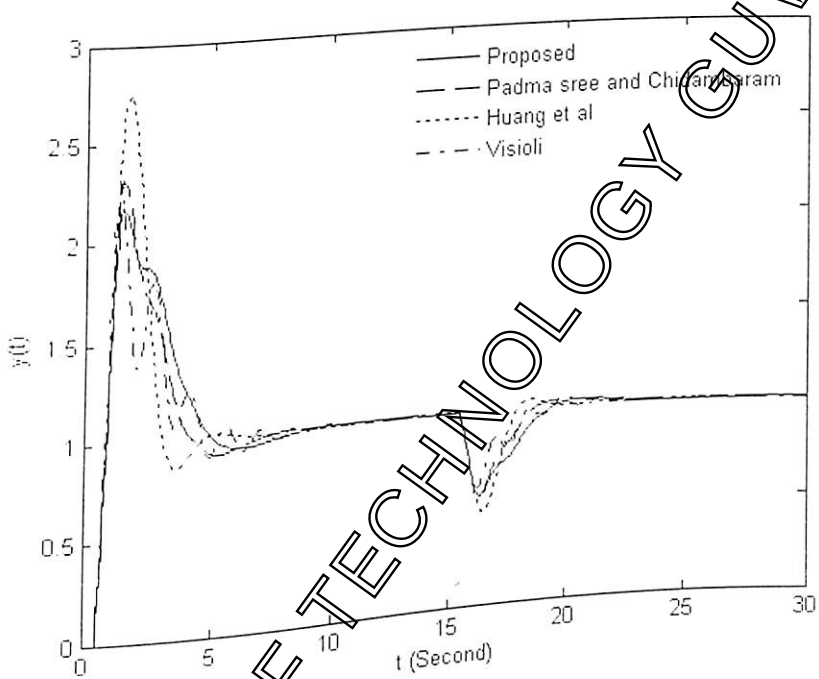

Fig. 4.10. Closed loop responses to step input and load disturbance for example 4.3

4.4.2 PI-PD Controller

The PID controller discussed in subsection 4.4.1 is the typically available controller for use in practice. However, derivative kick is an undesirable phenomenon that occurs because of the derivative action in the forward path. The derivative of the error signal can be written as

$$\frac{de(t)}{dt} = \frac{dr(t)}{dt} - \frac{dy(t)}{dt} \tag{4.20}$$

If there is a sudden change in the reference input to the controller, the first part of (4.20) yields a large change in the control signal temporarily, which is referred to as a derivative kick and it may drive the controller to saturation. To avoid this, the reference input may be excluded from the derivative action. The derivative action of the controller can be implemented in the feedback path. PI-PD structure is the commonly used configuration for this purpose which is a two degree of freedom and four parameter controller. In this

subsection, the PI-PD controller parameters are designed for the FOPDT model based on the loop phase and gain margin criteria. For fair comparison, some other two degree of freedom or four parameters controllers for stable and unstable processes such as set-point weighted PID controller [43, 44], PID-P controller [42] and PI-PD controller [40, 41] are considered in the simulation study.

4.4.2.1 Estimation of Controller Parameters

Setting the relay height to zero in Fig. 2.9, the PI-PD control structure is obtained. The forms of the PI and PD controllers are given in (2.22) and (2.23), respectively. At first, the inner feedback PD controller is designed based on the stability properties of the process model obtained by using the identification procedure given in subsection 2.2.1.6. Thereafter, the PI controller is designed for the stabilized process model $G'_m(s)$ that is the process model $G_m(s)$ coupled with the PD controller.

Design of PD controller

The stabilized process transfer function model (Fig.2.9) can be written as

$$G'_m(s) = \frac{G_m(s)}{1 + G_{c2}G_m(s)} = \frac{Ke^{-Ds}}{Ts + KK_f(1 + T_d s)e^{-Ds} \pm 1} \tag{4.21}$$

The first order Pade approximation is used for the time delay term in the denominator of (4.21). Let us choose

$$T_d = \frac{D}{2} \tag{4.22}$$

Then, (4.21) becomes

$$G'_m(s) = \frac{Ke^{-Ds}}{\left[\left(T - \frac{KK_f D}{2}\right)s + (KK_f \pm 1)\right]} \tag{4.23}$$

It is apparent from the denominator of (4.23) that $G_{c2}(s)$ is capable of stabilizing an unstable FOPDT process model and relocating the pole of a stable process model when

$$K_f \geq \frac{1}{K} \tag{4.24}$$

and

$$K_f \le \frac{2T}{KD} \tag{4.25}$$

Combining (4.24) and (4.25), one obtains

$$\frac{1}{K} \le K_f \le \frac{2T}{KD} \tag{4.26}$$

Then, one can use the following proportional gain to design the feedback PD controller

$$K_f = \frac{1}{K}\sqrt{\frac{2T}{D}} \tag{4.27}$$

Design of PI controller

Now, the outer loop transfer function becomes $G_{c1}G'_m(s)$ and the basic equations of the phase and gain margins criteria can be expressed as

$$\left|G_{c1}(j\omega_g)G'_m(j\omega_g)\right| = 1 \tag{4.28}$$

$$\left|G_{c1}(j\omega_p)G'_m(j\omega_p)\right| = \frac{1}{g_m} \tag{4.29}$$

$$\pi + \arg\left(G_{c1}(j\omega_g)G'_m(j\omega_g)\right) = \phi_m \tag{4.30}$$

$$\pi + \arg\left(G_{c1}(j\omega_p)G'_m(j\omega_p)\right) = 0 \tag{4.31}$$

Using (2.6) and (4.23) in (4.28-4.31) gives

$$KK_c = \omega_g T_I (KK_f \pm 1)\sqrt{\frac{\omega_g^2\tau^2+1}{\omega_g^2 T_I^2+1}} \tag{4.32}$$

$$g_m KK_c = \omega_p T_I (KK_f \pm 1)\sqrt{\frac{\omega_p^2\tau^2+1}{\omega_p^2 T_I^2+1}} \tag{4.33}$$

$$\phi_m = \frac{\pi}{2} + \tan^{-1}(\omega_g T_I) - \tan^{-1}(\omega_g\tau) - D\omega_g \tag{4.34}$$

$$\frac{\pi}{2} + \tan^{-1}(\omega_p T_I) - \tan^{-1}(\omega_p\tau) - D\omega_p = 0 \tag{4.35}$$

where

$$T_I = \frac{\left(T - \frac{KK_f D}{2}\right)}{KK_f \pm 1} \tag{4.36}$$

The approximation, $\tan^{-1} x = \frac{\pi}{2} - \frac{1}{x}$, for $\frac{1}{x} < 1$, is used to solve (4.34-4.35) and $\omega_p T_I$, $\omega_g T_I$, $\omega_p \tau$, $\omega_g \tau$ are assumed to be greater than one. Now, using the above approximation, the expressions (4.32-4.35) becomes

$$KK_c = \omega_g \left(T - \frac{KK_f D}{2} \right) \tag{4.37}$$

$$g_m KK_c = \omega_p \left(T - \frac{KK_f D}{2} \right) \tag{4.38}$$

$$\phi_m = \frac{\pi}{2} - \frac{1}{\omega_g T_I} + \frac{1}{\omega_g \tau} - D\omega_g \tag{4.39}$$

$$\frac{\pi}{2} - \frac{1}{\omega_p T_I} + \frac{1}{\omega_p \tau} - D\omega_p = 0 \tag{4.40}$$

Finally, the simultaneous solution of (4.37-4.40) gives

$$K_c = \left(\frac{C_1}{KD} \right) \left(T - \frac{KK_f D}{2} \right) \tag{4.41}$$

$$T_I = \frac{\tau}{1 + \left(\frac{C_2}{D} \right) \tau} \tag{4.42}$$

where

$$C_1 = \frac{2\phi_m + \pi(g_m - 1)}{2(g_m^2 - 1)} \quad \text{and} \quad C_2 = \frac{\pi}{2} g_m C_1 \left(1 - \frac{2 g_m C_1}{\pi} \right).$$

For a given process (K, T, D) and user specifications (g_m, ϕ_m), (4.41-4.42), (4.27) and (4.22) are used to estimate the PI-PD controller parameters (K_c, T_I, K_f, T_d).

4.4.2.2 Simulation Results

In this subsection, the control approach is demonstrated by several examples. The PI-PD controller for the process models obtained by the method given in subsection 2.2.1.6 is designed using suitable values of g_m and ϕ_m. We have considered two typical stable processes and two unstable processes for the simulation study. The process models and the PI-PD controller parameters for all the four examples are tabulated in Table 4.2.

Table 4.2 Actual process, process model parameters and PI-PD controller parameters

Examples	Processes	Process model parameters			PI-PD Controller parameters			
		K	T	D	K_c	T_I	K_f	T_d
1	$\frac{e^{-0.5s}}{(s+1)}$	1.0	1.0002	0.4976	0.3912	0.1543	2.0050	0.2488
2	$\frac{2}{(s+1)^4}$	2.0	4.6127	1.7726	0.2815	0.7870	1.1407	0.8863
3	$\frac{e^{-0.4s}}{(s-1)}$	1.0	0.9795	0.3998	0.4460	0.4124	2.2136	0.1999
4	$\frac{4e^{-2s}}{(4s-1)}$	4.0	3.9997	2.0013	0.0848	1.8788	0.4998	1.0007

Example 4.4

Consider the stable FOPDT process of example 4.1. The process model parameters and the PI-PD controller parameters obtained using $g_m = 3.6$ and $\phi_m = 30^0$ are tabulated in Table 4.2. The set-point weighted PID controller parameters by Chidambaram's method [43] are $K_c = 1.6$, $T_I = 0.9$, $T_d = 0.0$ with the set-point weight 0.28 and $K_c = 2.4$, $T_I = 1$, $T_d = 0.25$ with the set-point weight 0.54, respectively, by their dominant pole placement method and Ziegler and Nichols [36] tuning formulae. The closed loop performances of the proposed and Chidambaram's methods for both the set-point change and the step load disturbance are shown in Fig. 4.01. The proposed method rejects disturbance rapidly and shows good control performance in terms of overshoot and settling time.

Example 4.5

This example considers a higher order transfer function $G(s) = \frac{2}{(s+1)^4}$. Again, $g_m = 3.6$ and $\phi_m = 30^0$ are used to design the controller for the identified equivalent FOPDT model of the process. Chidambaram [43] designed a set-point weighted PID controller with the parameters $K_c = 0.831$, $T_I = 2.5823$, $T_d = 0.2540$ and $b = 0.2646$ for the higher order process

using the FOPDT model $G_m(s) = \frac{2e^{-1.5s}}{(3s+1)}$. The control performances of the proposed method and Chidambaram's method are shown in Fig. 4.12. The results show that the proposed method can also be extended to design the PI-PD controller for higher order processes.

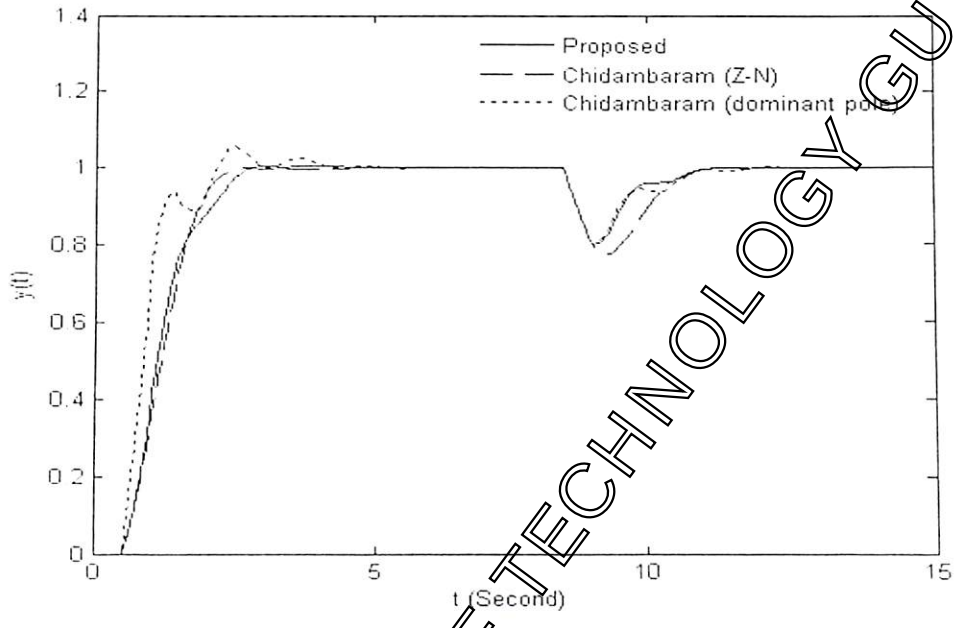

Fig. 4.11. Closed loop responses to step input and load disturbance for example 4.4

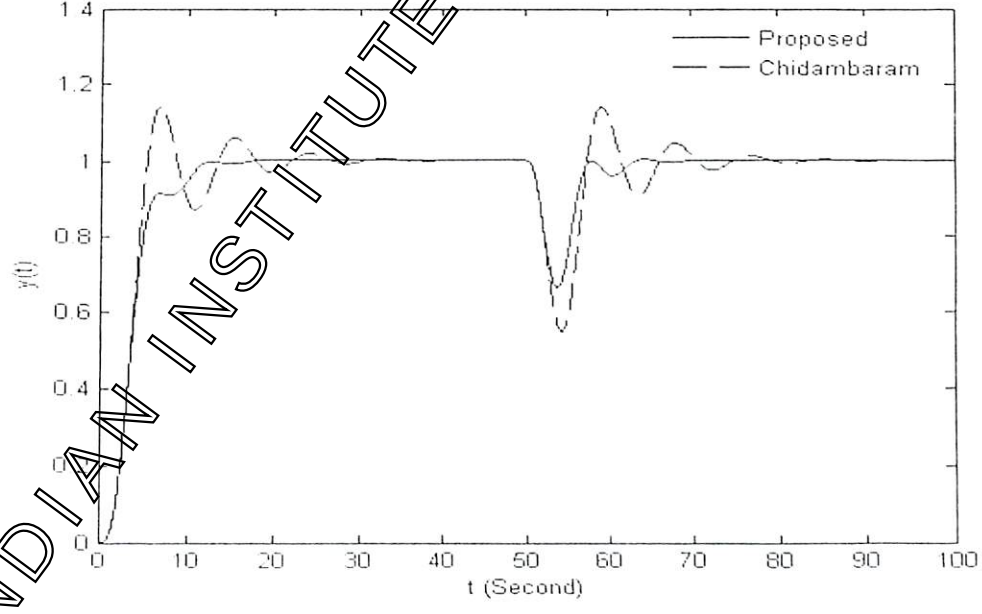

Fig. 4.12. Closed loop responses to step input and load disturbance for example 4.5

Example 4.6

Consider an unstable FOPDT process $G(s) = \frac{e^{-0.4s}}{(s-1)}$. The PI-PD controller parameters are estimated using the gain margin of 4.6 and phase margin of 60^0. Table 4.2 shows the identified process model parameters using the method discussed in subsection 2.2.1.6 and the designed controller parameters. For the same process, Padma Sree and Chidambaram [44] have proposed set-point weighted PID controllers using ISE and overshoot minimization techniques. The control performances of the proposed method for both the set-point change and the step load disturbance of magnitude 0.5 are compared with that of Padma Sree and Chidambaram's methods [44] as shown in Fig. 4.13. The proposed method shows excellent control performances in terms of the overshoot, speed of response and settling time. The main advantage of this control method is that the inner feedback PD controller manipulates the stabilization problem.

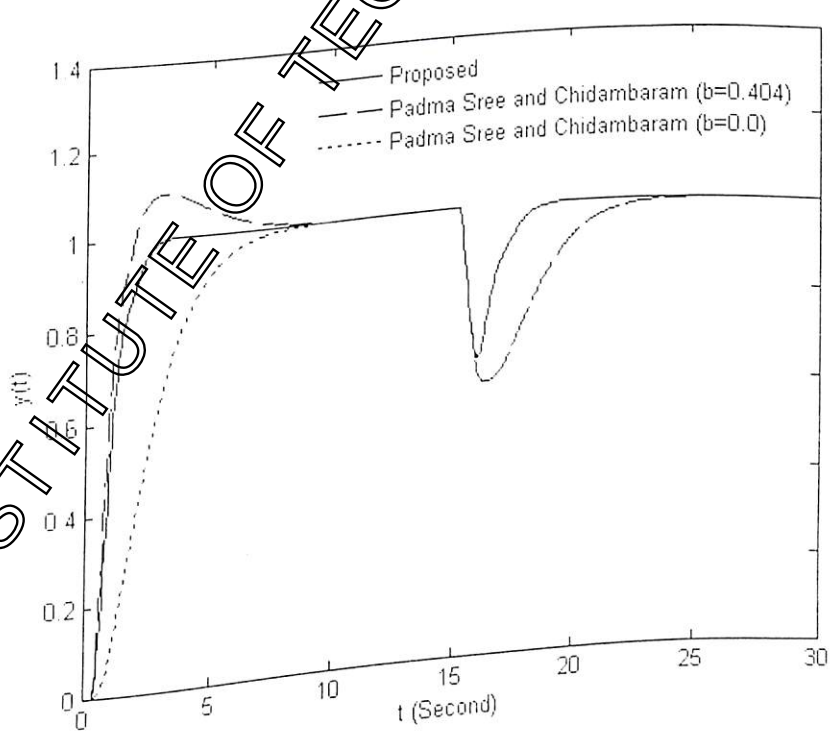

Fig. 4.13. Closed loop responses to step input and load disturbance for example 4.6

Example 4.7

Let the unstable FOPDT process be $G(s) = \dfrac{4e^{-2s}}{(4s-1)}$. The controller parameters obtained by the proposed method for the process model using $g_m = 4.5$ and $\phi_m = 60^0$ are given in Table 4.2. For the same process, the parameters of the PID-P controller suggested by Park et al. [42] are K_c = 0.068, T_I = 1.885, T_d = 4.296 and K_f = 0.35 and the PI-PD controller parameters by Majhi and Atherton [40] are K_c = 0.131, T_I =2, K_f= 0.5 and T_d = 1. Fig. 4.14 (a) shows the responses given by the set-point input and the static load disturbance of magnitude 0.1. The PI-PD control method proposed by Majhi and Atherton results in better overshoot and settling time than the Park et al.'s method. As expected, the proposed method shows the best control performance. The robust performance of the controller is verified by perturbing the steady state gain, time constant and the time delay of the process. Figs. 4.14 (b), 4.14 (c) and 4.14 (d) show the closed loop performances for ±10% variations in process parameters, thereby, indicating the robustness of the proposed controller.

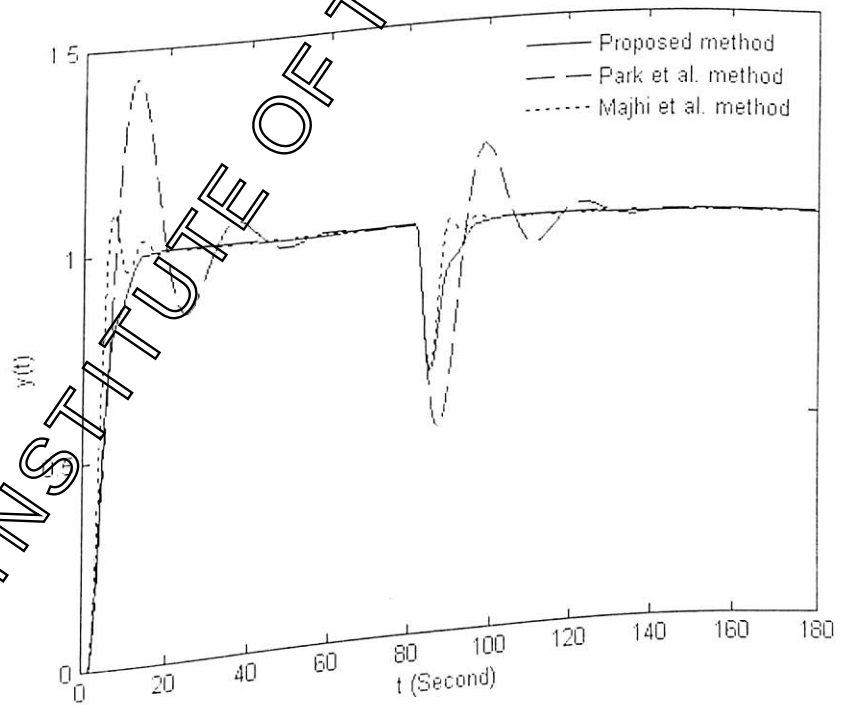

Fig. 4.14(a). Closed loop responses to step input and load disturbance for example 4.7

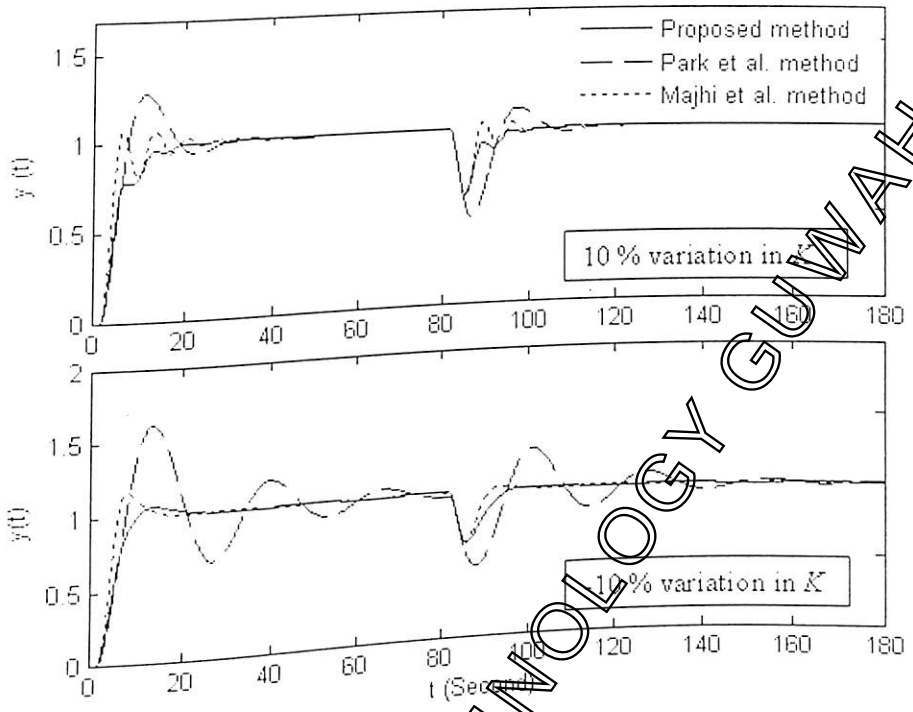

Fig. 4.14 (b). Closed loop responses to step input and load disturbance with ±10% variation in K for example 4.7

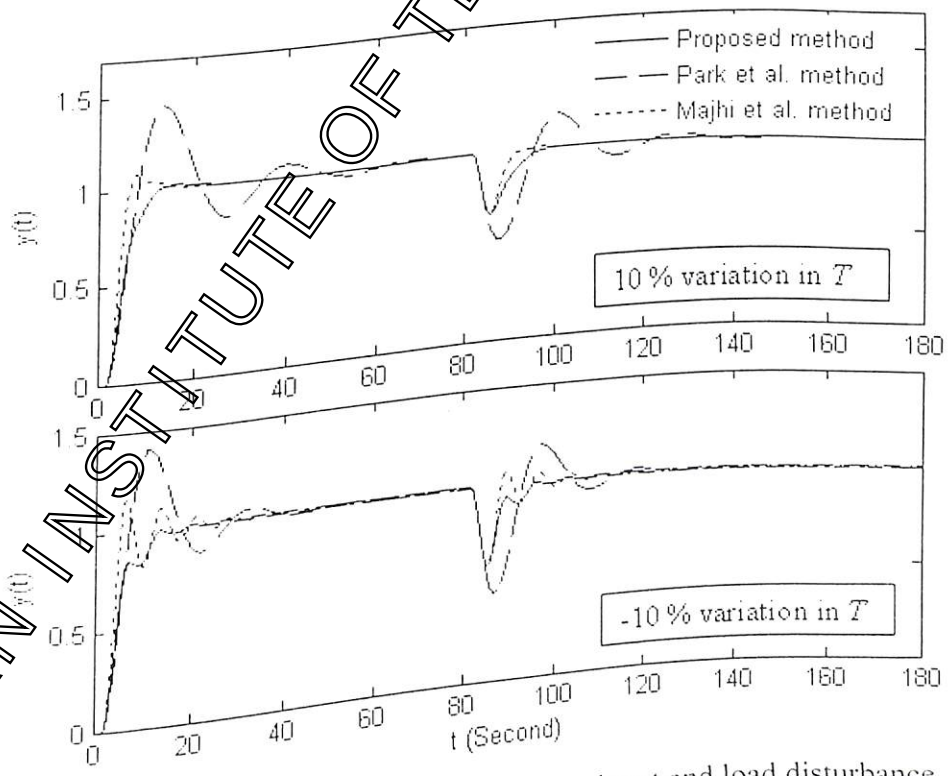

Fig. 4.14 (c). Closed loop responses to step input and load disturbance with ±10% variation in T for example 4.7

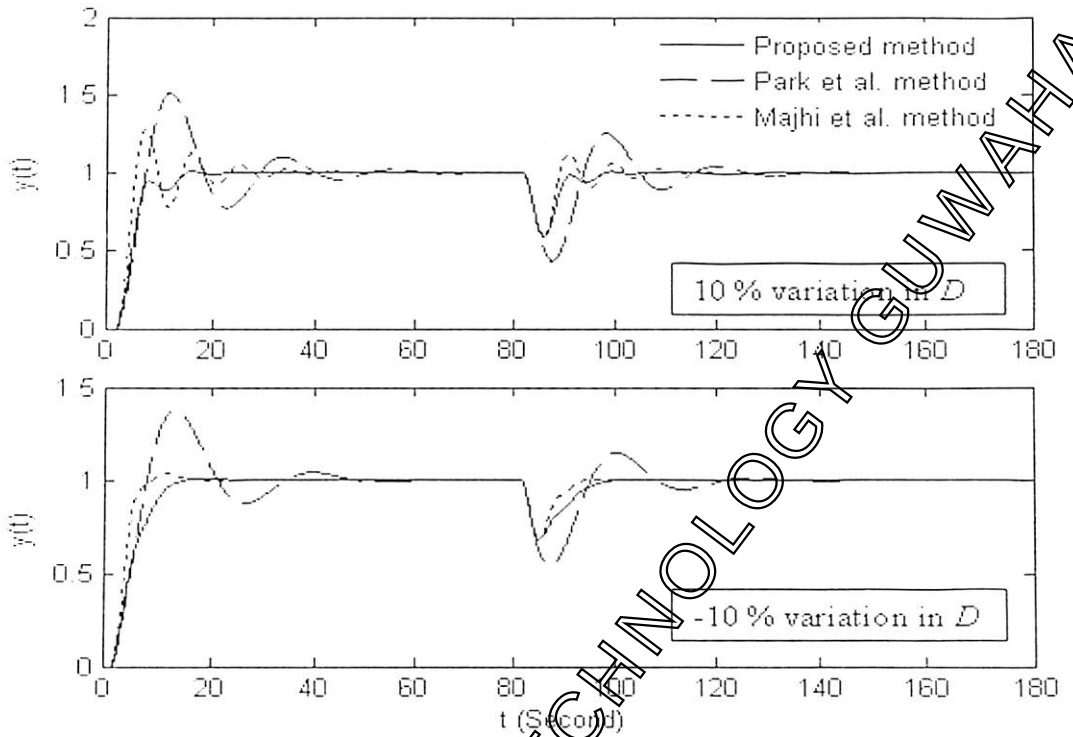

Fig. 4.14 (d). Closed loop responses to step input and load disturbance with ±10% variation in D for example 4.7

4.5 Controller Design for TITO Processes

According to industrial demand, there are many developments in the control of two-input-two-output processes. The uses of such processes are very often in power plants, aircraft, chemical industries and other fields. The control of these processes is difficult than the SISO processes due to interaction between the loops. Many methods have been presented in the literature for the control of TITO process [59-69]. In this subsection, the PID controller design method for the SISO process (given in subsection 4.4.1) is extended to design decentralized PID controllers for the TITO process. The PID controllers are designed for the identified SISO transfer function models discussed in subsection 3.3.1.

4.5.1 PID Controller

4.5.1.1 Estimation of Controller Parameters

At first, a diagonal transfer function model (3.1) of the TITO process dynamics is identified. Thereafter, two SISO controllers for the process model are designed using the loop phase and gain margin criteria. The form of the controller given in (3.3) is considered here. So, the loop transfer function becomes

$$\boldsymbol{G}_m\boldsymbol{G}_{cl}(j\omega)=\begin{bmatrix} G_{m1}G_{cl1}(j\omega) & 0 \\ 0 & G_{m2}G_{cl2}(j\omega) \end{bmatrix} \tag{4.43}$$

Let us assume

$$T'_{li}=T_i \tag{4.44}$$

Then, (4.43) can be written as

$$G_{mi}G_{cli}(j\omega)=\frac{K_i K'_{ci}e^{-j\omega D_i}}{(j\omega T_i+1)}\left(1+\frac{1}{j\omega T'_{li}}\right) \tag{4.45}$$

The phase margin and gain margin criteria for each loop can be expressed as

$$\left|G_{pi}G_{cli}(j\omega_{gi})\right|=1 \tag{4.46}$$

$$\left|G_{pi}G_{cli}(j\omega_{pi})\right|=\frac{1}{g_{mi}} \tag{4.47}$$

$$\pi+\arg\left(G_{pi}G_{cli}(j\omega_{gi})\right)=\phi_{mi} \tag{4.48}$$

$$\pi+\arg\left(G_{pi}G_{cli}(j\omega_{pi})\right)=\phi_{mi} \tag{4.49}$$

where ω_{gi} and ω_{pi} are the i^{th} loop gain crossover and phase crossover frequencies, respectively. Similarly, g_{mi} and ϕ_{mi} are the gain and phase margins of i^{th} loop.

Using (4.45) in (4.46-4.49) we have

$$K_i K'_{ci}=\omega_{gi}T'_{li}\sqrt{\frac{\omega_{gi}^2T_i^2+1}{\omega_{gi}^2T_{li}'^2+1}} \tag{4.50}$$

$$g_{mi}K_iK'_{ci}=\omega_{pi}T'_{li}\sqrt{\frac{\omega_{pi}^2T_i^2+1}{\omega_{pi}^2T_{li}'^2+1}} \tag{4.51}$$

$$\frac{\pi}{2}+\tan^{-1}(\omega_{gi}T'_{li})-\tan^{-1}(\omega_{gi}T_i)-D_i\omega_{gi}=\phi_{mi} \tag{4.52}$$

$$\frac{\pi}{2} + \tan^{-1}(\omega_{pi}T'_{li}) - \tan^{-1}(\omega_{pi}T_i) - D_i\omega_{pi} = 0 \tag{4.53}$$

By using the approximation given in (4.10)

$$K_i K'_{ci} = \omega_{gi} T'_{li} \tag{4.54}$$

$$g_{mi} K_{pi} K'_{ci} = \omega_{pi} T'_{li} \tag{4.55}$$

$$\frac{\pi}{2} - \frac{1}{4\omega_{gi}T'_{li}} + \frac{1}{4\omega_{gi}T_i} - D_i\omega_{gi} = \phi_{mi} \tag{4.56}$$

$$\frac{\pi}{2} - \frac{1}{4\omega_{pi}T'_{li}} + \frac{1}{4\omega_{pi}T_i} - D_i\omega_{pi} = 0 \tag{4.57}$$

Simultaneous solution of (4.54-4.57) gives

$$K'_{ci} = \left(\frac{C_{1i}}{K_i}\right)\left(\frac{T_i}{D_i}\right) \tag{4.58}$$

$$T'_{li} = \frac{T_i}{1 + \left(C_{2i}\left(\frac{T_i}{D_i}\right)\right)} \tag{4.59}$$

where

$$C_{1i} = \frac{2\phi_{mi} + \pi(g_{mi} - 1)}{2(g_{mi}^2 - 1)} \tag{4.60}$$

$$C_{2i} = 2g_{mi}C_{1i}\left(1 - \frac{2g_{mi}C_{1i}}{\pi}\right) \tag{4.61}$$

The decentralized PID controller parameters (K'_{ci}, T'_{li} and T'_{di}) are obtained from (4.58-4.59) and (4.44) for user defined gain margin g_{mi} and phase margin ϕ_{mi}. Then, the parameters of the parallel form PID controller K_{ci}, T_{li} and T_{di} are obtained using (3.36-3.38). Robustness of the system can be found out by choosing suitable gain and phase margins for each loop. The range of loop gain and phase margin is suggested as $g_{mi} \geq 2$, $\phi_{mi} \geq 30$ [59]. Approximate analytical formulae to compute phase and gain margins of PID control systems can be obtained to facilitate on-line computation which would be particularly useful for implementing adaptive control.

4.5.1.2 Simulation Results

Two examples are considered here to illustrate the control methodology discussed in the preceding subsection. At first, a diagonal process model is identified using the method discussed in subsection 3.2.4. Thereafter, the controller parameters K_{ci}, T_{Ii} and T_{di} are designed by using (4.58-4.59), (4.44) and (3.36-3.38) for the specified loop phase and gain margins. The methods proposed by Zhuang and Atherton [62] and Ziegler and Nichols tuning formulae given in [66] have been considered here for comparison of results. Another typical example is given in appendix B2 to highlight the control technique.

Example 4.8

Consider a fourth order TITO process discussed in example 3.1. Using the identification procedure described in subsection 3.2.4, the process is modeled as

$$\boldsymbol{G}_m(s) = \begin{bmatrix} \dfrac{0.849\,e^{-0.3422s}}{(1.8790s+1)^2} & 0 \\ 0 & \dfrac{0.678\,e^{-0.3271s}}{(1.7573s+1)^2} \end{bmatrix}$$

Choosing $\phi_m = 45^0$ and $g_m = 2.0$ for both the loops, the parameters of the controller $G_{c1}(s)$ are estimated as $K_{c1} = 10.1388$, $T_{I1} = 3.7600$, $T_{d1} = 0.9400$ and that of $G_{c2}(s)$ are $K_{c2} = 12.4033$, $T_{I2} = 3.5165$ and $T_{d2} = 0.8791$. Using the method given in [62], $K_{c1} = 7.156$, $K_{c2} = 7.717$, $T_{I1} = T_{I2} = 0.713$ and $T_{d1} = T_{d2} = 2.925$ are obtained. Similarly Ziegler and Nichol's tuning formula [66] gives $K_{c1} = 6.072$, $K_{c2} = 6.547$, $T_{I1} = T_{I2} = 0.457$ and $T_{d1} = T_{d2} = 1.903$ for the considered TITO process. The responses of all the three methods to unit step set-point input and static disturbance are shown in Fig. 4.15(a). The figure shows improved performance, in terms of speed of response and overshoot, by the proposed control method. To test the robust performance of the controllers, the process parameters are perturbed by ±10%. The closed loop responses to step input and load disturbance with 10 % and -10 % variations in parameters of the process are shown in Figs. 4.15(b) and 4.15(c), respectively. It is evident from the figures that the proposed PID controllers have the best set-point responses and disturbance rejection for perturbed process as compared to other two discussed methods.

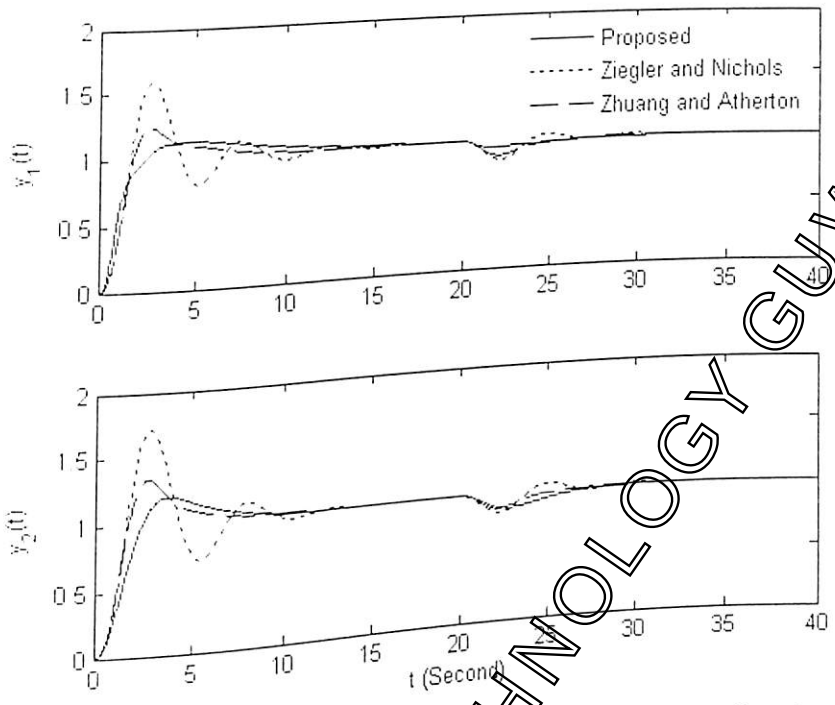

Fig. 4.15(a). Closed loop responses to step input and load disturbance of loop 1 and loop 2 for example 4.8

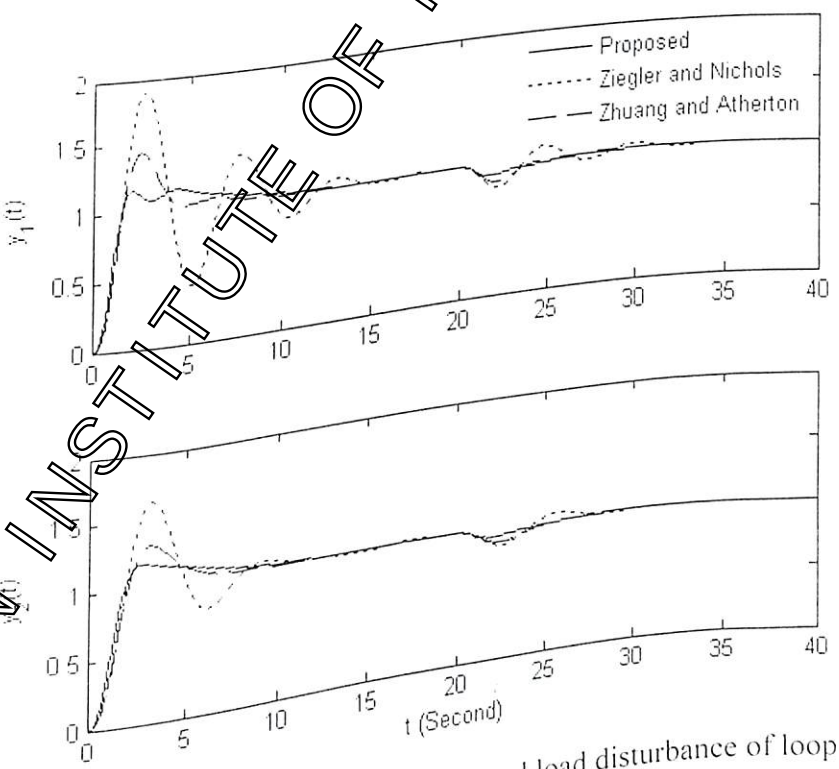

Fig. 4.15(b). Closed loop responses to step input and load disturbance of loop 1 and loop 2 with 10% variation in all parameters of the process

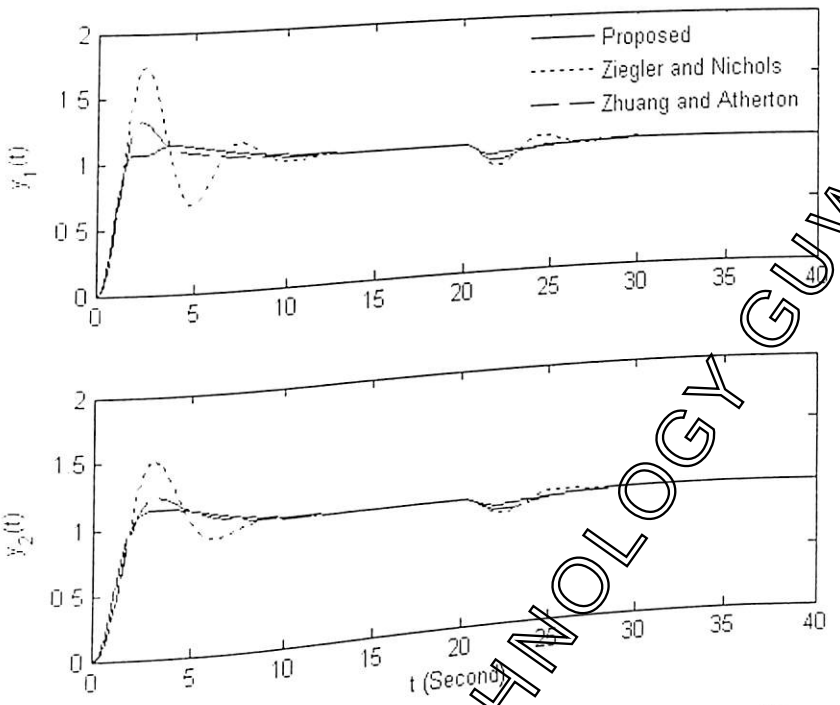

Fig. 4.15(c). Closed loop responses to step input and load disturbance of loop 1 and loop 2 with −10% variation in all parameters of the process

Example 4.9

This example considers the high order process of example 3.2. The dynamics of the proces is modeled as

$$\boldsymbol{G}_m(s) = \begin{bmatrix} \dfrac{2.1925\,e^{-0.0419s}}{(0.4119s+1)^2} & 0 \\ 0 & \dfrac{2.1925\,e^{-0.0419s}}{(0.4119s+1)^2} \end{bmatrix}$$

For this study, the choice of $\phi_m = 45^0, g_m = 2.0$ for both the loops yield the controller parameters as $K_{c1} = K_{c2} = 7.0162$, $T_{I1} = T_{I2} = 0.8246$ and $T_{d1} = T_{d2} = 0.2061$. Zhuang and Atherton's CL method [62] gives $K_{c1} = K_{c2} = 5.83$, $T_{I1} = T_{I2} = 0.140$ and $T_{d1} = T_{d2} = 0.561$. Similarly, $K_{c1} = K_{c2} = 6.40$, $T_{I1} = T_{I2} = 0.091$ and $T_{d1} = T_{d2} = 0.364$ are estimated by the use of Ziegler and Nichols's method [66]. The unit step input and load disturbance responses of the TITO process are shown in Fig. 4.16. It is apparent from the figures that superior performances are achievable by the proposed control technique.

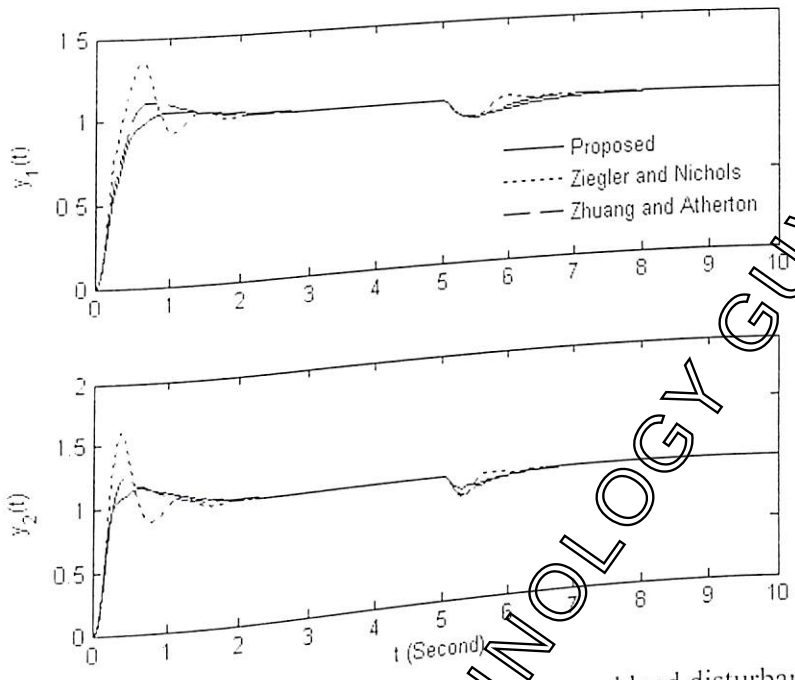

Fig. 4.16. Closed loop responses to step input and load disturbance of loop 1 and loop 2 for example 4.9

4.5.2 PID-P Controller

The PID-P controller structure is obtained when the relay heights in Fig. 3. 4 are set to zero. A diagonal transfer function model of the TITO process is obtained as given in subsection 3.2.4. Then, the parameters of PID-P controller are designed for the process model. Using block diagram reduction of the PID-P controller structure (setting the relay heights in Fig. 3. 4 to zero), one can easily obtain the equivalent PID control structure as shown in Fig. 4.17 which is equivalent to a set-point weighted PID controller. Let the new PID controller be

$$G^*_{ch}(s) = G_{ch}(s) + K_{bi} = K^*_{ci}\left(1 + sT^*_{di}\right)\left(1 + \frac{1}{T^*_{Ii}}\right) \qquad \forall\, i = 1,2 \tag{4.62}$$

The controller $G_{ch}(s)$ is given in (3.35). The controller parameters K^*_{ci}, T^*_{di} and T^*_{Ii} are designed for the identified process models $G_{mi}(s)$ using the method given in the preceding subsection 4.5.1. Then, the controller parameters K_{ci}, T_{di} and T_{Ii} of $G_{ch}(s)$ are obtained using the relations

$$K_{ci} = K^*_{ci}\left(1 + \frac{T^*_{di}}{T^*_{Ii}}\right) - K_{bi} \tag{4.63}$$

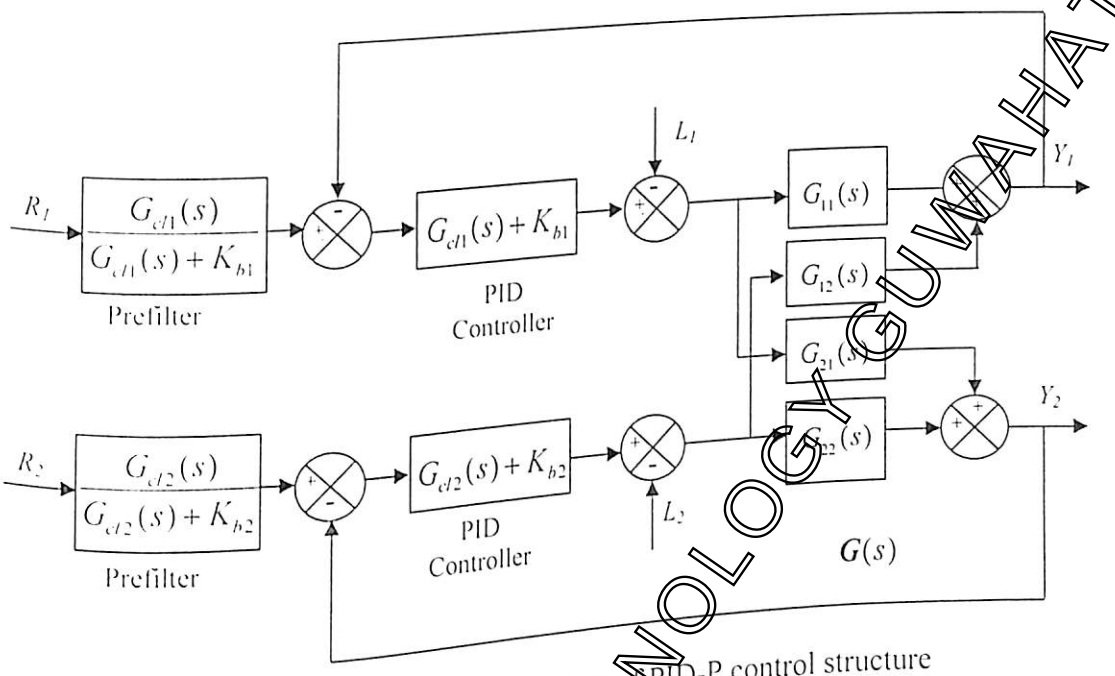

Fig. 4.17. Equivalent PID structure of PID-P control structure

$$T_{di} = \frac{T_{di}^*}{\left(1 + \frac{T_{di}^*}{T_{Ii}^*} - \frac{K_{bi}}{K_{ci}^*}\right)} \tag{4.64}$$

$$T_{Ii} = T_{Ii}^*\left(1 + \frac{T_{di}^*}{T_{Ii}^*} - \frac{K_{bi}}{K_{ci}^*}\right) \tag{4.65}$$

It is clear from (4.63-4.65) that K_{bi} should be less than $K_{ci}^*\left(1+\frac{T_{di}^*}{T_{Ii}^*}\right)$ to obtain a stable closed loop output response. Therefore, one has to satisfy the relation

$$K_{bi} = \varepsilon K_{ci}^* \tag{4.66}$$

by choosing $\varepsilon \le 1$ since $\left(1+\frac{T_{di}^*}{T_{Ii}^*}\right) \ge 1$. In the following example, $K_{b1} = K_{b2}$ that satisfy (4.66) is chosen to reduce the loop interaction during the on-line identification and control of the process. However, one can use suitable values of K_{b1} and K_{b2} to improve the controller performances.

Example 4.10

Consider the TITO process discussed in example 3.3. The identified process model parameters are given in Table 3.3 (a). Choosing $g_m = 4$, $\phi_m = 30^0$ for loop 1 and $g_m = 3$, $\phi_m = 45^0$ for loop 2, the parameters of the controller $G_{cl1}(s)$ are estimated as $K_{c1} = 0.0638$, $T_{I1} = 0.4119$, $T_{d1} = 1.3349$, $K_{b1} = 0.2$ and that of $G_{cl2}(s)$ are $K_{c2} = 0.1121$, $T_{I2} = 0.3561$, $T_{d2} = 0.6708$, $K_{b2} = 0.2$. For comparison of results, the controller setting suggested by Chien et al. [63] is considered. Their method shows superiority over some decentralized controller design methods [48, 49, 53, 54] for the TITO processes. Chien et al.'s method gives $K_{c1} = 0.3634$, $T_{I1} = 1.42$, $T_{d1} = 0.1614$, $K_{c2} = 0.2252$, $T_{I2} = 1.77$ and $T_{d2} = 0.2011$. Fig. 4.18 shows the closed loop responses for the above controller settings, where the unit step set-point change in R_1 occurs at $t = 0$ and in R_2 at $t = 20$ hour. It can be seen from Fig. 4.18 that the proposed controller design method gives satisfactory performances although the TITO process is not diagonal dominant.

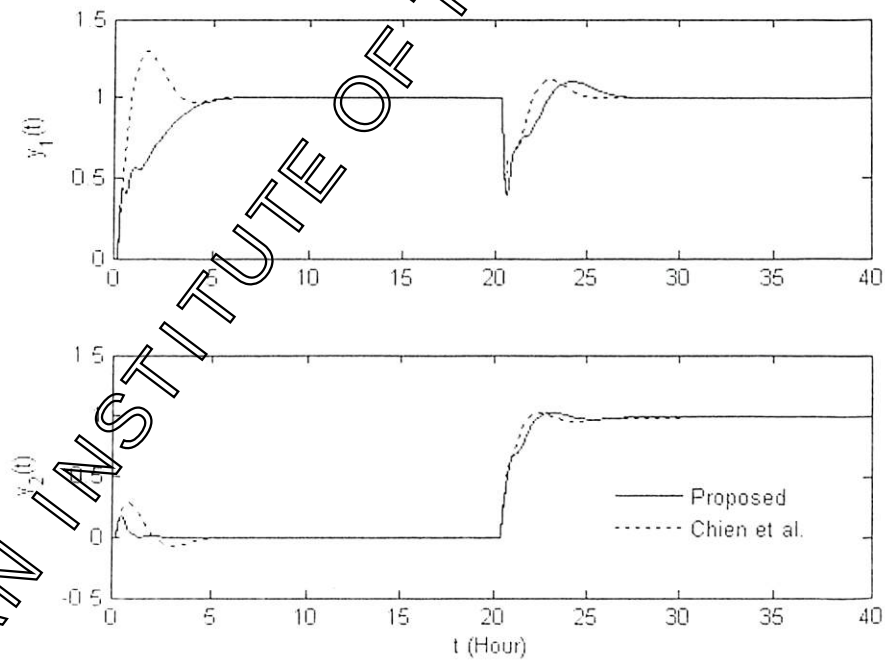

Fig. 4.18. Closed loop responses to step input and load disturbance of loop 1 and loop 2

4.6 Conclusions

In subsection 4.4.1, simple formulae are derived to tune PID controller for stable and unstable SISO processes to meet gain and phase margin specifications. Further, the method is extended to design PI-PD controller to improve the controller performances in subsection 4.4.2. The PD controller in the inner feed back loop plays an important role in stabilizing the open loop processes. It is apparent from the simulation results that the proposed method is capable of giving quite satisfactory performances compared with several previous methods when suitable phase and gain margins are used.

A method for finding the parameters of decentralized PID controllers for the TITO processes has been developed in subsection 4.5.1. The controller parameters are designed for the SISO models of the TITO process for specified loop phase and gain margins. The controller scheme is modified by inserting proportional controllers in the inner feedback paths, thereby, reducing the loop interaction and improving the stability of the process. From the simulation, it is observed that the method gives improved performances with respect to overshoot, settling time and speed of responses.

Chapter 5

Model-Free Controller Design

5.1 Introduction

The auto-tuning of PID controllers which do not require a mathematical model of the process was first suggested by Ziegler and Nichols [36] in 1942. The tuning method is basically based on the concepts of the critical point on the process Nyquist curve as discussed in section 4.3 of chapter 4. The critical point is obtained by inserting a proportional controller of suitable gain in the error path of the feedback control loop that makes the process output oscillatory. Thereafter, many contributions have been made to improve the above tuning technique. Åström and Hägglund [2] used a relay in place of proportional controller for the automatic tuning of PID controllers. The auto-tuning method is improved by using a modified relay [20, 22], iterative feedback tuning [33] and on-line non-iterative method [39].

In this chapter, we propose a modified relay based automatic tuning method for stable processes. The proposed method has the following advantages. Firstly, the method estimates the critical gain and critical frequency more accurately than the existing conventional relay auto-tuning methods due to the presence of the PI controller in the modified relay. Secondly, the auto-tuning method gives a symmetrical and smooth limit cycle output in presence of static load disturbance and measurement noise thereby improving the measurement accuracy of the critical gain and critical frequency. Finally, the method does not require prior information about the process and needs to design only two controller parameters (a proportional gain and a derivative time constant) from the modified relay experiment.

5.2 Proposed Auto-tuning Scheme

The proposed auto-tuning scheme is shown in Fig. 5.1. The modified relay comprises of an ideal relay, N, connected in series with a PI controller of unity proportional gain, $G_{cN}(s)$. The static load disturbance L and the random additive noise M appear at the input and output of the process, respectively. The auto-tuning of PID controller is carried out based on the criterion that the closed loop system maintains a phase margin of at least 30^0 during the process identification and control.

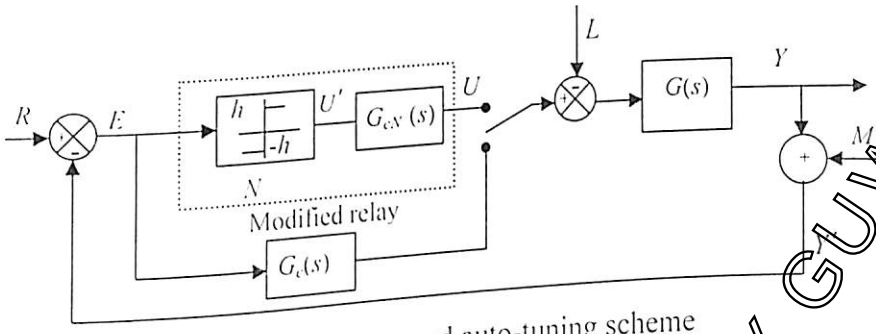

Fig.5.1. Proposed auto-tuning scheme

The series form of the PID controller given in (2.51) is used for analysis in the proposed method. The PID controller can be expressed as

$$G_c(s) = G_{cN}(s)G_{cPD}(s) \tag{5.1}$$

where

$$G_{cN}(s) = \left(1 + \frac{1}{T_I' s}\right) \tag{5.2}$$

$$G_{cPD}(s) = K_c'\left(1 + T_d' s\right) \tag{5.3}$$

The auto-tuning test is carried out in two stages of relay test as T_I' of $G_{cN}(s)$ is unknown initially. In the initial stage, the value of T_I' is chosen between 10-20 so as to induce the limit cycle output with a critical frequency ω_{cr}'. Thereafter, T_I' is updated using the expression (referring (5.2))

$$T_I' = \frac{1}{\omega_{cr}' \tan\phi'} \tag{5.4}$$

where, $\phi' \geq 30^0$ is the user defined phase angle. Then, the modified relay in the feedback loop induces limit cycle output with a critical frequency ω_{cr} in the second stage. From extensive simulation, it is found that the frequency ω_{cr} is less than ω_{cr}' for stable processes for the suggested initial choice of T_I'. Therefore, the phase angle contributed by the modified relay $\phi = \tan^{-1}\left(\frac{1}{\omega_{cr} T_I'}\right)$ is more than ϕ'. The Nyquist curves of the uncompensated process, the process with the modified relay and the process with the

controller are shown in Fig. 5.2. The modified relay identifies a point in the third quadrant (A_1 in Fig. 5.2) with the critical frequency ω_{cr} that lags from the negative real axis by an angle of ϕ. The loop phase margin ϕ_m is calculated with respect to the gain crossover point A_2 as shown in Fig. 5.2 which is more than 30^0 for a user defined phase angle of $\phi' \geq 30^0$ ensuring a stable limit cycle output. Once the identification is over, the PID controller is designed based on the limit cycle parameters obtained from the second stage of relay test. The integral time constant of the PID controller is the integral time constant of G_{cN}. The remaining controller parameters K_c' and T_d' are designed using the amplitude and frequency of the limit cycle output signal.

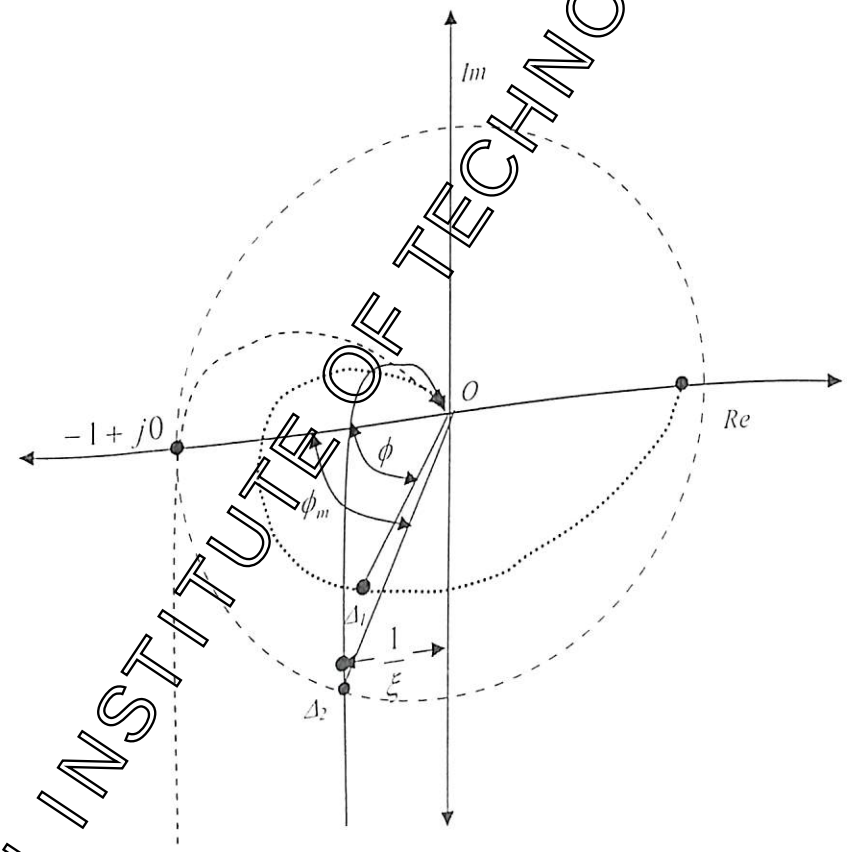

Fig. 5.2. Nyquist curves of the uncompensated process (.....), the process with the modified relay (-----) and the process with the controller (—)

5.3 Accuracy of the Proposed Scheme

The describing function analysis produces accurate results only when the limit cycle is near sinusoidal and this is certainly not the case with the majority of processes. The describing function approximation leads to estimation error in the critical gain and frequency. In the proposed method, the ratios of amplitudes of the harmonic components to the fundamental decrease because of integral action of the PI controllers in the modified relay. Thus the accuracy of the describing function analysis is improved. Let $e(t) = A\sin\omega t$ be the input signal to the modified relay where A is the peak amplitude of the error signal. The ideal relay output $u'(t)$, in response to $e(t)$, is a square wave with the fundamental frequency ω. Using Fourier series expansion, the periodic output $u'(t)$ can be written as

$$u'(t) = \sum_{k=1}^{r} \mu'_{2k-1} \sin\left((2k-1)\omega t\right) \tag{5.5}$$

where $\mu'_{2k-1} = \dfrac{4h}{\pi(2k-1)}$ are the amplitudes of the harmonic components of $u'(t)$ and h is the relay height. The amplitude ratios of higher harmonic components to the fundamental component of ideal relay output are given in Table 5.1. The expression of the output of the modified relay $u(t)$ is

$$u(t) = \sum_{k=1}^{r} \mu'_{2k-1} \sin\left((2k-1)\omega t\right) + \sum_{k=1}^{r} \frac{\mu'_{2k-1}}{\omega T_I'(2k-1)} \sin\left((2k-1)\omega t - \frac{\pi}{2}\right) \tag{5.6}$$

The expression for the amplitudes of the frequency components of $u(t)$ can be written as

$$\mu_{2k-1} = \frac{4h}{\pi(2k-1)^2}\sqrt{(2k-1)^2 + \frac{1}{(\omega T_I')^2}} \tag{5.7}$$

Table 5.1 indicates that the modified relay reduces the effect of 3rd, 5th, 7th and 9th harmonics from 33% to 11%, 20% to 4%, 14% to 2% and 11% to 1%, respectively.

Table 5.1 Harmonic analysis of relay methods

Ideal relay				Modified relay			
μ'_3/μ'_1	μ'_5/μ'_1	μ'_7/μ'_1	μ'_9/μ'_1	μ_3/μ_1	μ_5/μ_1	μ_7/μ_1	μ_9/μ_1
0.3333	0.2	0.1429	0.1111	0.1111	0.0400	0.0204	0.0123

5.4 Effects of Load Disturbance and Measurement Noise

The static disturbances during the ideal relay feedback test result in an asymmetrical limit cycle output that leads to errors in the estimates of the limit cycle parameters. Because of the integral action in the loop in the proposed scheme, the effects of load disturbance is eliminated successfully as described in the subsection 2.2.1.5 of chapter 2. Again, another problem in estimating limit cycle parameters is the measurement noise. Fourier series based curve fitting technique discussed in subsection 2.2.1.6 is used in this work to obtain the best fit output signal from the noisy one.

5.5 Controller Design

During an auto-tuning test, the modified relay induces the limit cycle output with a user defined phase of ϕ' degree. According to the Nyquist stability criterion, limit cycle exists when

$$NG_{cN}G(j\omega_{cr}) = -1 \tag{5.8}$$

Using (5.2) in (5.8), one obtains

$$G(j\omega_{cr}) = \frac{\cos\phi}{N} e^{j(-180+\phi)} \tag{5.9}$$

where $|G_{cN}(j\omega_{cr})| = \dfrac{1}{\cos\phi}$ and $\phi = \tan^{-1}\left(\dfrac{1}{\omega_{cr}T_l'}\right)$.

At the critical frequency, the process $G(j\omega_{cr})$ has the phase lag of $-180+\phi$ degrees and its Nyquist curve passes through the point A_l in the 3rd quadrant as shown in Fig. 5.2. The controller is tuned based on the following design criteria. Firstly, the phase lag of the loop transfer function $G_c G(j\omega_{cr})$ is to be $-180+\phi$ degrees so as to maintain the minimum phase margin of 30^0. Secondly, the real part of $G_c G(j\omega_{cr})$ is set to $-\dfrac{1}{\xi}$ where $\xi > 1$. The design parameter ξ satisfies both the gain margin (g_m) and phase margin (ϕ_m) requirements because $g_m > \xi$ and $\phi_m > \cos^{-1}(1/\xi)$. The closed loop performance of the process can be improved with the proper choice of ξ. Then, the design criteria become

$$\angle G_c G(j\omega_{cr}) = -180 + \phi \tag{5.10}$$

$$|G_c G(\omega_{cr})| \cos\phi = \frac{1}{\xi} \tag{5.11}$$

With the help of (5.1-5.3) and (5.9-5.11), it is easy to obtain

$$\angle G_{cPD}(j\omega_{cr}) = \phi \tag{5.12}$$

$$|G_{cPD}(j\omega_{cr})| = \frac{N}{\xi \cos\phi} \tag{5.13}$$

Solving (5.12) and (5.13), the expressions for the proportional gain and derivative time constant of the PID controller become

$$\left.\begin{aligned} K_c' &= \frac{4h}{\pi A \xi} \\ T_d' &= \frac{\tan\phi}{\omega_{cr}} \end{aligned}\right\} \tag{5.14}$$

Similarly, the expression for the integral time constant of the PID controller using (5.2) is

$$T_I' = \frac{1}{\omega_{cr} \tan\phi} \tag{5.15}$$

The PID controller parameters K_c', T_I' and T_d' are thus found using (5.14) and (5.15). Thereafter, the PID controller parameters K_c, T_I and T_d of (2.7) are obtained using the expressions given in (2.52-2.54). The following steps are suggested for the automatic tuning of the PID controller.

- The auto-tuning test starts with the initial choice of T_I' value which is between 10 and 20 for stable processes. Next, T_I' is updated using (5.4) for a user-defined phase angle of $\phi' \geq 30^0$ before beginning of the second stage of relay test.
- The amplitude A and the frequency ω_{cr} of the limit cycle output are measured in the second stage of the auto-tuning test. The parameters of the PID controller are then obtained from (5.14) and (5.15) for a chosen value of ξ.
- For fine-tuning of the controller, the above steps may be repeated with different user defined phase angles, ϕ'.

5.6 Simulation Results

Two typical stable processes and a non-minimum phase process are considered in this section and two high-order process are taken in appendix B3 for the simulation studies to show the robustness and effectiveness of the new auto-tuning method. Initially, setting $T_l' = 20$ the relay experiment is performed to obtain the limit cycle parameters ω_{cr}' for the processes in the following examples. Thereafter, the value of T_l' is updated for a user defined phase angle of $\phi' \geq 30^0$. The critical gain and frequency are estimated from the second stage of relay test. Then, the controller parameters are obtained from (5.14) and (5.15). A relay with height $h = 0.5$ is considered in all the examples. Again, the value of the derivative filter constant is chosen to be 1% of the derivative time constant of the PID controller.

Example 5.1

Considers a second order stable process transfer function with repeated roots [39]

$$G(s) = \frac{e^{-s}}{(s+1)^2}.$$

For a user-defined $\phi' = 30^0$, T_l' is updated as 1.3414 before beginning the second stage of auto-tuning test. The modified relay induces limit cycle output giving the phase lag of $\phi = 38.5414^0$ (see Fig. 5.2). A measurement noise $M(0, \sigma_M^2 = 0.0917 \times 10^{-2})$ is added to the process output during the relay test. The noisy output signal with SNR = 20dB and the recovered signal obtained from the curve fitting method are shown in Fig. 5.3. The PID controller parameters are designed using $\xi = 2$ and (5.14-5.15). The estimated PID parameters along with those suggested by Åström and Hägglund [2], Tan et al. [39] and Ziegler and Nichols [36] are given in Table 5.2. The closed loop output responses to a unit step input and a step load disturbances of magnitude 0.5 at 40 sec are shown in Fig.5.4. As is evident from Fig. 5.4(a), Åström and Hägglund's PID shows overdamped and sluggish responses to both the inputs. The Ziegler and Nichols's method gives improved disturbance rejection with poor set-point response. Highly oscillatory closed loop responses are obtained by Tan et al.'s PID controller. However, the proposed method gives excellent control for the second order process in terms of the overshoot, speed of response and settling time for both

the set-point and load disturbance inputs. To test robustness of the proposed auto-tuning method, it is assumed that there are ±10% of parameter perturbations in K, T and D, respectively. Figs. 5.4(b), 5.4(c) and 5.4(d) show that the proposed method is robust to parameter perturbation in this example.

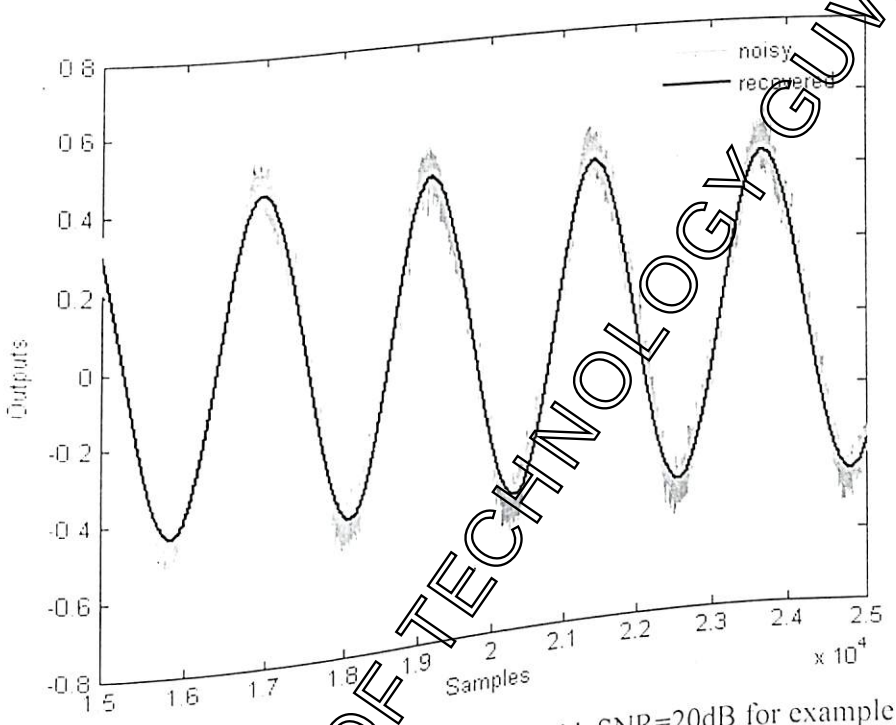

Fig. 5.3. Recovered and noisy output signal with SNR=20dB for example 5.1

Table 5.2 PID controller settings for example 5.1

Methods	PID controller parameters
Proposed	$1.1443\left(1+\frac{1}{2.1926s}+\frac{0.5208s}{0.0052s+1}\right)$
Åström and Hägglund	$0.8940\left(1+\frac{1}{3.6680s}+0.9170s\right)$
Tan et al.	$0.621\left(1+\frac{1}{0.9s}+0.23s\right)$
Ziegler and Nichols	$1.5325\left(1+\frac{1}{2.388s}+0.5970s\right)$

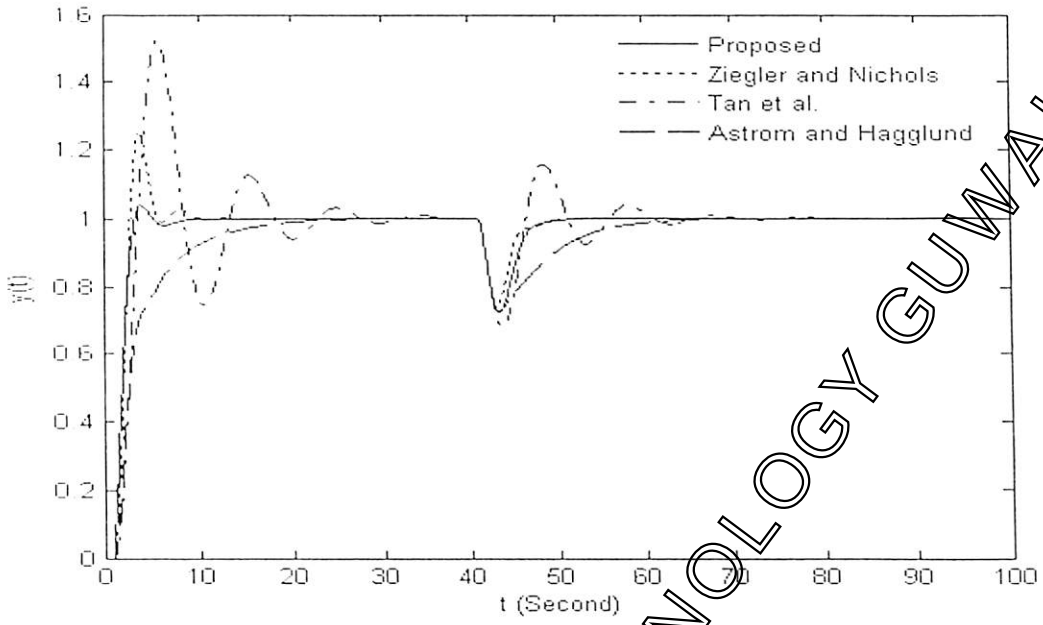

Fig.5.4 (a). Closed loop responses to step input and load disturbance for example 5.1

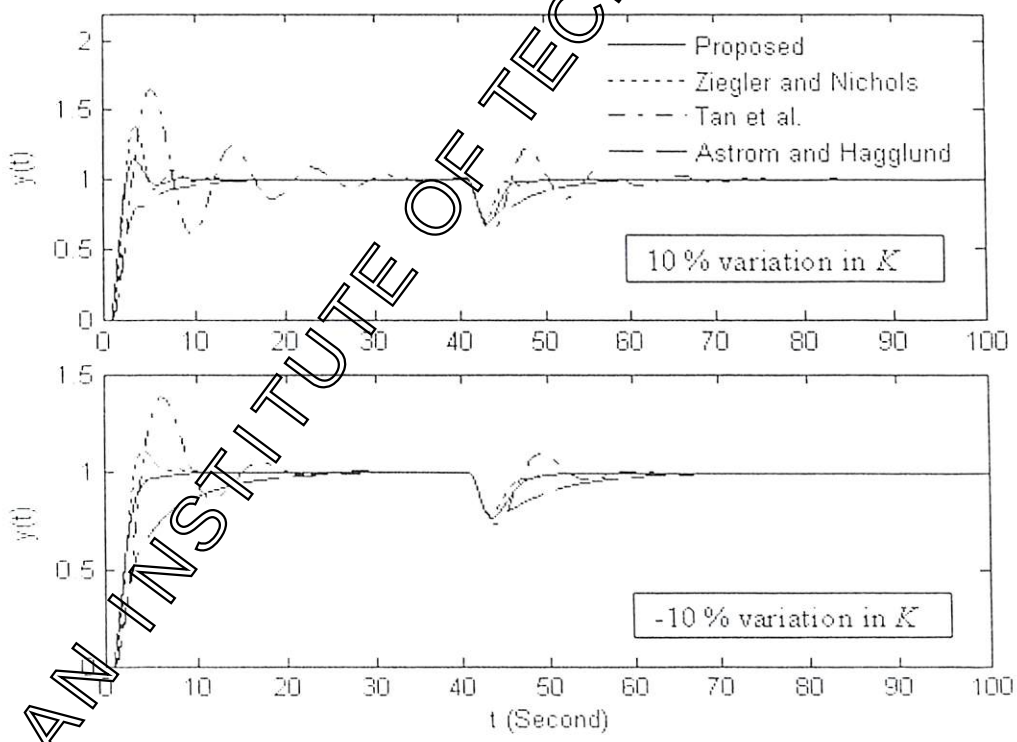

Fig.5.4 (b). Closed loop responses to step input and load disturbance with ±10% variation in K for example 5.1

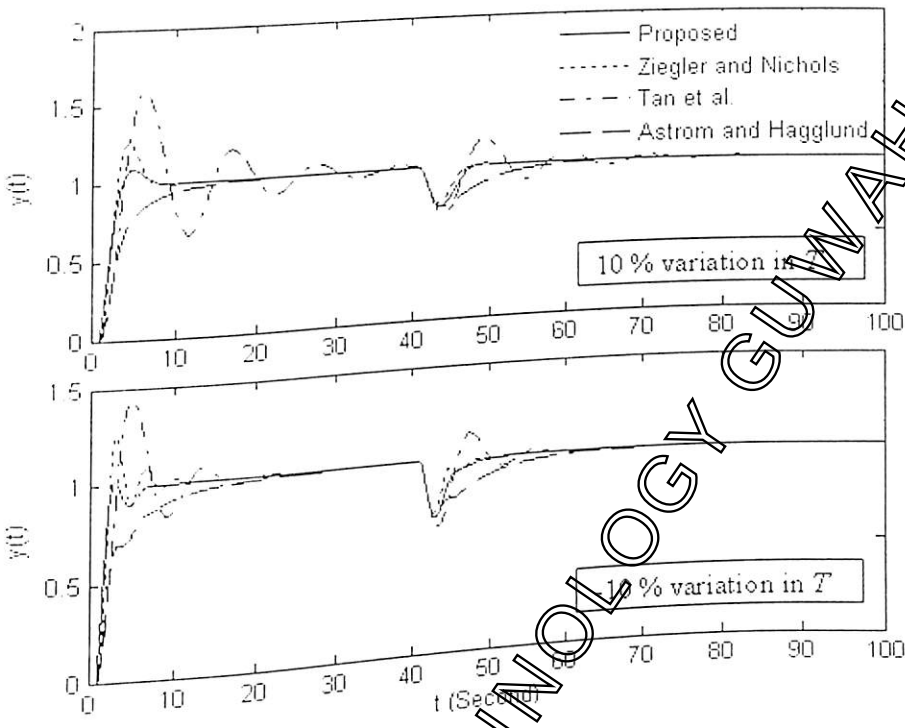

Fig.5.4 (c). Closed loop responses to step input and load disturbance with ±10% variation in T for example 5.1

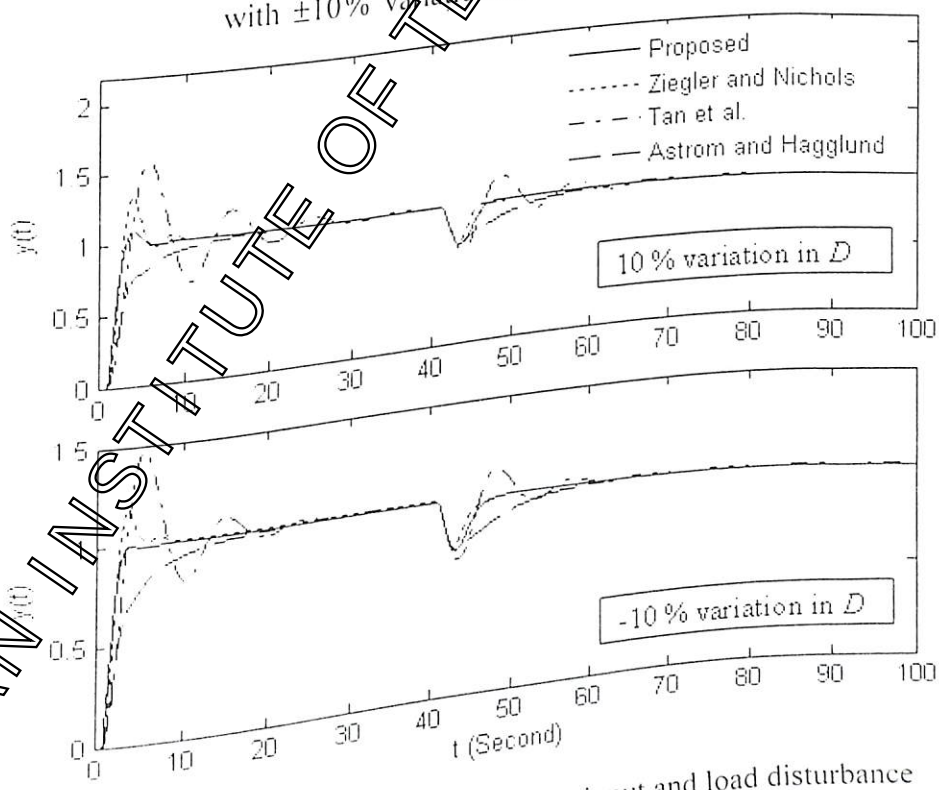

Fig.5.4 (d). Closed loop responses to step input and load disturbance with ±10% variation in D for example 5.1

Example 5.2

This example considers a sixth order process [33] with the transfer function

$$G(s) = \frac{1}{(s+1)^6}.$$

The integral time constant T_i' is estimated as 3.1045 during the auto-tuning test using $\phi' = 30^0$. The noisy limit cycle output with SNR = 20dB which results upon the addition of $M(0, \sigma_N^2 = 0.0970 \times 10^{-2})$ during the modified relay experiment and the recovered signal are shown in Fig. 5.5. Using (5.14) and (5.15) and the recovered limit cycle data, the PID parameters are estimated with the choice of $\xi = 2$. The methods proposed by Åström and Hägglund [2], Ho et al. [33] and Ziegler and Nichols [36] have been considered for comparison of the results. Table 5.3 gives the PID controller parameters designed by the above mentioned methods. Fig. 5.6 shows the responses of the controller settings to unit step reference and step load disturbance of magnitude 0.05 appearing at 80 seconds.

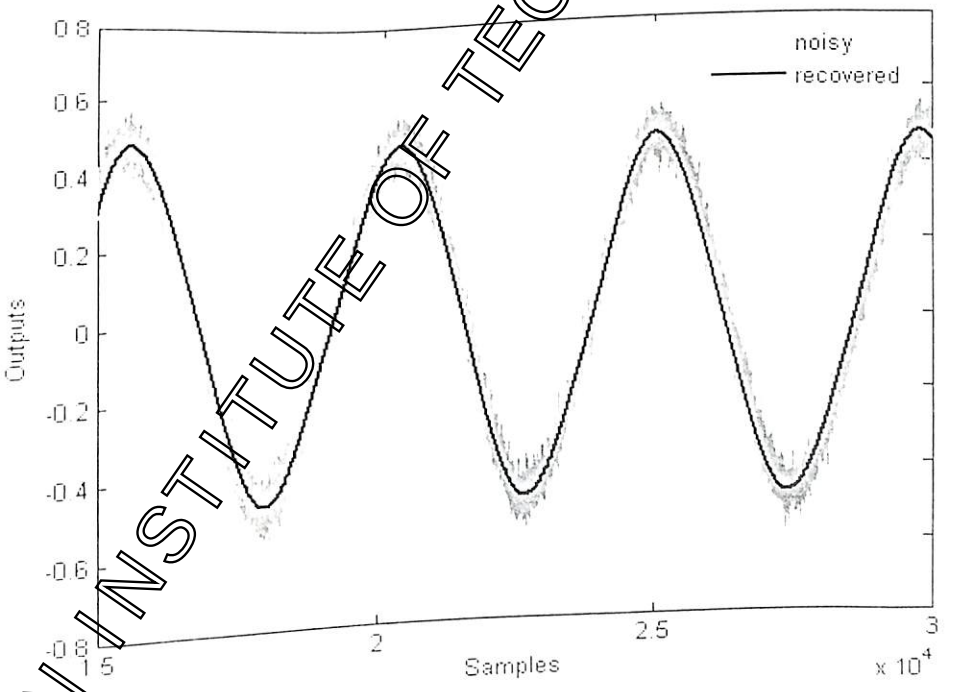

Fig. 5.5. Recovered and noisy output signal with SNR=20dB for example 5.2

Table 5.3 PID controller settings for example 5.2

Methods	PID controller parameters
Proposed	$1.0384\left(1+\frac{1}{4.7433s}+\frac{1.0726s}{0.0107s+1}\right)$
Åström and Hägglund	$0.8200\left(1+\frac{1}{8.3589s}+2.0897s\right)$
Ho et al.	$1.3\left(1+\frac{1}{5.291s}+\frac{1.3s}{0.13s+1}\right)$
Ziegler and Nichols	$1.4057\left(1+\frac{1}{5.4420s}+1.3605s\right)$

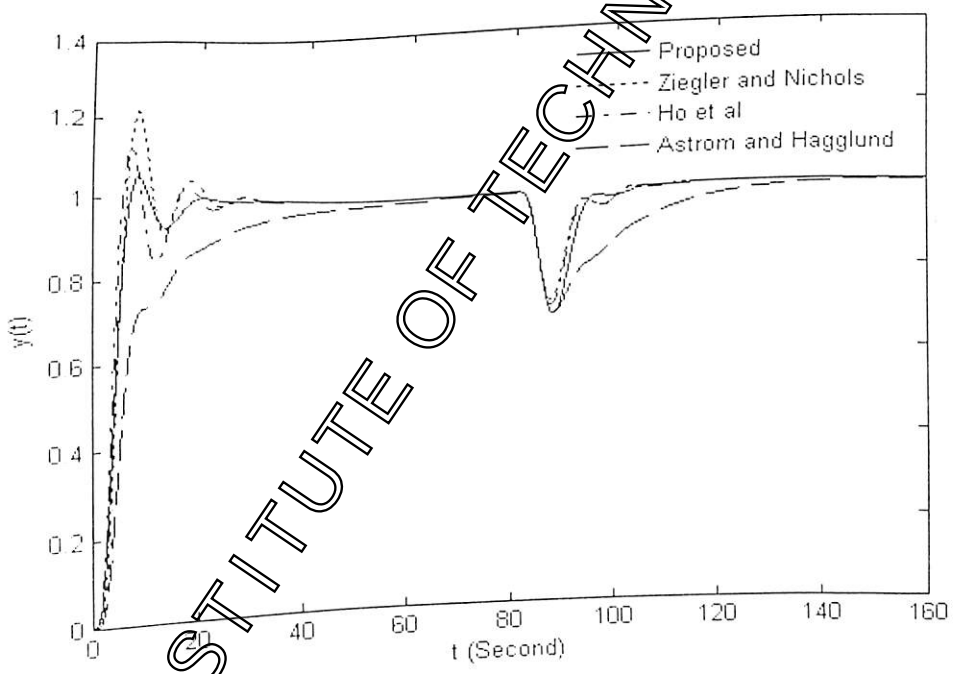

Fig.5.6. Closed loop responses to step input and load disturbance for example 5.2

It is clear from Fig.5.6 that Ziegler and Nichols's and Ho et al.'s methods show more overshoot with almost similar disturbance rejection ability. The method proposed by Åström and Hägglund reduces the overshoot, however, the responses are sluggish. The overall comparisons show that the proposed method gives faster response with shorter settling time and good disturbance rejection ability in comparison to the other three.

Example 5.3

A non-minimum phase process with the transfer function $G(s) = \dfrac{1-5s}{(1+10s)(1+20s)}$ is considered. The relay auto-tuning test is carried out with a user defined phase angle of $\phi' = 45^0$ which results subsequently in $T_l' = 8.1981$ and $\phi = 56.68^0$. The additive random noise $M(0, \sigma_M^2 = 0.188\times10^{-2})$ is introduced at the process output during the relay experiment. Fig. 5.7 shows the corresponding noisy output signal with SNR = 20dB and the recovered output signal. Table 5.4 gives the controller settings by the proposed method for a design value of $\xi = 1.2$. For comparison, Åström and Hägglund's method [2] and Ziegler and Nichols's method are considered and their controller parameters are given in Table 5.4. The closed loop performances of all the controllers are shown in Fig. 5.8. The magnitude of the step load disturbance applied at 130 sec is 0.5. Results have been compared with those obtained with the usual technique based on the relay feedback. It is clear from Fig. 5.8 that the overall performance of the proposed method is satisfactory with respect to the other methods.

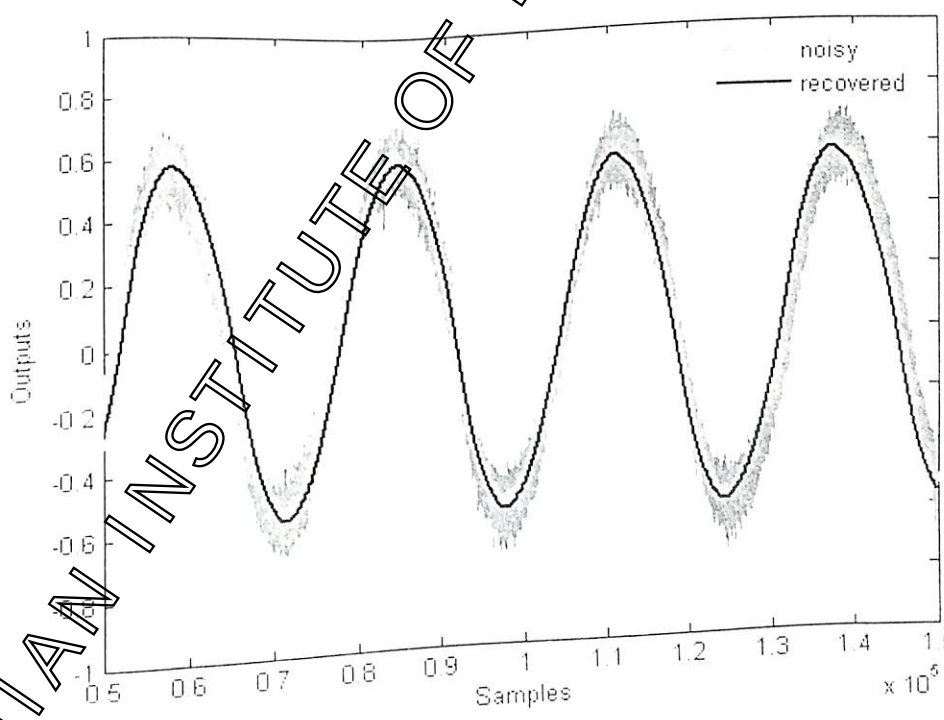

Fig. 5.7. Recovered and noisy output signal with SNR=20dB for example 5.3

Table 5.4 PID controller settings for example 5.3

Methods	PID controller Parameters
Proposed	$3.4744\left(1+\frac{1}{27.1732s}+\frac{5.7247s}{0.0572s+1}\right)$
Åström and Hägglund	$4.4563\left(1+\frac{1}{29.5649s}+7.3912s\right)$
Ziegler and Nichols	$7.6394\left(1+\frac{1}{19.2480s}+4.8120s\right)$

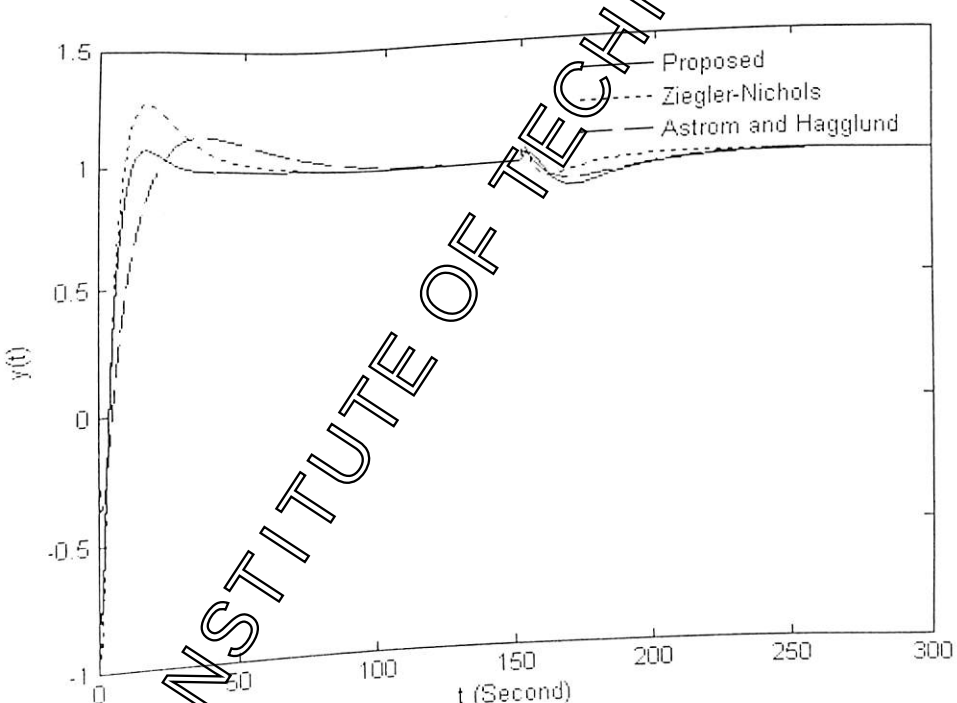

Fig.5.8. Closed loop responses to step input and load disturbances for example 5.3

5.7 Conclusions

In this work, a modified relay based auto-tuning method for the PID controller is proposed. The method improves the describing function approximation and ensures a symmetrical and smooth limit cycle output compared to the conventional relay based auto-tuning methods even in the presence of static load disturbance and measurement noise. The distance of the Nyquist curve of the loop transfer function from the imaginary axis of complex plane and the loop phase margin are used in designing the controller parameters. The proposed control method has been illustrated by various typical process transfer functions. It shows improved results as compared to some previous work on PID control for stable processes.

Chapter 6

Conclusions

This thesis has investigated various identification and control methods for SISO and TITO processes based on relay induced limit cycles. In the following concluding remarks we first briefly summarize the main contributions of the thesis and then discuss about the various possible extensions.

6.1 Summary

Relay feedback identification and control are two topics in control engineering that present many interesting problems. The main purpose of this thesis has been to investigate some relay based identification and control methods for SISO and TITO processes.

In chapter 2, relay based on-line identification methods for stable and unstable SISO processes are proposed. At first, the DF analysis is used and simple expressions are derived to obtain the FOPDT process model parameters. The method estimates the model parameter with less estimation error as compared to some recent identification methods available in the literature. Further, the on-line identification structure (relay with PID controller) is modified (relay with PI-PD controller) to improve the accuracy of the method. The modified identification structure gives significantly improved estimates of the model parameters for unstable processes. The accuracy of the method depends on the estimation of the critical gain (K_{cr}) which is not accurate for some typical processes in case of DF analysis. Hence, an exact method using the state space analysis is proposed for the on-line identification of stable and unstable processes in subsection 2.2.2. The advantage of this method is that it does not require any approximation to estimate model parameters. It is shown in simulation examples that the exact identification method gives better estimates than the describing function method. However, one needs to solve simultaneously a set of nonlinear equations to estimate the model parameters. This is not the case with the describing function analysis. Therefore, although approximation is involved, the DF analysis is generally preferred for the relay feedback systems.

The effects of static load disturbances during the on-line identification is successfully removed by the continuous action of the integral controller in the loop and best fit limit cycle is obtained from the noisy one using the Fourier series based curve fitting method. Although the Fourier series based curve fitting method enables one to obtain the best fit noise-free limit cycle, it is a time consuming process and the noisy signal being feedback to the relay results in multiple switching. These limitations are taken care of by inserting an

adaptive low pass filter in the feedback path. The method is able to estimate the model parameters accurately even in the presence of load disturbance and measurement noise from a single relay test.

Chapter 3 presents some identification methods for the TITO processes. An on-line identification method for TITO processes for the decentralized relay based tests is presented in the subsection 3.2.1. The proposed method identifies two second order plus delay SISO transfer function models of the process in the presence of load disturbance and measurement noise. A modification of the identification method is given in the subsection 3.2.2 by inserting proportional controllers in the inner feedback loops. The proportional controllers stabilize the process and reduce the loop interaction at critical frequency thereby increasing the accuracy of the identified model. Further, a P_relay based identification method is proposed in section 3.3 for the identification of two SISO transfer function models of the process from a single relay test in the presence of large loop interaction and measurement noise. The novelty of the proposed approach lies in that it successfully reduces the loop interactions and can cope with the presence of measurement noise during the process identification. Most importantly, the steady state gains of the transfer function models are estimated in a simple manner.

Some controller design methods are provided in chapter 4. Firstly, simple formulae are derived to design PID controller for stable and unstable FOPDT processes to meet gain and phase margin specifications. Further, the method is extended to design PI-PD controller to improve the controller performances. The PD controller in the inner feed back loop plays an important role in stabilizing the open loop processes. Also, it avoids the chance of derivative kick which is possible due to the presence of derivative action in the forward path. A method for finding the parameters of decentralized controllers for a TITO process based on the loop phase and gain margins is presented in subsection 4.5.1. The controller parameters are tuned on-line without disrupting the closed loop operation. The controller scheme is modified by inserting proportional controllers in the inner feedback paths to improve the control performances.

A modified relay based auto-tuning method for PID controller is proposed in chapter 5. The method does not require the intermediate stage (identification of process model), improves the describing function approximation and ensures a symmetrical and noise free limit cycle

output even in the presence of static load disturbance and measurement noise. The distance of the Nyquist curve of the loop transfer function from the imaginary axis of complex plane and the loop phase margin are used in designing the controller parameters. The proposed control method has illustrated by various typical process transfer functions. It shows improved results as compared to some previous work on PID control for stable processes.

6.2 Future Work

Some identification and control methods have been proposed in this thesis. However, it is still possible to undertake further extensions of the proposed research work. Some of the issues that require further investigations are explained below.

1. The on-line identification method for SISO processes using the DF analysis is very simple and efficient. But, the error in the estimation of the critical gains (K_{cr}) is significant due to the approximations involved in DF method specially for under damped and delay dominated processes . The above problem is overcome by using the state space analysis. However, the method requires solving nonlinear equations which again gives estimation errors for incorrect choice of initial solutions. Hence, further scope to obtain an exact model of the process dynamics using some exact methods exists.
2. In chapter 3, different identification methods for highly interactive TITO processes are proposed. The loop interaction is reduced during the identification of process model to improve the accuracy. However, the method is not able to eliminate the loop interaction. The accuracy of the identification method will be improved if the loop interaction is eliminated during the identification.
3. There are many ways to improve the controller design methods for the multivariable processes. Chapter 4 gives controller design methods based on the model of the TITO process. But, the model based design methods depend on efficient and reliable modeling of the process dynamics. Chapter 5 provides a step in this direction, by presenting an auto-tuning method for SISO processes where parametric model identification is not required. The same technique may be extended for the control of TITO processes.

We proposed a modified relay based auto-tuning method for stable processes (in chapter 5) that shows improved results over some existing techniques. So, the

extension of the auto-tuning method for unstable and integrating processes may prove useful.

5. The identification and control methods proposed in the thesis are applicable only to the linear time-invariant processes. Hence, the techniques may be extended for nonlinear processes.

Appendix A

A1 Derivation of Steady State Gains (Subsection 3.2.1.2)

Looking at Fig. 3.1 (neglecting the effect of disturbance and measurement noise), the expressions for the process inputs ($U_1(s)$ and $U_2(s)$) and outputs ($Y_1(s)$ and $Y_2(s)$) at two different set-point or reference inputs (R_1 and R_2) can be written as

$$\begin{bmatrix} Y_1^1 \\ Y_2^1 \\ Y_1^2 \\ Y_2^2 \end{bmatrix} = \begin{bmatrix} U_1^1 & U_2^1 & 0 & 0 \\ 0 & 0 & U_1^1 & U_2^1 \\ U_1^2 & U_2^2 & 0 & 0 \\ 0 & 0 & U_1^2 & U_2^2 \end{bmatrix} \begin{bmatrix} G_{11} \\ G_{12} \\ G_{21} \\ G_{22} \end{bmatrix} \tag{A.1}$$

The dependency on s is suppressed in the expressions for ease in analysis. Solving (A.1), one obtains

$$\begin{bmatrix} G_{11} \\ G_{12} \\ G_{21} \\ G_{22} \end{bmatrix} = \frac{1}{(U_1^1 U_2^2 - U_1^2 U_2^1)} \begin{bmatrix} U_2^2 & 0 & -U_2^1 & 0 \\ -U_1^2 & 0 & U_1^1 & 0 \\ 0 & U_2^2 & 0 & -U_2^1 \\ 0 & -U_1^2 & 0 & U_1^1 \end{bmatrix} \begin{bmatrix} Y_1^1 \\ Y_2^1 \\ Y_1^2 \\ Y_2^2 \end{bmatrix} \tag{A.2}$$

If the process is decoupled by using the decoupler given in [51], the effective transfer function of each loop can be expressed as

$$\left.\begin{aligned} G_1 &= \frac{G_{11}G_{22} - G_{12}G_{21}}{G_{22}} \\ G_2 &= \frac{G_{11}G_{22} - G_{12}G_{21}}{G_{11}} \end{aligned}\right\} \tag{A.3}$$

Using (A.2) in (A.3), we obtain

$$\left.\begin{aligned} G_1 &= \frac{(U_2^2 Y_1^1 - U_2^1 Y_1^2)(U_1^1 Y_2^1 - U_1^2 Y_1^1) - (U_1^1 Y_2^1 - U_1^2 Y_1^1)(U_2^2 Y_1^1 - U_2^1 Y_2^2)}{(U_1^1 Y_2^1 - U_1^2 Y_1^1)(U_1^1 U_2^2 - U_1^2 U_2^1)} \\ G_2 &= \frac{(U_2^2 Y_1^1 - U_2^1 Y_1^2)(U_1^1 Y_2^1 - U_1^2 Y_1^1) - (U_1^1 Y_2^1 - U_1^2 Y_1^1)(U_2^2 Y_1^1 - U_2^1 Y_2^2)}{(U_2^2 Y_1^1 - U_2^1 Y_1^2)(U_1^1 U_2^2 - U_1^2 U_2^1)} \end{aligned}\right\} \tag{A.4}$$

where G_1 and G_2 are the effective transfer functions between Y_1, U_1 and Y_2, U_2 respectively. Hence, the steady state gains can be estimated by taking the average values of process inputs and outputs during the relay test. Therefore, the expression for the steady state gains can be written as

$$\left.\begin{aligned} K_1 &= \frac{\chi}{(u^1_{1avg}.y^2_{2avg} - u^2_{1avg}.y^2_{1avg})(u^1_{1avg}u^2_{2avg} - u^2_{1avg}u^1_{2avg})} \\ K_2 &= \frac{\chi}{(u^2_{2avg}.y^1_{1avg} - u^1_{2avg}.y^1_{2avg})(u^1_{1avg}u^2_{2avg} - u^2_{1avg}u^1_{2avg})} \end{aligned}\right\} \quad (A.5)$$

where

$$\chi = (u^2_{2avg}.y^1_{1avg} - u^1_{2avg}.y^1_{2avg})(u^1_{1avg}.y^2_{2avg} - u^2_{1avg}.y^2_{1avg}) - (u^1_{1avg}.y^1_{2avg} - u^2_{1avg}.y^1_{1avg})(u^2_{2avg}.y^1_{1avg} - u^1_{2avg}.y^2_{2avg})$$

and the subscript avg indicates the average value of the concerned variables (subsection 3.2.1.2).

A2 Derivation of Steady State Gains (Subsection 3.3.4)

Looking at Fig. 3.5, the expressions for the inputs of the process in conjunction with the noise filters ($\bar{U}_1(s) = G_{II}U_1(s)$ and $\bar{U}_2(s) = G_{II}U_2(s)$) and the filtered output signals (Y'_1 and Y'_2) at two different set-point or reference inputs (R_1 and R_2) can be written as

$$\begin{bmatrix} Y'^1_1 \\ Y'^1_2 \\ Y'^2_1 \\ Y'^2_2 \end{bmatrix} = \begin{bmatrix} \bar{U}^1_1 & \bar{U}^1_2 & 0 & 0 \\ 0 & 0 & \bar{U}^1_1 & \bar{U}^1_2 \\ \bar{U}^2_1 & \bar{U}^2_2 & 0 & 0 \\ 0 & 0 & \bar{U}^2_1 & \bar{U}^2_2 \end{bmatrix} \begin{bmatrix} G_{11} \\ G_{12} \\ G_{21} \\ G_{22} \end{bmatrix} \quad (A.6)$$

The dependency on s is suppressed in the expressions for ease in analysis. As explained in Appendix A1, (A.6) can be simplified as

$$\begin{bmatrix} G_{11} \\ G_{12} \\ G_{21} \\ G_{22} \end{bmatrix} = \frac{1}{(\bar{U}^1_1\bar{U}^2_2 - \bar{U}^2_1\bar{U}^1_2)} \begin{bmatrix} \bar{U}^2_2 & 0 & -\bar{U}^1_2 & 0 \\ -\bar{U}^2_1 & 0 & \bar{U}^1_1 & 0 \\ 0 & \bar{U}^2_2 & 0 & -\bar{U}^1_2 \\ 0 & -\bar{U}^2_1 & 0 & \bar{U}^1_1 \end{bmatrix} \begin{bmatrix} Y'^1_1 \\ Y'^1_2 \\ Y'^2_1 \\ Y'^2_2 \end{bmatrix} \quad (A.7)$$

Using (A.7) in (A.5), we obtain

$$\left.\begin{aligned} G_1 &= \frac{(\bar{U}^2_2Y'^1_1 - \bar{U}^1_2Y'^1_2)(\bar{U}^1_1Y'^2_2 - \bar{U}^2_1Y'^2_1) - (\bar{U}^1_1Y'^1_2 - \bar{U}^2_1Y'^1_1)(\bar{U}^2_2Y'^1_1 - \bar{U}^1_2Y'^2_2)}{(\bar{U}^1_1Y'^2_2 - \bar{U}^2_1Y'^2_1)(\bar{U}^1_1\bar{U}^2_2 - \bar{U}^2_1\bar{U}^1_2)} \\ G_2 &= \frac{(\bar{U}^2_2Y'^1_1 - \bar{U}^1_2Y'^1_2)(\bar{U}^1_1Y'^2_2 - \bar{U}^2_1Y'^2_1) - (\bar{U}^1_1Y'^1_2 - \bar{U}^2_1Y'^1_1)(\bar{U}^2_2Y'^1_1 - \bar{U}^1_2Y'^2_2)}{(\bar{U}^2_2Y'^1_1 - \bar{U}^1_2Y'^1_2)(\bar{U}^1_1\bar{U}^2_2 - \bar{U}^2_1\bar{U}^1_2)} \end{aligned}\right\} \quad (A.8)$$

Then the expressions for the steady state gains can be written as

$$\left.\begin{aligned} K_1 &= \frac{\bar{\chi}}{(\bar{u}^1_{1avg}.y'^2_{2avg} - \bar{u}^2_{1avg}.y'^2_{1avg})(\bar{u}^1_{1avg}\bar{u}^2_{2avg} - \bar{u}^2_{1avg}\bar{u}^1_{2avg})} \\ K_2 &= \frac{\bar{\chi}}{(\bar{u}^2_{2avg}.y'^1_{1avg} - \bar{u}^1_{2avg}.y'^1_{2avg})(\bar{u}^1_{1avg}\bar{u}^2_{2avg} - \bar{u}^2_{1avg}\bar{u}^1_{2avg})} \end{aligned}\right\} \quad (A.9)$$

where

$$\bar{\chi} = (\bar{u}^2_{2avg}.y'^1_{1avg} - \bar{u}^1_{2avg}.y'^1_{2avg})(\bar{u}^1_{1avg}.y'^2_{2avg} - \bar{u}^2_{1avg}.y'^2_{1avg}) - (\bar{u}^1_{1avg}.y'^1_{2avg} - \bar{u}^2_{1avg}.y'^1_{1avg})(\bar{u}^2_{2avg}.y'^1_{1avg} - \bar{u}^1_{2avg}.y'^2_{2avg})$$

and the subscript avg indicates the average value of the concerned variables (subsection 3.3.4).

Appendix B

B1 Simulation Examples of On-line Identification Methods

In these examples, the proposed limit cycle based online identification method with PID controller in the loop is applied to high order SISO processes with and without time delay. For the assessment of its accuracy, identification error in the frequency domain is considered. The comparison is made with other on-line identification methods i.e. area method [73], step response methods [74], reduced order modeling methods using swarm optimized eigen spectrum analysis [80] and stability equation method [81] to show the performance enhancement. Also, the on-line identification method with PID controller in the loop is illustrated for a typical TITO process.

Example B.1

Consider a high-order process with large time delay

$$G(s) = \frac{e^{-10s}}{(s+1)^2(2s+1)^3}.$$

$K_c = 0.1$, $T_I = 1$ and $T_d = 0$ is used in the initial stage of relay test and the design values of $\alpha = 0.2$, $g_m = 3$ and $\phi_m = 60^0$ are used to obtain the controller parameters for the next stage of test. The controller and the process model parameters of both the stages of the relay test are given in Table B.1. The model parameters obtained by the area method [73] are $K = 1.08$, $T = 3.96$, $D = 14.04$ with $EE = 1.27\%$. The Nyquist curves of the actual process, process models obtained by the area method and by the proposed method are given in Fig. B.1. As seen from the Nyquist curves and Table B.1, the proposed method can estimate the model parameters more accurately than the method given in [73].

Table B.1 Controller and process model parameters for example B.1

Stage 1	$G_c(s)$	$K_c = 0.1, T_I = 1, T_d = 0$	
	$G_m(s)$	$K = 1.0, T = 3.927, D = 14.09$	
Stage 2	$G_c(s)$	$K_c = 0.2725, T_I = 6.1833, T_d = 1.5337$	EE=0.0019
	$G_m(s)$	$K = 1.0, T = 4.12, D = 14.01$	

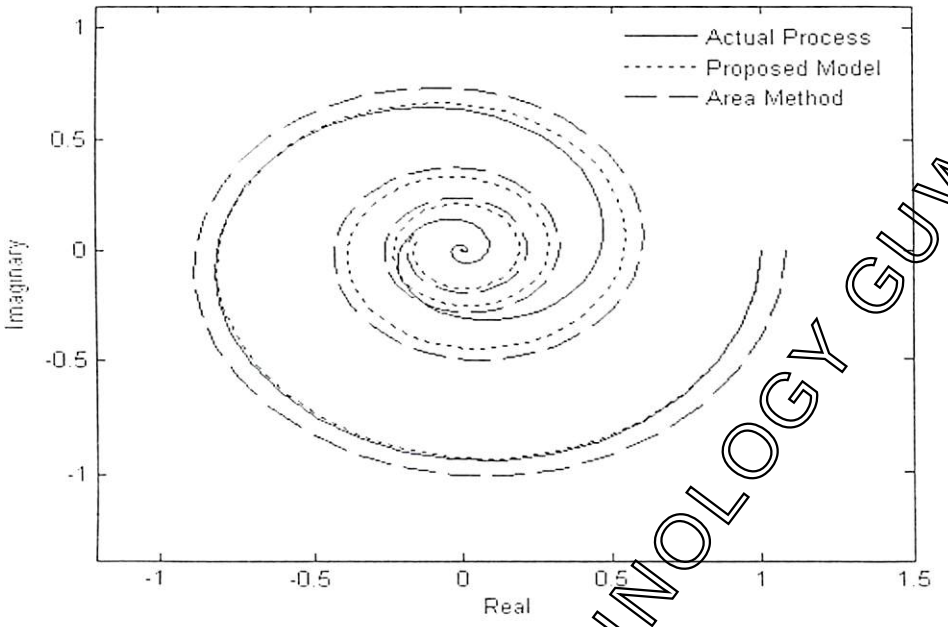

Fig.B.1. Nyquist curves of process models for example B.1

Example B.2

Let the process transfer function of a high-order process without time delay be

$$G(s) = \frac{1}{(s+1)^5}.$$

The relay test starts with the initial controller $K_c = 0.1$, $T_I = 1$ and $T_d = 0$ and then updates the controller using the design values of $\alpha = 0.2$, $g_m = 3$ and $\phi_m = 60^0$. The controller and the process model parameters along with the estimation error index are given in Table B.2. The model parameters obtained by the area method [73] are $K = 1.0$, $T = 2.3772$, $D = 2.6400$ with $EE = 17.48\%$.

Table B.2 Controller and process model parameters for example B.2

Stage 1	$G_c(s)$	$K_c = 0.1, T_I = 1, T_d = 0$	
	$G_m(s)$	$K = 1.0, T = 3.5927, D = 2.6697$	
Stage 2	$G_c(s)$	$K_c = 0.9596, T_I = 4.0960, T_d = 0.4643$	EE=0.0421
	$G_m(s)$	$K = 1.0, T = 3.6021, D = 2.6705$	

The identification method by step response method [74] gives the FOPDT model as $K = 1.0,\ T = 2.60,\ D = 3.31$. The resulting estimation error index by the later method is 12.76%. The proposed method identifies the process dynamics more accurately in terms of the estimation error index in comparison to the above discussed methods.

Example B.3

Let us consider a typical high-order process [80] $G(s) = \dfrac{s^3 + 7s^2 + 24s + 24}{s^4 + 10s^3 + 35s^2 + 50s + 24}$. The relay test is performed and the resulting process model parameters are obtained with the choice of design values $\alpha = 0.2$, $g_m = 3$ and $\phi_m = 60^0$ for controller design required in the second stage of the relay test.

Table B.3 Process models for example B.3

Methods	Identified Models
Proposed	$\dfrac{e^{-0.0005s}}{0.8231s+1}$
Parmar et al.	$\dfrac{0.6349s+4}{s^2+5s+4}$
Chen et al.	$\dfrac{0.6997(s+1)}{s^2+1.4577s+0.6997}$

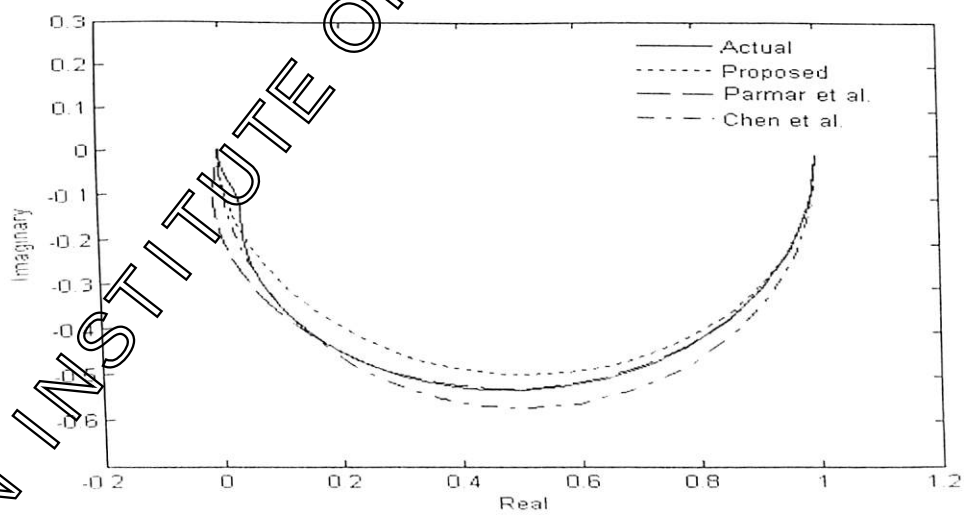

Fig.B.2. Nyquist curves of process models for example B.3

The identified models obtained by Parmar et al. [80], Chen et al.[81] and by proposed methods are given in Table B.3. The Nyquist curves of the actual process and the process models by the above methods are shown in Fig.B.2. Parmar et al. and Chen et al. give second order models whereas the proposed identified model is a first order with time delay. However, it is clear from Fig. B.2 that the Nyquist curves of the proposed model and actual process are close to each other at high frequency which is related to the transient response of the process, showing that the higher order processes can also be approximated by a FOPDT model using the proposed on-line identification method.

Example B.4

Consider a typical time delay TITO process [62] with the transfer matrix

$$\boldsymbol{G}(s) = \frac{1}{s+1}\begin{bmatrix} 2e^{-0.5s} & 0.2e^{-0.1s} \\ 0.3 & 1.1e^{-0.5s} \end{bmatrix}$$

The auto-tuning test starts with the choice of $K'_{ci} = 0.1$, $T'_{Ii} = 1$ and $T'_{di} = 0$. The estimated process model and the controller parameters for both the stages of relay tests are given in Table B.4. The design values $g_{m1} = 2$, $\phi_{m1} = 60^0$ and $g_{m2} = 2$, $\phi_{m2} = 65^0$ are used to calculate the controller settings required for the second stage of the relay test. The accuracy of the identified model is illustrated in the example B.6 and compared with other methods.

Table B.4 Controller and process model parameters for example B.4

	Loop 1	Loop 2
Stage 1	$K'_{c1} = 0.1,\ T'_{I1} = 1,\ T'_{d1} = 0$	$K'_{c2} = 0.1,\ T'_{I2} = 1,\ T'_{d2} = 0$
	$K_1 = 1.0455,\ T_1 = 0.4190,\ D_1 = 0.3103$	$K_2 = 1.04,\ T_2 = 0.3241,\ D_2 = 0.3783$
Stage 2	$K'_{c1} = 0.6055,\ T'_{I1} = 0.8802,\ T'_{d1} = 0.4190$	$K'_{c2} = 0.7188,\ T'_{I2} = 0.4855,\ T'_{d2} = 0.3241$
	$K_1 = 1.9556,\ T_1 = 0.4192,\ D_1 = 0.3103$	$K_2 = 1.04,\ T_2 = 0.3245,\ D_2 = 0.3784$

B2 Simulation Examples of Model based Controller Design

In this section, the controller performance for the high-order process given in example B.2 is illustrated and compared with the Leva et al.'s auto-tuning method [79] where, the controller parameters are obtained from the closed loop characteristics of the process. Again, the controller performance for the TITO process (example B.4) is compared with the methods proposed by Zhuang and Atherton [62] and by Ziegler and Nicholas [66].

Example B.5

Consider the high-order process discussed in example B.2. The specifications for the controller design are set as $\alpha = 0.2$, $g_m = 3.0$ and $\phi_m = 60^0$. The controller parameters obtained for the process model are $K_c = 0.9596$, $T_I = 4.0960$, $T_d = 0.4643$. The PID settings by Leva et al.'s method [79] are $K_c = 1.05$, $T_I = 11.66$, $T_d = 2.27$. Fig. B.3 shows the comparisons of the closed loop output responses to unit step input and step load disturbance of magnitude 0.1 applied at $t = 100$ second for all the controller settings. The proposed method shows improved set-point and disturbance response in comparison to Leva et al.'s methods.

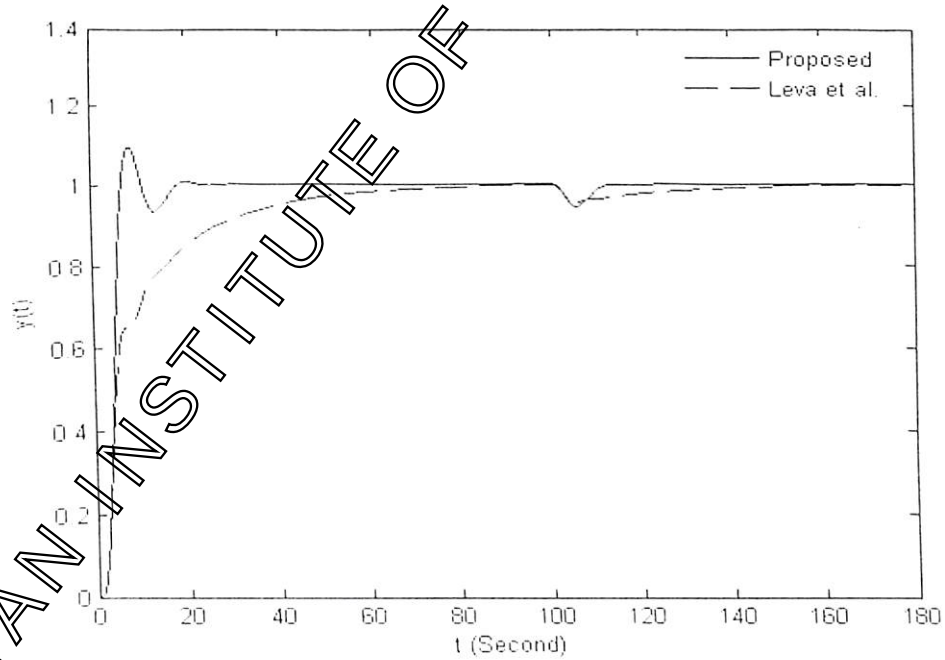

Fig.B.3. Closed loop responses to step input and load disturbance for example B.5

Example B.6

Consider the TITO process discussed in example B.4. Using the identification procedure described in subsection 3.2.4, the process is modeled as

$$\boldsymbol{G}_m(s) = \begin{bmatrix} \dfrac{1.9556\, e^{-0.3103s}}{(4192s+1)^2} & 0 \\ 0 & \dfrac{1.04\, e^{-0.3784s}}{(0.3245s+1)^2} \end{bmatrix}$$

Choosing $g_{m1} = 2,\ \phi_{m1} = 60^0$ and $g_{m2} = 2,\ \phi_{m2} = 65^0$, the parameters of the controller $G_{c1}(s)$ are estimated as $K_{c1} = 0.8938$, $T_{I1} = 1.2991$, $T_{d1} = 0.2839$ and that of $G_{c2}(s)$ are $K_{c2} = 1.1453$, $T_{I2} = 0.9220$ and $T_{d2} = 0.2102$. Using the method given in [62], $K_{c1} = 1.014$, $K_{c2} = 1.480$, $T_{I1} = 1.258$, $T_{I2} = 1.038$ and $T_{d1} = 0.220$, $T_{d2} = 0.221$ are obtained. Similarly Ziegler and Nichol's tuning formula [66] gives $K_{c1} = 1.192$, $K_{c2} = 1.743$, $T_{I1} = T_{I2} = 0.908$ and $T_{d1} = T_{d2} = 0.218$ for the considered TITO process.

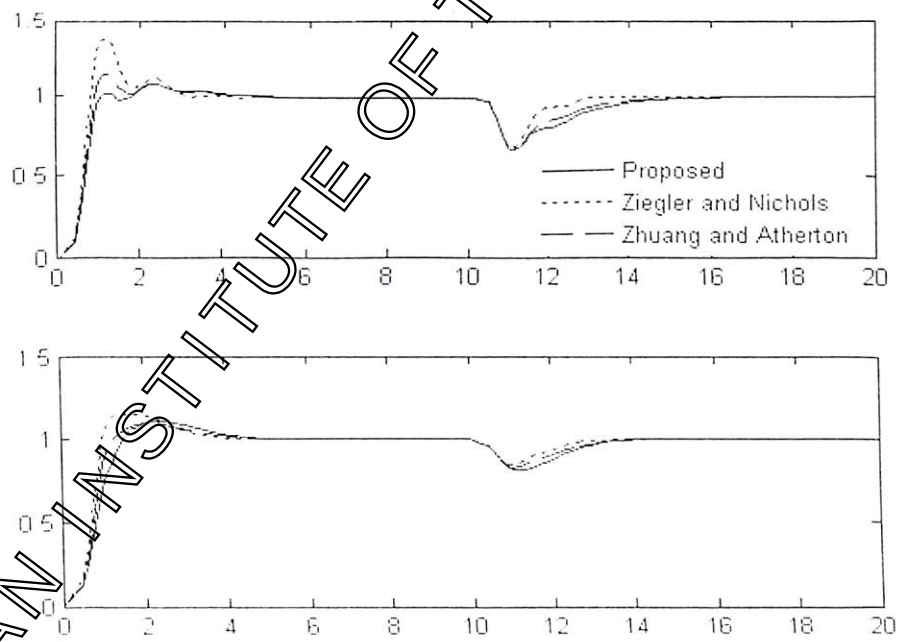

Fig.B.4. Closed loop responses to step input and load disturbance of loop 1 and loop 2 for example B.6

The responses of all the three methods to unit step set-point input and static disturbance are shown in Fig.B.4. The figure shows improved performance, in terms of speed of response and overshoot by the proposed control method.

B3 Simulation Examples of Model-free Controller Design

Two typical stable processes are considered in this section for the simulation studies to show the robustness and effectiveness of the new auto-tuning method. Chen et al,'s iso-damping method [77] and Jeng et al.'s modified relay (relay connected in series with a time delay) method [78] are considered for comparison. Both the methods do not require the intermediate process model for the controller design.

Example B.7

Considers a third order stable process transfer function with repeated roots [77] $G(s) = \frac{e^{-s}}{(s+1)^3}$.

For a user-defined $\phi' = 30^0$, T_l is updated as 1.9319 before beginning the second stage of auto-tuning test. The modified relay induces limit cycle output giving the phase lag of $\phi = 37.2796^0$. A measurement noise $M(0, \sigma_M^2 = 0.0917\times10^{-2})$ is added to the process output during the relay test. The PID controller parameters are designed using $\xi = 2$. The estimated PID parameters along with those suggested by Chen et al. are given in Table B.5. The closed loop output responses to a unit step input and a step load disturbances of magnitude 0.5 at 40 sec are shown in Fig.B.5. As is evident from Fig.B.5, Chen et al.'s PID gives highly oscillatory closed loop responses. The proposed method gives excellent control in terms of the overshoot, speed of response and settling time for both the set-point and load disturbance inputs.

Table B.5: PID controller settings for example B.7

Methods	PID controller parameters
Proposed	$1.0749\left(1+\frac{1}{3.0513s}+\frac{0.7088s}{0.007s+1}\right)$
Chen et al.	$1.024\left(1+\frac{1}{1.241s}+1.539s\right)$

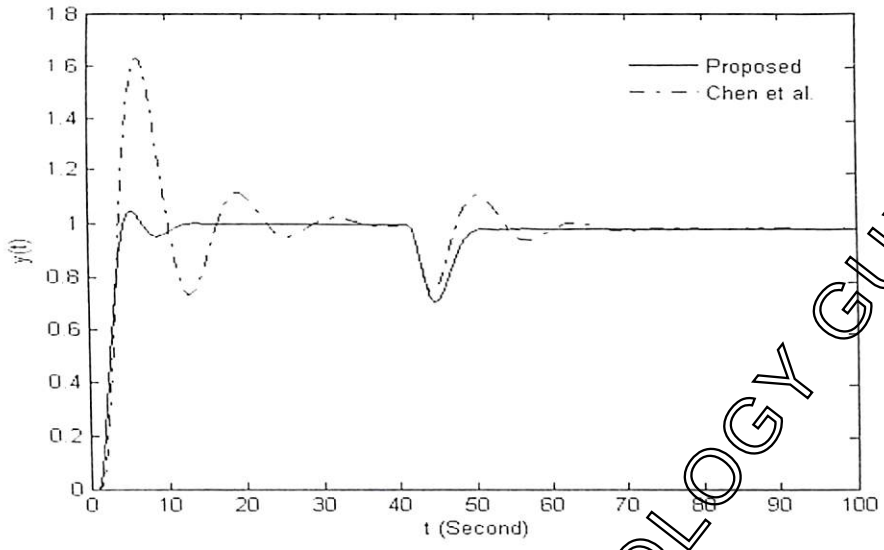

Fig.B.5. Closed loop responses to step input and load disturbance for example B.7

Example B.8

This example considers a high order process [78] with the transfer function

$$G(s) = \frac{1}{(s+1)^5}.$$

The integral time constant T_i is estimated as 2.4644 during the auto-tuning test using $\phi' = 30^0$. Using the recovered limit cycle data, the PID parameters are estimated with the choice of $\xi = 2$. The methods proposed by Chen et al. [77] and Jeng et al. [78] have been considered for comparison of the results.

Table B.6: PID controller settings for example B.8

Methods	PID controller parameters
Proposed	$1.1734\left(1+\frac{1}{3.8470s}+\frac{0.8857s}{0.0088s+1}\right)$
Chen et al.	$0.921\left(1+\frac{1}{1.961s}+1.969s\right)$
Jeng et al.	$1.207\left(1+\frac{1}{3.651s}+0.913s\right)$

Table B.6 gives the PID controller parameters designed by the above mentioned methods. Fig. B.6 shows the responses of the controller settings to unit step reference and step load disturbance of magnitude 0.05 appearing at 80 seconds. It is clear from Fig. B.6 that Chen et al.'s and Jeng et al.'s methods show more overshoot with almost similar disturbance rejection ability. The overall comparisons show that the proposed method gives faster response with shorter settling time and good disturbance rejection ability in comparison to the other.

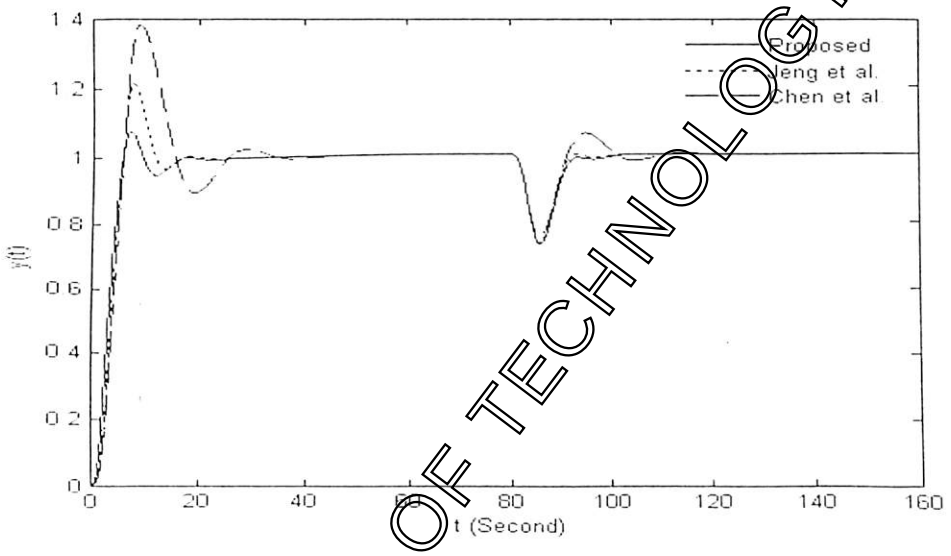

Fig. B.6 Closed loop responses to step input and load disturbance for example B.8

Appendix C

C1 On-line Identification for Non-linear Processes

In this section, on-line identification of the non-linear processes is discussed. In the suggested scheme, Hammerstein type or Wiener type models using relay feedback are identified where the models configure linear dynamics and non-linear static gain functions (N_s) as blocks in series. The series of blocks gives good description of the phenomena really going on a physical process. The above mentioned models are very useful in modeling of the non-linear processes. The features of the response in the relay feedback test for linear and non-linear processes (Wiener and Hammerstein types) are given in Table C.1 [75, 76]. Figs. C.1 and C.2 show the block diagram of the Wiener and Hammerstein type processes.

Table C.1 Features of the response in the relay feedback test

	Linear Model	Wiener Model	Hammerstein Model
Half period (T_{cr})	$T_{cr+} = T_{cr-}$	$T_{cr+} = T_{cr-}$	$T_{cr+} \neq T_{cr-}$
Amplitude (A)	$A_+ = A_-$	$A_+ \neq A_-$	$A_+ \neq A_-$

Fig.C.1. Wiener type process

Fig.C.2. Hammerstein type process

The non-linear process can be identified in any of the above mentioned structure (Wiener or Hammerstein types). The proposed auto-tuning scheme can be extended for the identification and control of the non-linear process. The block diagrams of the suggested on-line identification method for non-linear processes are shown in Figs. C.3 and C.4.

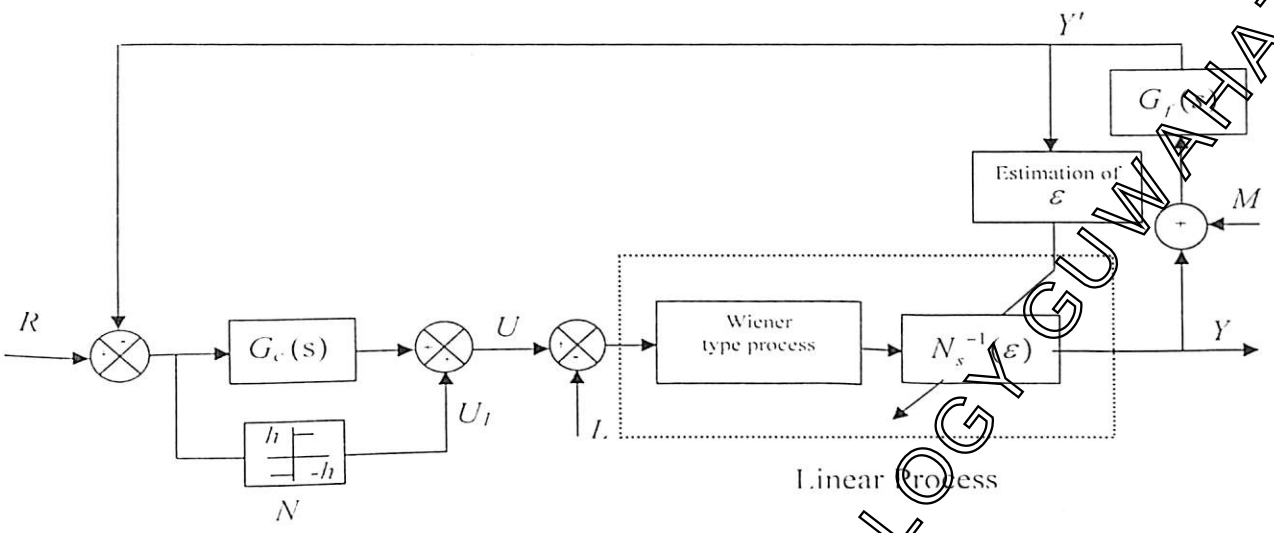

Fig.C.3. Proposed on-line identification scheme for Wiener type process with adaptive noise filter

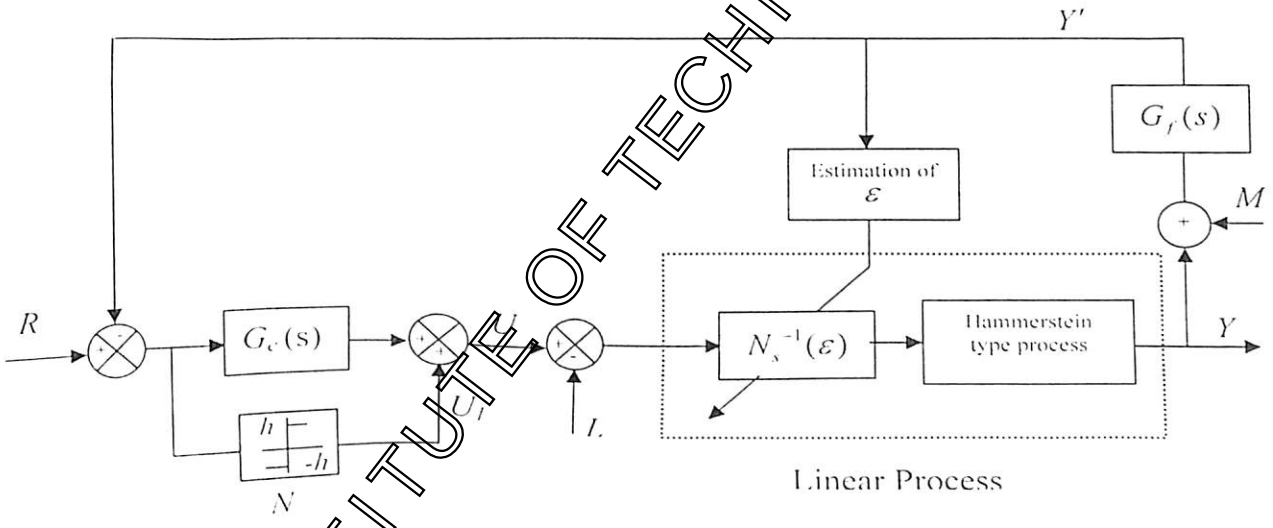

Fig.C.4. Proposed on-line identification scheme for Hammerstein type process with adaptive noise filter

For linear processes, the symmetric input signals causes the symmetric output responses. Hence, if the static non-linearity (N_s) of the non-linear process is cancelled, then the performance of the non-linear process becomes that of a linear one. Hence, a linear PID controller can be designed for the linear process model. The non-linearity can be removed by minimizing the parameter ε which is described as

$$\varepsilon = \min_{\lambda} \sum_{n=1}^{\infty} \left[\left(\frac{A_+(n)}{A_-(n)} - 1 \right)^2 + \left(\frac{a_+(n)}{a_-(n)} - 1 \right)^2 + \left(K(n) - 1 \right)^2 \right]$$

where,

$A_+(n)$ and $A_-(n)$ are the positive and negative amplitudes of the n^{th} period of the limit cycle

$a_+(n)$ and $a_-(n)$ are the positive and negative areas of the n^{th} period of the limit cycle

$K(n)$ are the steady state gains of the linearized model obtained from n^{th} period

Thus, the identification procedure can be divided into two parts. In the first part, the parameters of the non-linear function are obtained by minimizing ε via a simple optimization procedure which aims to obtain a symmetric limit cycle output. In the second part, the linear transfer function model is obtained by using the procedure given in section 2.3. Hence, the identified linear and non-linear parts are fully decoupled. The PID controller is designed for the identified linear model.

C2 Tuning Problems Associated with Real Life Controller

The auto-tuning of PID controller can be used in aerospace, motion control, process control, medicine, communication system, electrical, mechanical, chemical and numerous engineering applications. A few applications are given below.

1. Communication System

Adaptive channel quality indicator (CQI) used in wireless communication system:

The auto-tuning method can be implemented for adaptively biasing a channel quality indicator (CQI) used for setting a configuration of communication between a transmitter and a receiver in a wireless communication system. The receiver sends a CQI and positive acknowledgement (ACK)/negative acknowledgement (NACK) messages to the transmitter. The ACK/NACK messages indicate the absence or presence of error, respectively, in a transmitted data packet. The CQI is derived from the signal-to-interference ratio (SIR) and the ACK/NACK messages. The transmitter calculates the block error rate (BLER) of the transmitted data packets based upon the ACK/NACK messages sent from the receiver. The transmitter compares the BLER of the transmitted data packets to a target BLER and biases the CQI based on the comparison in order to achieve the target BLER.

2. Medicine

Automatic control of anesthetic depth during surgery

Continuous infusions, delivered by digitally programmed pumps, are a commonly used approach for delivering intravenous anesthetic during surgical procedures. This allows the physician to set the flow rate of anesthetic precisely into the patient in an attempt to maintain the appropriate levels of the anesthetic depth. The advantage of the infusion method is that the drug level in the body can be kept more constant, in contrast to the sequence of peaks and valleys that result from periodic injections. Thus less drug is needed for the safety of the patient.

3. Robotics

Mobile robot path tracking using a robust PID controller

The important issues in this field is the path-tracking (PT), which is concerned with the ability to drive a mobile robot autonomously as close as possible to a previously defined reference path. This path is usually specified as either a sequence of consecutive reference points or by a set of geometrical primitives such as straight lines or arcs of circumferences.

Motion control of robot manipulator

These manipulators are used in materials handling, welding, grinding, guided missile etc. The main challenge in this area is the motion control under complexity of dynamics and uncertainties arises from joint and link flexibility, actuator dynamics, friction, sensor noise and unknown disturbances.

4. Power system

STATCOM (Static Compensator)/SVC (Static VAR Compensator) for automatic voltage stabilization

In electrical transmission systems, the voltage of the system is largely controlled by reactive power. A STATCOM/SVC are the devices that is capable of producing or absorbing reactive power using a combination of capacitors, reactors and power electronic switches. Hence, the proposed auto-tuning scheme can be used for the voltage stabilization in transmission systems.

List of Publications

Published research papers related to this thesis work

1. Padhy, P.K. and Majhi, S., Tuning of PI controller for stable systems, *Journal of Systems Science and Engineering*, vol. 13, pp. 55-59, 2006.
2. Padhy, P.K. and Majhi, S., Relay based PI-PD design for stable and unstable FOPDT Processes, *Journal of Computers and Chemical Engineering*, vol. 30, pp. 790-796, 2006.
3. Padhy, P.K. and Majhi S., An exact method for on-line identification of FOPDT processes, *Proc. of IEEE International Conference on Industrial Technology*, IIT Bombay, pp. 1528-1532, Dec. 2006.
4. Padhy, P.K. and Majhi S., Identification of TITO processes, *Proc. of IEEE International Conference of Industrial Technology*, IIT Bombay, pp. 664-669, Dec. 2006.
5. Padhy, P.K. and Majhi, S., IMC based PID controller for FOPDT stable and unstable processes, *Proc. of 30th National System Conference*, Dona Paula, Goa, Nov. 2006.
6. Majhi, S. and Padhy, P.K., Relay based identification of time delay processes, *Proc. of 30th National System Conference*, Dona Paula, Goa, Nov. 2006.
7. Padhy, P.K. and Majhi S., On-line mobile robot path tracking using PI controller, *Proc. of IEEE INDICON*, Delhi, Sept. 2006.
8. Padhy, P.K. and Majhi, S., Automatic tuning of fuzzy PID controller, *Proc. of 29th National System Conference*, IIT Bombay, Dec. 2005.
9. Padhy, P.K. and Majhi, S., Relay based PI-PD design for stable FOPDT processes, *Proc. of DICHCAT*, Korea, Oct. 2005.
10. Padhy, P.K., Majhi, S. and Atherton, D.P., PID-P controller for TITO systems, *Proc. of 16th IFAC World Congress*, May. 2005.
11. Padhy P.K. and Majhi S., Closed loop identification of TITO systems, *Proc. of SICPRO*, Moscow, pp. 849-856, Jan. 2005.

12. Padhy P.K. and Majhi S., Relay based PID controller tuning of a TITO system, *Proc. of SICPRO*, Moscow, pp. 857-865, Jan. 2005.

13. Padhy, P.K. and Majhi, S., Parametric identification of nonlinear systems, *Proc. of IEEE INDICON*, IIT, Kharagpur, pp. 220-224, Dec. 2004.

14. Padhy, P.K. and Majhi, S., PI-PD controller for unstable FOPDT systems, *Proc. of National Conference on Recent Advances in Power, Signal Processing and Control*, NIT, Rourkela, Nov. 2004.

Research paper communicated

1. Padhy, P.K. and Majhi, S., Tuning of PID Controller for stable processes, communicated to *International Journal of Systems and Control Letters*.

Bibliography

[1] Mukherjee, S., Satakshi and Mittal, R. C., Model order reduction using response-matching technique, *Journal of the Franklin Institute*, vol. 342, pp. 503-519, 2005.

[2] Åström, K. J. and Hägglund, T., Automatic tuning of simple regulators with specifications on phase and amplitude margins, *Automatica*, vol. 20, pp. 645-651, 1984.

[3] Luyben, W. L., Derivations of transfer functions for highly non-linear distillation columns, *Ind. Eng. Chem. Res.*, vol. 26, pp. 2490-2495, 1987.

[4] Li, W., Eskinat, E. and Luben, W. L., An improved auto tune identification method, *Ind. Eng. Chem. Res.*, vol. 30, pp. 1530-1541, 1991.

[5] Leva, A., PID auto tuning algorithm based on relay feedback, *IEE Proc. on Control Theory and Applications*, vol. 140, pp. 328-338, 1993.

[6] Lee, T. H., Wang, Q. G. and Tan, K. K., A modified relay-based technique for improved critical point estimation in process control, *IEEE Transactions on Control Systems Technology*, vol. 3, pp. 330-337, 1995.

[7] Sung, S. W., Park, J. H, Lee, I., Modified relay feedback method, *Ind. Eng. Chem. Res.*, vol. 34, pp. 4133–4135, 1995.

[8] Shen, S., Wu, J. S., and Yu, C. C., Use of biased-relay feedback for system identification, *AIChE journal*, vol. 42, pp. 1174–1180, 1996.

[9] Wang, Q. G., Zhang, Y. and Guo, X., Robust closed loop identification with application to auto-tuning, *Journal of Process Control*, vol. 11, pp. 519-530, 2001.

[10] Tan, K. K., Lee, T. H., Huang, S., Chua, K. Y. and Ferdos, R., Improved critical point estimation using a preload relay, *Journal of Process Control*, vol. 16, pp. 445-455, 2006.

[11] Tyagrajan, T. and Yu, C. C., Improved auto tuning using shape factor from relay feedback, *Ind. Eng. Chem. Res.*, vol. 42, pp. 4425-4440, 2003.

[12] Srinivasan, K. and Chidambaram, M., Modified relay feedback method for improved system identification, *Computers and Chemical Engineering*, vol. 27, pp. 727-732, 2003.

[13] Vivek, S. and Chidambaram, M., Identification using single symmetrical relay feedback, *Computers and Chemical Engineering*, vol. 29, pp. 1625-1630, 2005.

[14] Vivek, S. and Chidambaram, M., An improved relay auto tuning of PID controllers for unstable FOPDT systems, *Computers and Chemical Engineering*, vol. 29, pp. 2060-2068, 2005.

[15] Chang, R. C., Shen, S. H. and Yu, C. C., Derivations of transfer functions from relay feedback systems, *Ind. Eng. Chem. Res.*, vol. 31, pp. 855-860, 1992.

[16] Wang, Q. G., Hang, C. C and Zou, B., Low order modeling from relay feedback systems, *Ind. Eng. Chem. Res.*, vol. 36, pp. 375-381, 1997.

[17] Atherton, D. P., Improving accuracy of autotuning parameters estimation, *Proc. IEEE Int. Conf. on Control Applns.*, Hartford, USA, pp. 51-56, 1997.

[18] Majhi, S and Atherton, D.P., Autotuning and controller design for processes with small time delays, *IEE Proc. on Control Theory and Applications*, vol. 146, pp. 415-424, 1999.

[19] Panda, R. C. and Yu, C. C., Shape factor of relay response curves and its use in autotuning, *Journal of Process Control*, vol. 15, pp. 894-906, 2005.

[20] Wei, T., Songjiao, S. and Mengxiao, W., Model identification and control of long time-delay processes, *Proc. IEEE Conference on Intelligent Control and Automaton*, pp. 974-976, 2002.

[21] Jin, H. P., Sung, S. W. and Lee, I. B., Improved relay autotuning with static load disturbance, *Automatica*, vol. 33, pp. 711-715, 1997.

[22] Scali, C, Marchetti, G and Semino, D., Relay with additional delay for identification and auto-tuning of completely unknown processes, *Ind. Eng. Chem. Res.*, vol. 38, pp. 1987-1997, 1987.

[23] Majhi, S. and Litz, L., Relay based identification of process model parameters, *Proc. of IEEE American Control Conference*, Denver, USA, pp.2949-2953, 2003.

[24] Majhi, S. and Litz, L., Relay based closed loop tuning of PID controller, *Automatisierungstechnik*, vol.52, pp.202-208, 2004.

[25] Majhi, S., On-line PI control of stable processes, *Journal of Process Control*, vol. 13, pp. 769-786, 2005.

[26] Normey-Rico, J. E., Alcala, I, Gomez-Ortega, J and Camacho, E. F., Mobile robot path tracking using a robust PID controller, *Control Engineering Practice*, vol. 9, pp. 1209-1214, 2001.

[27] Thuilot, B, D'andrea, N. B. and Micaellli, A., Modeling and feedback control of mobile robots equipped with several steering wheels, *IEEE Transaction on Robotics and Automation*, vol. 12, pp. 375-390, 1996.

[28] Freund, E and Mayr, R., Nonlinear path control in automated vehicle guidance, *IEEE Transaction on Robotics and Automation*, vol. 13, pp. 49-60, 1997.

[29] Hwang, S. H., Closed loop auto-tuning of single-input-single-output systems, *Ind. Eng. Chem. Res.*, vol. 34, pp. 2406-2417, 1995.

[30] Huang, H. P., Jeng, J. C. and Luo, K. Y., Auto-tune system using single run relay feedback test and model based controller design, *Journal of Process Control*, vol. 15, pp. 713-727, 2005.

[31] Ho, W.K., Hang, C. C. and Cao, L. S., Tuning of PID controllers based on gain and phase margin specifications, *Automatica*, vol. 31, pp. 497-502, 1995.

[32] Ho, W.K. and Xu, W., Online PID tuning for unstable processes based on gain and phase margin specification, *IEE Proc. on Control Theory and Application*, vol. 145, pp. 392-399, 1998.

[33] Ho, W. K., Hong, Y., Hansson, A. Hjalmarsson, H. and Deng, J. W., Relay auto-tuning of PID controllers using iterative feedback tuning, *Automatica*, vol. 39, pp. 149-157, 2003.

[34] Padma Sree, R., Srinivas, M. N. and Chidambram, M., A simple method of tuning PID controllers for stable and unstable FOPDT systems, *Computers and Chemical Engineering*, vol. 192, pp. 2201-2218, 2004.

[35] Visioli, A., Optimum tuning of PID controllers for integrating and unstable processes, *IEE Proc. on Control Theory and Applications*, vol. 148, pp. 180-188, 2001.

[36] Ziegler, J. G. and Nichols, N. B., Optimum settings for automatic controllers, *ASME Transactions*, vol. 64, pp. 759-767, 1942.

[37] Wang, Q. C., Hang, C. C. and Yang, X. P., Single loop controller design via IMC principle, *Automatica*, vol. 37, pp. 2041-2048, 2001.

[38] Huang, H. P., and Chen, C. C., Auto-tuning of PID controllers for second order unstable systems having dead time, *Journal of Chemical Engineering (Japan)*, vol. 32, pp. 579-588, 1999.

[39] Tan, K. K., Lee, T. H and Jiang, X., Robust on-line relay automatic tuning of PID control systems, *ISA Transactions*, vol. 39, pp. 219-232, 2000.

[40] Majhi, S. and Atherton, D.P., Online tuning of controllers for an unstable FOPDT process, *IEE Proc. on Control Theory and Applications*, vol. 147, pp. 421-427, 2000.

[41] Kaya, I., Tan, N. and Atherton, D.P., A simple procedure for improving performance of PID controller, *IEEE Conf. on Control Applications*, vol. 2, pp. 882-891, 2003.

[42] Park, J. H., Sung, S. W. and Lee, I., An enhanced PID control strategy for unstable processes, *Automatica*, vol. 34, pp. 751-762, 1998.

[43] Chidambram, M., Set point weighting PI/PID controllers, *Chem. Eng. Comm.*, vol. 179, pp. 1-13, 2000.

[44] Padma Sree, R. and Chidambram, M., Set point weighted PID controllers for unstable processs, *Chem. Eng. Comm*, vol. 192, pp. 1-13, 2005.

[45] Skogestad, S. and Morari, M., Robust performance of decentralized control systems by independent design, *Automatica*, vol. 25, pp. 119-125, 1989.

[46] Lee, J., Cho, W. and Edgar, T. F., Multiloop PI controller design for interacting multivariable process, *Computers and Chemical Engineering*, vol. 22, pp. 1711-1723, 1998.

[47] Choi, J. Y., Lee, J., Jung, J. H., Lee, M. and Han, C., Sequentional loop closing identification of multivariable process models, *Computers and Chemical Engineering*, vol. 24, pp. 809-814, 2000.

[48] Shen, S. H. and Yu, C. C., Use of relay feedback test for automatic tuning of multivariable systems, *AIChE journal*, vol. 40, pp. 627–646, 1994.

[49] Luyben, W. L., Simple method for tuning SISO controllers in multivariable systems, *Industrial and Engineering Chemestry Process Design and Development*, vol. 25, pp. 654-660, 1986.

[50] Wang, Q.G, Zou, B., Lee, T.H. and Bi, Q., Auto tuning of multi variable PID controller from decentralized relay feedback, *Automatica*, vol. 33, pp. 319-330, 1997.

[51] Wang, Q. G., Huang, B. and Guo, X., Auto tuning of TITO decoupling controllers from step tests, *ISA Transactions*, vol. 39, pp. 417-418, 2000.

[52] Tavakoli, S, Griffin, I and Fleming, P. J., Tuning of decentralize PI (PID) controllers for TITO processes, *Control Engineering Practice*, vol. 14, pp. 1069-1080, 2006.

[53] Palmor, Z. J., Halevi, Y.and Kranse, N., Automatic tuning of decentralized PID controller for TITO processes, *Automatica*, vol. 31, pp. 1001-1010,1995.

[54] Loh, A. P., Hang, C. C., Quek, C. K. and Vasnani, V. U., Autotuning of multiloop proportional-integral controllers using relay feedback, *Ind. Eng. Chem. Res.*, vol. 32, pp. 1102-1107, 1993.

[55] Loh, A.P and Vasnani, V.U., Necessary conditions for limit cycles in multi loop relay systems, *IEE Proc. on Control Theory and Applications*, vol. 141, pp. 163-168, 1994.

[56] Lin, C. H. and Han, K. W., Prediction of limit cycles in nonlinear two-input-two-output control systems, *IEE Proc. on Control Theory and Applications*, vol. 146, pp. 253-258, 1999.

[57] Lee, J. and Edgar, T. F., Interaction measure for decentralized control of multivariable processes, *Proc. of IEEE American Control Conference*, Anchorage, pp.454-458, 2002.

[58] Grosdidier, P. and Morari, M., Interaction measures under decentralized control, *Automatica*, vol. 22, pp. 309-319, 1986.

[59] Ho, W. K., Lee, T. H. and Gan, O. P., Tuning of multiloop proportional-integral-derivative control based on phase and gain margin, *Ind. Eng. Chem. Res.*, vol. 36, pp. 2231-2238, 1997.

[60] Huang, H. P., Jeng, J. C., Chiang, C. H. and Pan, W, A., direct method for multi-loop PI/PID controller design, *Journal of Process Control*, vol. 13, pp. 769- 786, 2003.

[61] Åström, K. J, Johanson, K. H. and Wang, Q. G., Design of decoupled PI controllers for two-by-two-systems, *IEE Proc. on Control Theory and Applications*, vol. 149, pp. 74-81, 2002.

[62] Zhuang, M. and Atherton, D.P., PID controller design for a TITO system, *IEE Proc. on Control Theory and Applications*, vol. 141, pp.111-120, 1994.

[63] Chien, I. L. Huang, H. P. And Yang, J. C., A simple multiloop tuning method for PID controllers with no proportional kick, *Ind. Eng. Chem. Res.*, vol. 38, pp.1456-1468, 1999.

[64] Chien, I.L. Huang, H.P. and Yang, J.C., A simple TITO method suitable for industrial application, *Chem. Eng. Comm.*, vol. 182, pp. 181-196, 2000.

[65] Majhi, S., SISO controller for TITO systems, *International conference on Energy, Automation and Information Technology*, IIT Kharagpur, pp. 723-726, 2001.

[66] Neiderlinski, A., A heuristic approach to the design of linear multivariable interacting control systems, *Automatica*, vol. 7, pp.691-701, 1971.

[67] Bristol, E. H., On a new measure of interaction for multivariable process control, *IEEE Trans. on Automatic Control*, vol. 2, pp. 133-134, 1966.

[68] Shinskey, F. G., The stability of interacting control loops with and without decoupling, *Proc. of IFAC Multivariable Technol Syst. Conf.*, pp. 21-30,1997.

[69] Maciehowski, J. M., Multivariable feedback design, Addison-Wesley, Workingham, U.K, 1989.

[70] Kuo, B. C., Automatic control systems, 7th edition, Prentice Hall international, 1995.

[71] Atherton, D. P., Non-linear control engineering, Describing function analysis and design, Van Nostraind Rheinhold Co, London, 1975.

[72] Åström, K. J. and Hägglund, T., Automatic tuning of PID controllers, Instrument Society of America, Research Triangle Park, NC, 1988.

[73] Åström, K. J. and Hägglund, T., Theory, Design and Tuning, 2nd edition, Instrument Society of America, Research Triangle Park, NC, 1995.

[74] Mamat, R. and Fleming, P. J., Method for on-line identification of a first order plus dead-time process model. *Electronics Letters*, vol. *31*, pp. 1297-1298, 1995.

[75] Sung, S. L. and Lee, J., Modeling and Control of Wiener type processes, *Chemical Engineering Science*, vol. 59, pp. 1515-1521, 2004.

[76] Giri, F., Chaoui, F. Z. and Rochdi, Y., Parameter identification of a class of Hammerstein plants, *Automatica*, vol. 37, pp. 749-756, 2001.

[77] Chen, Y. Q. and Moore, K. L., Relay feedback tuning of robust PID controllers with iso-damping property, *IEEE Transactions on Systems, Man and Cybernetics-Part B*, vol. 35, pp. 23-31, 2005.

[78] Jeng, J. C. Huang, H. P.and Lin, F. Y., Modified relay feedback approach for controller tuning based on assessment of gain and phase margins, *Ind. Eng. Chem. Res.*, vol. 45, pp. 4043-4051, 2006.

[79] Leva, A., Bascetta, L and Schiavo, F., Model based proportional-integral/proportional-integral-derivative (PI/PID) autotuning with fast relay identification, *Ind. Eng. Chem. Res.*, vol. 45, pp. 4052-4062, 2006.

[80] Parmar, G., Mukherjee, S. and Prasad, R., Reduced order modelling of linear dynamic systems using particle swarm optimized eigen spectrum analysis, *International Journal of Mathematics Sciences*, vol. 1, pp. 45-52, 2007.

[81] Chen, T. C., Chang, C. Y. and Han, K. W., Model reduction using the stability equation method and continued fraction method, *International Journal of Control*, vol. 32, pp. 81-94, 1980.